AIR SAMPLING WITH SOLID PHASE MICROEXTRACTION

by

Perry Anthony Martos

A thesis

presented to the University of Waterloo

in fulfillment of the

thesis requirement for the degree of

Doctor of Philosophy

in

Chemistry

Waterloo, Ontario, Canada, 1997

BORROWER'S PAGE

The University of Waterloo requires the signatures of all persons using or photocopying this thesis. Please sign below, and give address and date.

ABSTRACT

There is an increasing need for simple yet accurate air sampling methods. The acceptance of new air sampling methods requires compatibility with conventional chromatographic equipment, and the new methods have to be environmentally friendly, simple to use, yet with equal, or better, detection limits, accuracy and precision than standard methods. Solid phase microextraction (SPME) satisfies the conditions for new air sampling methods. Analyte detection limits, accuracy and precision of analysis with SPME are typically better than with any conventional air sampling methods. Yet, air sampling with SPME requires no pumps, solvents, is re-usable, extremely simple to use, is completely compatible with current chromatographic equipment, and requires a small capital investment.

The first SPME fiber coating used in this study was poly(dimethylsiloxane) (PDMS), a hydrophobic liquid film, to sample a large range of airborne hydrocarbons such as benzene and octane. Quantification without an external calibration procedure is possible with this coating. Well understood are the physical and chemical properties of this coating, which are quite similar to those of the siloxane stationary phase used in capillary columns. The log of analyte distribution coefficients for PDMS are linearly related to chromatographic retention indices and to the inverse of temperature. Therefore, the actual chromatogram from the analysis of the PDMS air sampler will yield the calibration parameters which are used to quantify unknown airborne analyte concentrations (ppb_v to ppm_v range).

The second fiber coating used in this study was PDMS/divinyl benzene (PDMS/DVB) onto which *o*-(2,3,4,5,6-pentafluorobenzyl) hydroxylamine (PFBHA) was adsorbed for the on-fiber derivatization of gaseous formaldehyde (ppb_v range), with and without external calibration. The oxime formed from the reaction can be detected with conventional gas chromatographic detectors. Typical grab sampling times were as small as 5 seconds. With 300 seconds sampling, the formaldehyde detection limit was 2.1 ppb_v, better than any other 5 minute sampling device for formaldehyde. The first-order rate constant for product formation was used to quantify formaldehyde concentrations without a calibration curve. This spot sampler was used to sample the headspace of hair gel, particle board, plant material and coffee grounds for formaldehyde, and other carbonyl compounds, with extremely promising results.

The SPME sampling devices were also used for time-weighted average sampling (30 minutes to 16 hours). Finally, the four new SPME air sampling methods were field tested with side-by-side comparisons to standard air sampling methods, showing a tremendous use of SPME as an air sampler.

ACKNOWLEDGMENTS

I thank first and foremost Dr. Janusz Pawliszyn for his strong support from the time we met. His belief in me and vision provided the opportunities I needed to successfully complete this work.

I thank next my dear friend Dr. Tadeusz Górecki for his opinions and healthy scientific discussions which enhanced the way which I carried out my research.

I next thank and gratefully acknowledge the efforts of all my committee members, Dr. Barker, Dr. Corsi, Dr. Karanassios, Dr. Lipkowski., Dr. McMahon, and Dr. Sloan.

Finally, I thank all the group members for their help and friendship, especially Drs. Hiroyuki Daimon and Zhouyao Zhang.

DEDICATION

I dedicate this thesis to Lillian, Zoë, and Kyle. I have a special dedication for my mother, Gilda Maria Pirollo Martos, whose actions molded who I am and whose life lovingly touched so many.

TABLE OF CONTENTS

LIST OF TABLES

Chapter 2

LIST OF FIGURES

CHAPTER 1

INTRODUCTION

1.1 Air Sampling Considerations and Solid Phase Microextraction

1.1.1 Air and air sampling

The air that we breathe can generally be categorized as ambient or outdoor air, indoor air, and occupational air. Each of these categories differ considerably from one another by a number of perspectives, including the observed concentrations of analytes, the chemical and toxicological nature of the analytes, and the different air sampling requirements for each of these environments.

The hydrocarbon fraction of ambient air is due to natural sources, e.g., vegetation, emissions from industry, vehicles, power plants, oil refineries, and others (1). The concentrations can vary significantly depending on one's proximity to the sources, and are dependent on prevailing meteorological conditions, terrain, source strengths, and emission control systems. Indoor air constituents result primarily from indoor/outdoor air exchange, and a plethora of indoor sources such as household commercial cleaning products, building materials, pesticides, paints, kerosene stoves, smoking, and many others (2). Occupational air usually contains a significantly smaller number of airborne compounds, but those compounds can often be found at concentrations orders of magnitude higher than in both outdoor and indoor air (3). Some of the occupationally observed concentrations can be high enough that personal protection is required so the workers won't suffer from physiological symptoms such as lung disorders, neurological damage, and even immediate death (4).

1.1.1.a Analysis of ambient air

Establishing a safe concentration level of ambient air pollutants is in part dependent on the nature of the analyte from chemical and toxicological perspectives, the prevalence of the analyte in the atmosphere including any secondary reaction products, and the lowest detectable level of those analytes with today's sampling and analysis equipment.

The United States Environmental Protection Agency (U.S.EPA) lists 189 hazardous air pollutants (HAPs) which require air sampling and analysis to determine the concentrations and source emissions of those analytes. Sampling for those analytes necessitates considerable expertise and costs due to labour and equipment. For example, U.S. EPA Methods TO-1 and TO-14 are used for parts per trillion to parts per million concentrations of hydrocarbons. Both methods require large and costly sampling pumps which can draw air at very high flow rates with analysis by gas chromatography coupled to mass spectrometry (5,6).

1.1.1.b Analysis of indoor air

In indoor air, the main sources of pollution include local ambient air pollutants and pollutants such as those from the uncontrolled use of cleaners, solvents such as paint thinners, propellants in aerosol cans, pesticides for pets and carpets, acrylate monomers from floor shine, carpet protectors consisting of formaldehyde, building materials such as particle board, cosmetics, adhesives for tiling, and even from compounds found in household tap water (2,7). In addition, the trend towards increasing energy efficiency in buildings and dwellings found an increase in indoor pollutants due to their accumulation. Those pollutants include, among others, a large range of hydrocarbons and carbonyl compounds. The airborne hydrocarbon concentrations are currently extensively used to act as indicators of indoor air quality (8).

This marker of indoor air quality has been shown to correlate extremely well with expressed health complaints, even though most of those do not cause documented health effects. By contrast, an example of a highly toxic yet ubiquitous indoor air pollutant, formaldehyde (2, 9), has been shown to be directly responsible for a number of health effects. It is a strong pulmonary irritant which can weaken the lungs to other airborne chemicals which would otherwise go without effect, and it is a mucous membrane irritant with allergic properties which can result in lung disorders and asthma like symptoms. It has also been identified as a probable human carcinogen (4,7).

The sampling and analysis of indoor air pollutants is very difficult. There can be hundreds of indoor pollutants ranging in concentration from parts per trillion (v/v) (ppt_v) to parts per million (v/v) (ppm_v) (2). Therefore, sampling and analysis methods used for indoor air studies have to be very sensitive for the low concentrations yet flexible for the higher concentrations. There are no government regulated indoor air sampling methods; however, a combination of ambient and occupational air sampling methods, using sensitive detectors, can provide for accurate description of the airborne analyte concentration.

1.1.1.c Analysis of occupational air

There is a large segment of the population, the "worker" population, to which exposure to known toxic chemicals can occur on a daily basis and is permitted by law (10). Employers are obligated to establish the airborne concentration of chemicals to which the workers are exposed while on the job. This is facilitated with professional services who use "personal" sampling devices which acquire representative portions of the worker's "breathing" air, i.e., a sampling device specific for the compounds of interest which is worn by the worker. The samples are analyzed for the target compounds, then reported. The results are then

compared to allowable exposure levels. It is extremely important that accurate and representative sampling and analyses of the employees breathing air are carried out with the best available methods because inaccuracies at this stage could result in an employee's over exposure to toxic compounds and could go unchecked for months or even years.

1.1.1.c.i What is a toxic compound and when is it toxic?

The allowed exposure of workers to high concentrations of known toxic chemicals did not go without first thorough checking and understanding of the analytes using controlled and defined toxicity tests (11). The toxicological data for a chemical are evaluated using parameters such as the lethal dose, 50 %, (LD_{50}) and the lethal concentration, 50 % (LC_{50}) (11). In general, the LD_{50} provides toxicologists with a measure of how much of an analyte per kilogram of body weight causes 50 % (the median) of the test animal population to die. An analyte with an LD_{50} of 50 to 500 mg/Kg is considered highly toxic compound, while an LD_{50} of 5 to 15 g/Kg is considered slightly toxic. The LC_{50} provides an understanding of the relationship between the analyte, typically the airborne concentration, and 50 % of the deaths for that concentration. The value for the LC_{50} is not as well definable as the LD_{50}. This is because the former strongly depends on the route of exposure. For example, high ground level SO_2 concentrations due to thermal inversions in England from coal burning killed more than 4000 people (12). By contrast, ingestion of the same lethal quantity of SO_2 adsorbed onto particles may go completely unnoticed (4). Therefore, the LC_{50} airborne concentration is one of the important parameters in defining a chemical's toxicity. The LC_{50} for airborne chemicals, along with other toxicological data, are used by toxicologists and government agencies to define workplace "allowable exposure limits". These limits were defined so that a typical 70 Kg worker would not observe a health problem following 40 years of daily

exposure (2000 hours/year) at the proposed limit (13).

1.1.1.c.ii Allowable exposure limits to airborne contaminants (vapours)

Hippocrates, in the fourth century B. C., recognized lead toxicity in the mining industry (3) and since then, relationships have been developed between ones' occupation and observable diesease. Probably one of the most significant works in this regard was published by Ramazzini in 1700. His text, entitled "De Morbis Artificum" was the cornerstone of occupational medicine today. Considerable advancements in occupational medicine have been made since Ramazzini's text from many perspectives including the protection of the worker from the dangerous aspects of his/her work environment. Allowable exposure limits have been set and enforced by government to protect nearly all workers (4). One of the main groups of standards promulgated by the various government agencies, such as the Occupational Safety and Health Administration (OSHA) (14), were set for airborne analytes in the workplace. These analytes are generally categorized as vapours, gases, dusts, mists, fumes, particles not otherwise classifiable, and particles with known chemical composition.

Among the group of vapours, one can find compounds ranging from extremely low to very large allowable airborne concentrations. For example, the isocyanates, which are used in the polyurethane foam industry, have an allowable exposure level of 0.02 ppm_v for 8 hours, OSHA (10). There are others with moderate allowable airborne concentrations, such as for formaldehyde and benzene, (0.75 and 1.0 ppm_v for 8 hours, respectively, OSHA), to those with extremely high allowable airborne concentrations, such as for toluene (200 ppm_v for 8 hours, OSHA) (10).

It is generally understood that the allowable levels, or the "Threshold Limit Values" (TLV) were developed on a delicate blend of observed health effects to the worker population

from exposure to the insult analytes, laboratory toxicity tests (which include the LC_{50}), industry's ability to control the analytes, and risk ratio assessments (4). The TLV's for airborne analytes, such as formaldehyde and toluene, were set to protect nearly all workers from adverse health effects associated with long term exposure. Therefore, ensuring the general worker population is not overexposed to the target analyte(s) requires measuring the airborne concentrations of those analytes during the worker's routine work practice. This is effectively done with samples of breathing air or "personal samples" and with air samples around the worker or "area samples".

1.1.1.c.iii Sampling in occupational air

In contrast to ambient air monitoring, worker exposure monitoring requires sampling devices which can be used in a fairly small concentration range, but typically at orders of magnitude higher than those found in ambient air (15) and which must be portable so that it may be worn by the test subject. Sampling high analyte concentrations may initially seem advantageous, but presents a difficulty for some sampling systems. A problem has also arisen with the current occupational air sampling methods in that the trend towards lower allowable exposure levels has pressed the sampling methods to their limits (15).

The typical sampling procedure utilizes a solid sorbent tube, such as activated charcoal for hydrocarbons, through which air is drawn at a specific flow rate for eight hours (10,15). Another sampling method for hydrocarbons uses passive sampling devices which do not require air sampling pumps (15,16,17,18). The passive sampling method works on the principle of diffusion to an activated charcoal sorbent bed. In both sampling devices, the sorbent is chemically desorbed with carbon disulphide (a very toxic organic solvent), the analytes separated with a gas chromatograph, detected with flame ionization detection,

quantified, then reported on a time-weighted average basis. Also, since the sampling methods require the use of carbon disulphide, the device cannot be re-used, and further are not amenable to sampling ambient or indoor analyte concentrations due to the low analyte mass loading achieved with the low flow rate air sampling devices specially configured for occupational air sampling.

There are two options to overcome the limits of current air sampling methods for occupational air. First, increase the analyte mass loading on the sampling system by increasing the air volume sampled, and/or second, increase detector response to the target analytes; however, the trend has moved towards more analyte loading because instrument detector responses have not proportionally increased with the decreasing allowable levels. A third novel technique combines the first point with an increasing signal/noise ratio as a result of the sampling system itself, such as observed with solid phase microextraction (SPME) for air sampling. As shown in this thesis, SPME is a powerful alternative to air sampling occupational air with traditional methods.

1.1.2. Air sampling concepts

In general, air can be sampled with a number of techniques depending on the analyte of interest. Some of these techniques include "grab sampling" (instantaneous sampling) air with stainless steel canisters or nylon bags (3), concentration over a sorbent bed as described above, colorimetric tubes, portable real-time detectors and passive monitors. (15,19). The ideal scenario is invariably an extremely cost effective yet very accurate evaluation of the airborne analyte concentration which are two opposing demands. In practice, an acceptable balance is always sought among the speed of analysis, accuracy, practicality of sampling, the instrument used for quantitation and total cost. The sampling and analysis techniques of

choice depend on both the analyte of interest and the ultimate use of the results. For example, nylon bags are quite useful for tracer gas studies involving sulfur hexafluoride (20) but would not be practical to study airborne polyaromatic hydrocarbons due to losses of those hydrocarbons on the walls of the bags.

Traditional methods to examine airborne concentrations of aliphatic and aromatic compounds include active air sampling (15) and whole air sampling (21). Active air sampling is usually facilitated with mass flow controlled pumps drawing the air suspected to contain the analyte(s) of interest over a bed of charcoal (or other sorbents) with subsequent thermal or chemical desorption followed by separation with gas chromatography (GC) and detection with flame ionization detectors (GC/ FID) or other types of detectors. These sampling techniques are quite useful but at the same time are cumbersome, bulky to ship to field studies, can be difficult to employ at a moments notice and require toxic eluants for chemical desorption or require costly thermal sorbent desorbers. Whole air sampling in stainless steel canisters alleviates some of the drawbacks with active sampling, yet they introduce different problems such as the requirement for costly GC interfaces, not to mention the costs associated with cleaning the canisters and transfer lines. In the past ten years, or so, passive sampling for airborne hydrocarbons with charcoal beds (15,22,23) has provided a good substitute to the active sampling methods, but the analysis maintains the use of toxic solvents for chemical desorption and the system is limited by interfering organics from the charcoal bed holder which increase method detection limits. Furthermore, the current passive sampling methods were designed for high analyte concentration ranges and are not useful for the pending lower allowable concentrations of airborne analytes. Also, current passive sampling systems are not amenable to both grab sampling and time-weighted average sampling. Therefore, a sampling

system designed today for specific airborne analytes should be flexible for use when the allowable analyte concentrations are reduced. SPME will be shown in this thesis to be an alternative air sampling method which can satisfy the aforementioned passive sampling requirements.

1.1.3 Solid Phase Microextraction (SPME)

SPME, a sampling technique originally developed by Dr. Janusz Pawliszyn (24) as a sampler for the direct extraction of waterborne analytes, is shown in this thesis to be an alternative to traditional air sampling. SPME provides significant analytical advantages over traditional methods, both for active air sampling with sorbents and whole air sampling. It is also portable, accurate, reproducible, cost effective, simple to deploy and re-usable. It is possible to sample a large range of airborne compounds employing SPME using different fiber coatings.

A schematic of the SPME device is shown in Figure 1.1A. There are two basic components to this device. They are the holder and the needle assembly. The assembly includes the analyte extraction polymer and a needle to protect the polymer (discussed below). The SPME holder and needle system are very simple to use, and anyone who can use a syringe can use SPME with little training. The SPME holder is used to guide the polymer into and out of the needle. The needle serves three purposes. First, to protect the SPME fiber coating when it is not used for sampling. Second, to provide the mechanism to position the fiber into a chromatographic injector interface as shown in Figure 1.1B. Third, to act as a diffusion path length for time-weighted average sampling (Chapter 5).

The heart of the sampling device is a fused silica rod coated with a polymer. The fused silica rod is approximately 100 μm in diameter. The rod can be coated with different

polymers, depending on which analytes require sampling. The polymer coated rod can be termed the "fiber coating". The length of the fiber coating is typically 1.0 cm with the polymer thickness ranging from 7 μm to 100 μm. A number of polymers and polymer aggregates make up the range of commercially available SPME fiber coatings. The most commonly used polymer is the 100 μm thick poly(dimethylsiloxane) (PDMS) fiber coating. This coating is a fixed liquid film and analytes partition to it via absorption, such as with a liquid-liquid extraction. By contrast, PDMS/divinylbenzene (PDMS/DVB) supports adsorptive analyte mass loading.

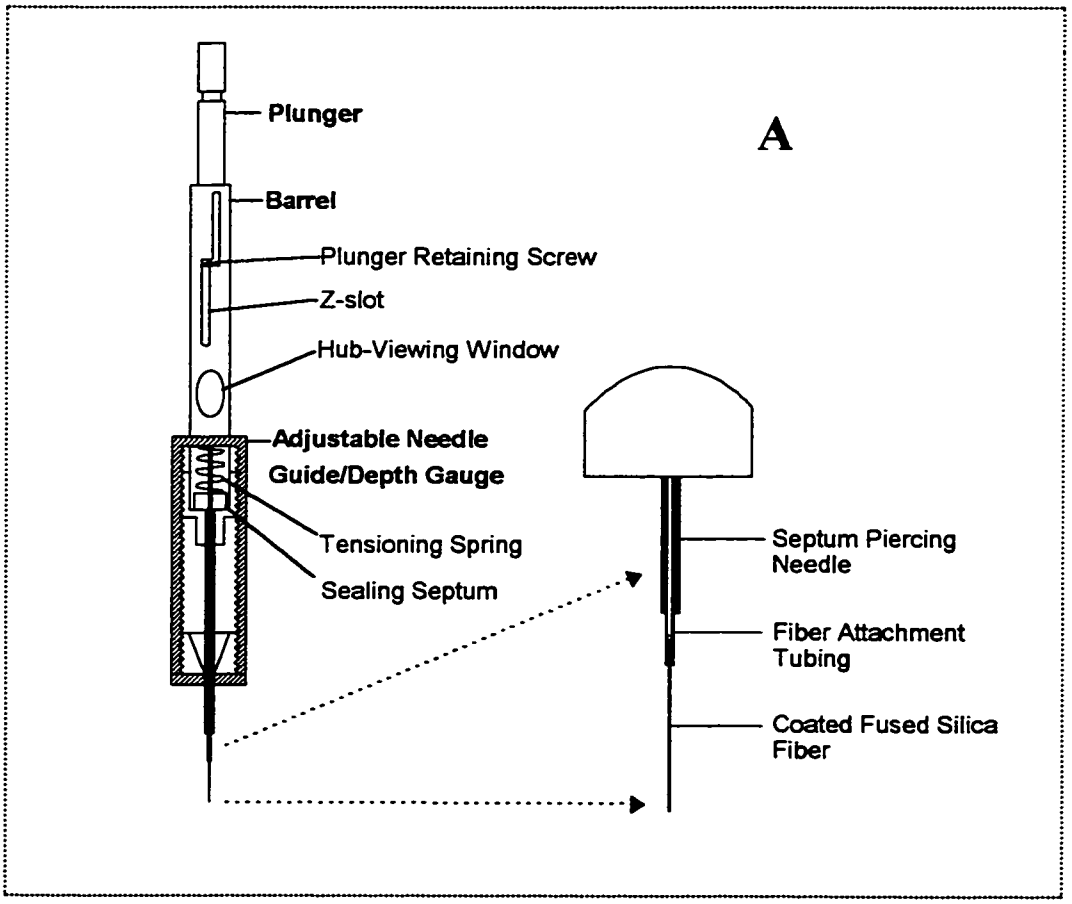

Figure 1.1A: The SPME device.

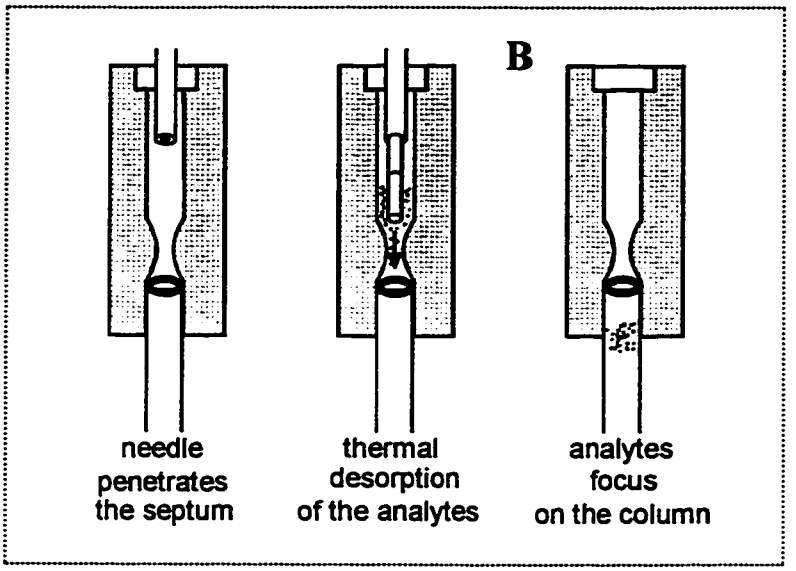

Figure 1.1B: The septum programmable injector (SPI) interface.

There are two modes, or fiber positions, in which air sampling with SPME can take place, regardless of fiber coating composition. The first mode is termed "exposed" (fiber) sampling while the second mode is termed "retracted" (fiber) sampling. The modes differ in the position of the fiber coating, during sampling, with respect to the fiber needle opening, i.e., outside of the needle opening (exposed) versus inside the needle opening (retracted). Each sampling mode posses an advantage, namely, the latter is used for long-term sampling, i.e., greater than 30 minutes, while the former is used for grab sampling, i.e., 5 minutes and less.

For exposed fiber sampling, the fiber (Figure 1.1A and Figure 1.2) is directly exposed to the test gas of interest. After a suitable exposure time, the fiber is retracted into the needle, then injected into a heated GC injector interface, such as that depicted in Figure 1.1B. The stages of injection, from left to right in Figure 1.1B, require placing the needle inside the GC narrow diameter injector liner, exposing the fiber coating to the hot carrier gas for a specific amount of time which provides for both a narrow analyte injection band and loading of analyte

at the head of the GC column. The airborne analytes partition to the fiber coating during the time the fiber is exposed to the test gas, but then reversibly desorb in the injector interface due to the 250 °C temperature as well as the high linear velocity of the carrier gas. With a narrow bore insert such as that used to desorb the SPME fiber coating, i.e., an insert with dimensions of slightly larger internal diameter than the SPME needle, a significant chromatographic advantage is achieved. The band of analyte injection is significantly narrower for volatile compounds compared to a liquid injection or whole gas injection without cryofocusing, the result being better chromatographic resolution, shorter analysis times, higher sample throughput but also no need for costly coolants (24).

Exposure of the SPME fiber coating to a test gas mixture is considered a two phase system. The first phase is the analyte gas mixture and the second phase is the SPME fiber coating, as depicted in Figure 1.2 for a static sampling bulb, i.e., no net gas movement in the bulb. If the 100 μm PDMS fiber coating is used, the system is considered to be liquid-gas. With enough exposure time between the two phases, the gas phase analytes will eventually reach equilibrium between the two phases. The ratio of analyte concentration in the fiber coating at equilibrium C_f^{∞} and the analyte concentration in the gas at equilibrium C_g^{∞} is the distribution constant, K_{fg} (Equation 1.1) which is how K_{fg} values are experimentally determined (see below),

$$K_{fg} = \frac{C_f^{\infty}}{C_g^{\infty}} \qquad \text{Equation 1.1}$$

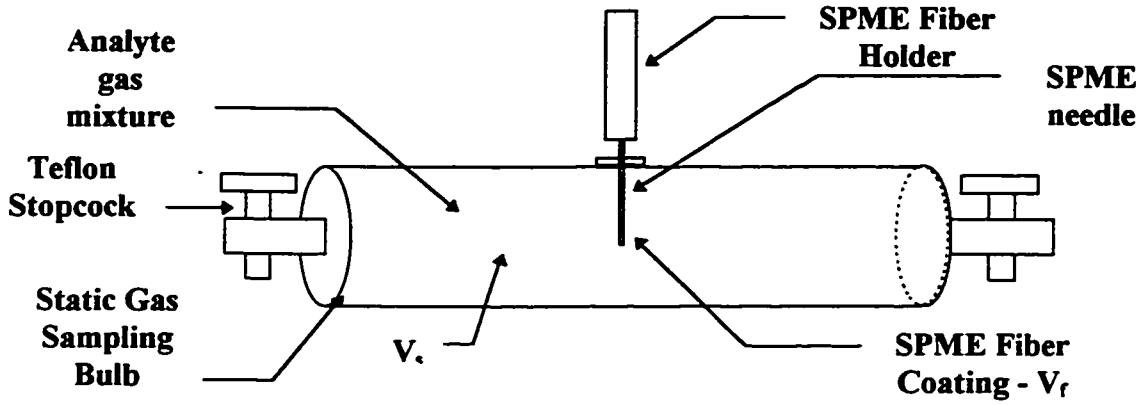

Figure 1.2: The two phase system for SPME exposed fiber exposure to a test gas contained in a glass sampling bulb for static sampling. Both V_S and V_f are the sample volume and fiber volume, respectively.

A mass balance expression can be written for the two phase system between PDMS and a gas phase analyte at equilibrium (Equation 1.2),

$$n_{Total} = C_0 V_g = C_f^{\infty} V_f + C_g^{\infty} V_g \qquad \text{Equation 1.2}$$

where n_{Total} is the total amount (mass) of analyte in the two phase system, C_O is the analyte concentration in the gas phase prior to its exposure to PDMS (mass/vol.), and V_f and V_g are volumes for the 100 μm PDMS fiber coating and the gas. When Equation 1.2 is combined with Equation 1.1 and rearranged, Equation 1.3 results,

$$n_f^{\infty} = \frac{K_{fg} V_f V_g C_O}{K_{fg} V_f + V_g} \qquad \text{Equation 1.3}$$

where n_f^{∞} is the amount of analyte mass loaded onto the PDMS fiber coating at equilibrium.

If $K_{fg} V_f + V_g \approx V_g$, (Consider if V_g=1 L, V_f=690x10^{-9} L, and K_{fg}=1,000, then

$K_{fg}V_f + V_g \approx V_g$), then Equation 1.3 can be expressed as Equation 1.4, which indicates

$$n_f^{\infty} \approx K_{fg} V_f C_O \qquad \text{Equation 1.4}$$

$$C_O = \frac{n_f^{\infty}}{V_f} \frac{1}{K_{fg}} \qquad \text{Equation 1.4a}$$

that Equation 1.4 can be used to determine the initial concentration of an analyte in the gas phase given knowledge of the amount of analyte loaded on the fiber at equilibrium and the V_f and K_{fg} (Equation 1.4a). The amount, n_f^{∞}, can be determined by analysis, the V_f is known for the 100 μm PDMS fiber coating (690 nL). The K_{fg} can be experimentally determined using Equation 1.1 after a correction is made for the reduction in C_g at equilibrium (Equation 1.2), which is shown with Equation 1.5a or Equation 1.5b after Equation 1.3 is rearranged to solve for K_{fg}.

$$K_{fg} = \frac{n_f^{\infty}}{V_f} \frac{V_g}{n_g^{\infty}} = \frac{\left(n_{Total} - n_g^{\infty}\right)}{V_f} \frac{V_g}{\left(n_{Total} - n_f^{\infty}\right)} \qquad \text{Equation 1.5a}$$

$$K_{fg} = \frac{n_f^{\infty} V_g}{V_f V_g C_O - n_f^{\infty} V_f} \qquad \text{Equation 1.5b}$$

where n_g^{∞} is the amount of analyte remaining in the gas after the system has reached equilibrium. Equations 1.5a or 1.5b are used when the K_{fg} is determined from a static gas sampling system, i.e., a finite amount of analyte in the gas phase, such as that system shown in Figure 1.2. In contrast, a dynamic gas sampling system, i.e., where the analyte amount in the gas phase is infinite compared to the amount which absorbs into the fiber coating, does not require correction for the amount of gas phase analyte remaining, as with Equations 1.5a and

1.5b. Instead, Equation 1.6 can be used without concern for analyte depletion from the gas.

$$K_{fg} = \frac{n_f^{\infty}}{V_f C_o} \qquad \text{Equation 1.6}$$

Also, a dynamic sampling system more closely resembles field sampling with SPME because the ambient, indoor, or occupational air has an infinite amount of analyte relative to the amount of analyte absorbed on the fiber at equilibrium. In contrast to static sampling, this system also eliminates the wall effects of the sampling vessel. A dynamic gas sampling system was developed for the research presented herein.

Preliminary work using 100 μm PDMS to sample airborne volatile organic hydrocarbons (VOCs) has been carried out (25), but this work focused predominantly on controlled static sampling conditions in gas sampling bulbs (Figure 1.2) and stainless steel canisters. The work indicated air sampling with SPME was feasible pending examination of a number of fundamental physical-chemical parameters.

As previously mentioned, a retracted fiber position relative to the needle opening provides another method to sample gas phase analytes. This type of sampling with SPME using PDMS and PDMS/DVB is useful for long-term air sampling, in contrast to short-term sampling, and is discussed in detail in Chapter 5. Both the PDMS and PDMS/DVB coating with on-fiber derivatization were used for exposed and retracted sampling.

1.2 Thesis Objectives

It is the overall objective of this thesis to develop SPME as a viable tool for air sampling by understanding the physical-chemical properties of analyte uptake onto different fiber coatings.

A dynamic standard gas sampling device was designed and built with the flexibility to control temperature and humidity. Efforts made in this regard allowed for detailed examination of a number of SPME sampling parameters which are discussed in the chapters to follow.

Chapters 2 and 3 focus on the use of PDMS for air sampling in the exposed fiber position. In these chapters, the analytes reach equilibrium with PDMS. Thermodynamic relationships revealed that the amount of analyte loaded at equilibrium is dependent on the analyte heat of vaporization and that the equilibrium can be accurately described from chromatographic retention indices. Also shown is a method to quantify total airborne hydrocarbons from gasoline vapour using the derived and proven relationships.

Chapter 4 deals with the use of PDMS/DVB as fiber coating to support on-fiber derivatization of formaldehyde (HCHO). The gas phase HCHO reacts with sorbed *o*-(2,3,4,5,6-pentafluorobenzyl)-hydroxylamine (PFBHA) to form a PFBHA-HCHO oxime which can be analyzed with conventional instrumentation. A first order rate constant developed for exposed fiber sampling proves to be quite useful for very fast grab sampling, i.e., less than 30 seconds.

Chapter 5 presents research from the use of SPME for gas sampling in the retracted fiber position. The fiber coatings used were 100 μm PDMS and PDMS/DVB for GC.

The ultimate usefulness of a sampling method is to test it under "real world" conditions. Chapter 6 details how the information in Chapters 2, 3, 4, and 5 were used in field sampling sessions; one using PDMS for airborne styrene and another using PDMS/DVB with PFBHA for formaldehyde.

Finally, Chapter 7 provides an overall summary of the scientific advancements from the compiled work presented herein.

1.3 References

1. Seinfeld, J. H., *Air Pollution, Physical and Chemical Funadamentals*, New York, McGraw-Hill, 1975

2. Otson, R. and Fellin, P., *Gaseous Pollutants: Characterization and Cycling*, John Wiley and Sons Inc., 1992, chapter 9 (Volatile Organics in the Indoor Environment: Sources and Occurrence)

3.. *The Industrial Environment - its Evaluation and Control*, U.S. Department of Health and Human Services, Public Health Service, Center for Disease Control, National Institute for Occupational Safety and Health, 1973

4. *Occupational Diseases*, U.S. Department of Health and Human Services, Public Health Service, Center for Disease Control, National Institute for Occupational Safety and Health, 1977

5. U.S.EPA Method T01 - *Method for the Determination of Volatile Organic Compounds in Ambient Air Using Tenax Adsorption and GCMS*, 1984

6 U.S.EPA Method T011 - *Determination of Volatile Organic Compounds in Ambient Air using SUMMA Passivated Canister Sampling and GC analysis*, 1988

7. McKone, T. E., Environ. Sci. Technol.,**21** (12) 1987 pp. 1194-1201

8. Batterman, S. and Peng, C., Am. Ind. Hyg. Assoc. J., **56** 1995 pp. 55-65

9. Bernstein, R.S., Stayner, L.T., Elliott, L.J., Kimbrough, R., Falk, H., and Blade, L., Am. Ind. Hyg. Assoc. J., **45** (11) 1984 pp. 778-785

10. *NIOSH Pocket Guide to Chemical Hazards*, U.S. Department of Health and Human Services, Public Health Service, Center for Disease Control, National Institute for Occupational Safety and Health, 1994

11. Casarett and Doull's Toxicology. *The Basic Science of Poisons*, 3rd edition, Macmillan Publishing Company, 1986

12. Davis, M. L. and Cornwell, D. A., *Introduction to Environmental Engineering*, McGraw-Hill, Inc. 2nd edition, 1991, Chapter 6

13. *American Conference of Governmental Industrial Hygienists*, TLVs and BEIs, 1996

14. *Occupational Safety and Health Act of 1970*, Title 84 U.S. Code

15. Adkins, J. E. and Norman, W. H., Anal. Chem., **65**, 1993, pp. 133R-155R

16. Underhill, D.W., Am. Ind. Hyg. Assoc. J., **44** (3) 1983 pp. 237-239

17. Occupational Health and Safety Products Laboratory, 3M Company, "Organic Vapor Analytical Method No. 4D", 1985

18. Yang, Y.Z., Fellin, P., and Otsen, R. *Sampling and Analysis of Airborne Pollutants*, Lewis Publishers, 1993, Chapter 5

19. Holdren, M.W., Smith, D.L., Smith, R.N., *Comparison of Ambient Air Sampling Techniques for Volatile Organic Compounds*, U.S.E.P.A., EPA/600/S4-85/067 1986

20. Giardino, N., Andelman, J B., Borrazzo, J. E., Davidson, C. I., JAPCA **38**, 1988, pp. 278-280

21. Winberry, W.T., Murphy, N.T., Riggan, R.M., EPA 600/4-89-107, 1988

22. Namiesnik, J., Gorecki, T., and Kozlowski, E., Sci. Total Env. **38** 1984 pp. 225-258

23. Pristas, R. Am. Ind. Hyg. Assoc. J., **52** (7) 1991 pp. 297-304

24. Pawliszyn, J. Solid Phase Microectraction - Theory and Practice, Wiley-VCH, 1997

25. Chai, M., Arthur, L., and Pawliszyn, J., Analyst, **118**, 1993, pp. 1501-1505

CHAPTER 2

SAMPLING HYDROCARBONS WITH SPME

2.1 Background

Airborne hydrocarbons are prevalent and as such there is concern for their point of origin, their distribution, and fate in the environment (1). The hydrocarbons also act as markers of air quality (1) and require appropriate sampling methods (2,3), some of which were discussed in Chapter 1. The hydrocarbons chosen for study herein include a range of volatile aliphatics and aromatics, and are summarized in Table 2.1. These hydrocarbons were selected to include compounds with a broad range of boiling points and vapour pressures. They were also chosen to represent compounds most familiar to environmental scientists concerned with hydrocarbons, e.g., terpenes, aliphatic hydrocarbons, mono aromatics and alkyl substituted aromatics. This chapter shows how SPME with the PDMS fiber coating is used as a sensitive air sampler for hydrocarbons (4,5).

Table 2.1: Summary of selected hydrocarbons.

Analyte	Formula / MW	B.P. (°C)	D_{AB} (cm^2/s)	V. P. (mm Hg)
Pentane (n-)	C_5H_{12} / 72	36	0.092	420
Hexane (n-)	C_6H_{14} / 86	69	0.084	124
Benzene	C_6H_6 / 78	80	0.090	75
Toluene	C_7H_8 / 92	111	0.082	21
Ethylbenzene	C_8H_{10} / 106	136	0.076	7
Xylene (*p*-)	C_8H_{10} / 106	138	0.076	9
Xylene (*o*-)	C_8H_{10} / 106	144	0.076	7
Pinene (α-)	$C_{10}H_{16}$ / 136	155	0.065	3
Mesitylene	C_9H_{12} / 120	165	0.071	2
Limonene (d-)	$C_{10}H_{16}$ / 136	176	0.065	1
Undecane (n-)	$C_{11}H_{24}$ / 156	195	0.061	<1

2.2 Theory

In air, the distribution constant, K_{fg}, (at a constant temperature) for an analyte between the PDMS fiber coating and air can be described by the Nernst distribution law shown in Equation 1.1 which describes the ratio of analyte concentrations in a closed two phase system when the amount of analyte is finite. Further, Equation 1.4 describes the case when the amount of gas phase analyte is infinite relative to the amount of analyte absorbed onto the PDMS fiber coating. Therefore, under the aforementioned conditions, Equation 1.4 can be written as Equation 2.1, i.e., infinite sample volume relative to the volume of the PDMS fiber coating (Equation 1.6),

$$K_{fg} = \frac{C_f^{\infty}}{C_g} = \frac{n_f^{\infty}}{V_f C_g} \qquad \text{Equation 2.1}$$

where the units for C_f and C_g can be μg/L, mg/m³, mol/L, etc.

Equation 2.1 can be rearranged to Equation 2.2 to provide an expression which can be used to determine unknown airborne analyte concentrations following the determination of n_f^{∞} and given the sampling temperature was the same as that at which K_{fg} was determined,

$$C_g = \frac{C_f^{\infty}}{K_{fg}} = \frac{n_f^{\infty}}{K_{fg} V_f} \qquad \text{Equation 2.2}$$

The main limitation to Equation 2.2 is that the sampling temperature must be the same as the temperature at which K_{fg} was determined. This poses serious limitations to the use of PDMS as a sorbent for air sampling. Under ideal laboratory conditions, acquiring K_{fg} for PDMS and sampling at the same temperature is simple to achieve; however, there is no guarantee that field sampling will occur at the same temperature as the calibration temperature. An understanding of the dependence of K_{fg} on temperature would alleviate this problem. This relationship can be theoretically determined, allowing the empirically determined K_{fg} to be used at any temperature.

For the dynamic process of analyte uptake on the fiber it must first be assumed that C_f does not change with time, i.e., the two phase system is at steady state where $dC_f/dt = 0$. The mass uptake of the analyte on the fiber in the system can be related by the analyte's partial pressure using Raoult's law for a non-ideal solution as shown in Equation 2.3.

$$p = \gamma_i' \times x_i \times p^{\bullet} \qquad \text{Equation 2.3}$$

where p is the partial pressure of the analyte a the gas/polymer interface, p° is the pure analyte

vapor pressure at a known temperature, x_i is the mole fraction of the analyte in the fiber and γ_i' is the analyte activity coefficient in the fiber. It is more convenient to describe the analyte concentration instead of mole fraction and so Equation 2.4(a) shows the constant A which is used to convert the mole fraction to concentration and Equation 2.4(b) shows a new activity coefficient which includes the constant A which is defined in Equation 2.4(c),

$$\gamma_i' \times x_i = \gamma_i' \times A \times C_f \quad \text{(a)}$$
$$\gamma_i' \times A \times C_f = \gamma_i \times C_f \quad \text{(b)} \qquad \text{Equation 2.4}$$
$$A = \frac{x_i}{C_f} \quad \text{(c)}$$

where γ_i is the new activity coefficient containing A. Substituting Equation 2.4(b) into Equation 2.3 we get:

$$p = \gamma_i \times C_f \times p^o \qquad \text{Equation 2.5}$$

The term for pressure, p, in Equation 2.5 can be described in terms of the ideal gas law, rearranging for p and shown in Equation 2.6,

$$p = \frac{n}{V} \times RT = C_g \times RT \qquad \text{Equation 2.6}$$

where n are the number of moles, V is the volume occupied, R is the universal gas constant, and T is the temperature. Equation 2.6 can be substituted into Equation 2.5 for p yielding Equation 2.7,

$$C_g \times RT = \gamma_i \times C_f \times p^o \qquad \text{Equation 2.7}$$

and upon rearrangement yields Equation 2.8, from which we can see the Nernst distribution coefficient, K_{fg}, (as in Equation 2.1),

$$\frac{RT}{\gamma_i \times p^o} = \frac{C_f}{C_g} = K_{fg} \qquad \text{Equation 2.8}$$

$$p^o = \frac{C_g \times RT}{\gamma_i \times C_f} \qquad \text{Equation 2.9}$$

The Clausius-Clapeyron equation, shown in Equation 2.10, is combined with Equation 2.9 with the result shown in Equation 2.11,

$$p^o = p^* \times e^{-\frac{\Delta H^v}{R}\left(\frac{1}{T} - \frac{1}{T^*}\right)} \qquad \text{Equation 2.10}$$

where p* is the analyte vapor pressure at a known temperature T* for a pure solute, ΔH^v is the heat of vaporization of the pure solute, and T is the temperature of interest.

$$\frac{C_g \times RT}{\gamma_i \times C_f} = p^* \times e^{-\frac{\Delta H^v}{R}\left(\frac{1}{T} - \frac{1}{T^*}\right)} \qquad \text{Equation 2.11}$$

By taking the natural logarithm of Equation 2.11 we can arrive at Equation 2.12 then rearranged to Equation 2.13 which yields Equation 2.14,

$$\ln\left(\frac{C_g \times RT}{p^* \times \gamma_i \times C_f}\right) = -\frac{\Delta H^v}{R}\left(\frac{1}{T} - \frac{1}{T^*}\right) \qquad \text{Equation 2.12}$$

$$\ln\left(\frac{p^* \times \gamma_i \times C_f}{C_g \times RT}\right) = \frac{\Delta H^v}{R}\left(\frac{1}{T} - \frac{1}{T^*}\right) \qquad \text{Equation 2.13}$$

$$\ln\left(\frac{K_{fg} \times p^* \times \gamma_i}{RT}\right) = \frac{\Delta H^v}{R}\left(\frac{1}{T} - \frac{1}{T^*}\right) \qquad \text{Equation 2.14}$$

Equation 2.17 can be arrived at from Equation 2.14 by converting the natural logarithm to base 10,.

$$\log_{10}\left(\frac{K_{fg}\times p^{\circ}\times \gamma_i}{RT}\right)=\frac{\Delta H^{v}}{2.303R}\left(\frac{1}{T}-\frac{1}{T^{\circ}}\right) \qquad \text{Equation 2.15}$$

$$\log_{10} K_{fg}+\log\left(\frac{p^{\circ}\times \gamma_i}{RT}\right)=\frac{\Delta H^{v}}{2.303RT}-\frac{\Delta H^{v}}{2.303RT^{\circ}} \qquad \text{Equation 2.16}$$

$$\log_{10} K_{fg}=\frac{\Delta H^{v}}{2.303RT}+\left(\log_{10}\left(\frac{RT}{\gamma_i\times p^{\circ}}\right)-\frac{\Delta H^{v}}{2.303RT^{\circ}}\right) \qquad \text{Equation 2.17}$$

Equation 2.17 shows the final form of the expression linearly relating $\log_{10}K_{fg}$ and T^{-1} as in the expression y = mx + b; it is emphasized that from Equation 2.17 the y-intercept (b) has a small dependence on temperature, but a careful examination reveals the dependence is <5% of that for the slope. Therefore, there is little error associated in ignoring the dependence of the y-intercept on temperature. From this we can simplify Equation 2.17 into Equation 2.18,

$$\log K_{fg}=a\times\left(\frac{1}{T}\right)+b \qquad \text{Equation 2.18}$$

where $a=\frac{\Delta H^{v}}{2.303R}$, $b=\left[\log_{10}\left(\frac{RT}{\gamma_i\times p^{\circ}}\right)-\frac{\Delta H^{v}}{2.303RT^{\circ}}\right]$ and $x=\frac{1}{T}$. Equation 2.18 can be rearranged and combined with Equation 2.2 yielding Equation 2.19,

$$C_g=n_f\times 10^{-\left(\frac{a}{T}+b\right)}\times V_f^{-1} \qquad \text{Equation 2.19}$$

where C_g is in mg/m³, the V_f is the fiber volume expressed in m³ (approximately 690 x 10^{-12} m³ for the 100 μm thick fiber and 140 x 10^{-12} m³ for the 30 μm thick fiber) and T is in Kelvin. Equation 2.19 provides a means to determine the airborne concentration of an analyte given the constants *a* and *b*, as well as the sampling temperature (T). Careful consideration should be made to consider fiber lengths since it is possible to overestimate or underestimate the

actual fiber volume based on the assumption that fiber length is 1.00 cm, as will be discussed in the section on inter-fiber reproducibility.

It is convenient to express the concentration of an airborne analyte in parts per million (volume/volume) (ppm_v) since it includes the molar volume and sample temperature (Equation 2.20). In this way, understanding the concentration does not require knowledge of sampling temperature and pressure; however, there are many different opinions as to the best way airborne analyte concentrations are expressed, with the two most common shown here. One of the other methods is mol/L in air, or typically, pmol/L to nmol/L.

$$ppm_{v\,(air)} = n_f \times \frac{R}{MW \times P \times V_f} \times \left[\frac{T}{10^{\left(\frac{a}{T} + b\right)}} \right] \qquad \text{Equation 2.20}$$

The symbol α can be used to replace the term $\frac{R}{MW \times P \times V_f}$, yielding a constant for a given analyte and fiber volume and having no dependence on temperature, the result shown in Equation 2.21,

$$ppm_{v\,(air)} = n_f \times \alpha \times \left[\frac{T}{10^{\left(\frac{a}{T} + b\right)}} \right] \qquad \text{Equation 2.21}$$

It is possible to provide data relating the temperature and a and b values for a specific analyte with the expression $\left[\frac{T}{10^{\left(\frac{a}{T} + b\right)}} \right]$ and define this as β as shown in Equation 2.22 which shows the new expression which can be used to determine the airborne concentration of an analyte at any temperature,

$$ppm_{v\,(air)} = n_f \times \alpha \times \beta \qquad \text{Equation 2.22}$$

Equation 2.22 requires the analyst to determine the mass of analyte loaded on the 100μm PDMS fiber, then look up the appropriate α and β values for the analyte of interest at a specific temperature. It is also possible to allow $\beta = \frac{T}{K_{fg}}$ when the analyte's K_{fg} was determined at the actual sampling temperature.

2.3 Experimental

2.3.1 Chemicals and Materials

2.3.1.a Chemicals

Benzene, toluene, ethylbenzene, *p*-xylene, *o*-xylene, 1,3,5-trimethylbenzene (mesitylene), α-pinene, d-limonene, n-pentane, n-hexane, and n-undecane were all purchased from Sigma-Aldrich (Mississauga, Ontario). Carbon disulphide (CS_2) was purchased from BDH (Toronto, Ontario). The CS_2 was used to chemically desorb analytes from charcoal tube air samples. After a purity check, all chemicals were used as purchased.

2.3.1.b Materials

Ultra high purity nitrogen, helium, and hydrogen gases for flame ionization detection and compressed air for standard gas generation as well as a two-stage regulator for the compressed air were purchased from Praxair (Waterloo, Ontario). Air for the flame ionization detector was generated from an air generator purchased from Balston. Very fine metering valves, 1/8 and 1/16" and adapters and tees for 1/8" tubing were purchased from Swagelock (Ontario). The syringe pump used to deliver the analyte mix for standard gas generation was purchased from Sage Syringe Instruments. All SPME equipment were purchased from Supelco (Supelco, Canada) as well as all syringes, impinger, charcoal scrubber, air diffusers,

silica gel, bubble flow meters, columns, passive badges, charcoal tubes and vials.

2.3.2 Preparation of analyte mixture

A standard mixture of benzene, toluene, ethylbenzene, *p*-xylene, *o*-xylene, mesitylene, α-pinene, d-limonene, n-pentane, n-hexane, and n-undecane was prepared by adding 0.75 g of each analyte, starting with n-undecane, into a Teflon capped flask. The mixture was then thoroughly mixed by flask inversion and then transferred to each of six 1.8 mL Teflon capped vials leaving no headspace. This mixture, which was made up of 9.1 % w/w of each analyte, was used in the syringe pump delivery system for generating the standard gas.

2.3.3 Standard gas generating device

A number of standard gas generation methods were examined prior to a commitment to one type. There are a considerable number of different methods to generate standard gas mixtures, even as early as 1957 (6,7). A syringe pump delivery system was decided on, and is shown as constructed in Figure 2.1. All copper and stainless steel tubing connecting the compressed air to the standard gas generating device was thoroughly cleaned with solvent, allowed to dry, then flamed. All air was filtered over a bed of a charcoal. Air flow rates into the mixing chamber were controlled with a very fine metering valve maintained at 20 p.s.i. head pressure. The 20 L chamber was lined with two consecutive layers of 1/16" Teflon, including the inside base and covered with a 1/8" thick piece of Teflon which was covered with 1/4" thick aluminum plate and bolted to an aluminum base, thereby squeezing the top layer of Teflon to the lip of the container. Pressure tests with helium in the chamber at 10 p.s.i. and a leak detector proved the chamber was gas tight. The outside of the chamber was uniformly covered in a coil of 3/8" copper tubing through which water was flowing from a temperature controllable water bath thus providing a constant

temperature to the chamber. All chamber temperatures were measured inside the chamber with a NIST calibrated thermocouple.

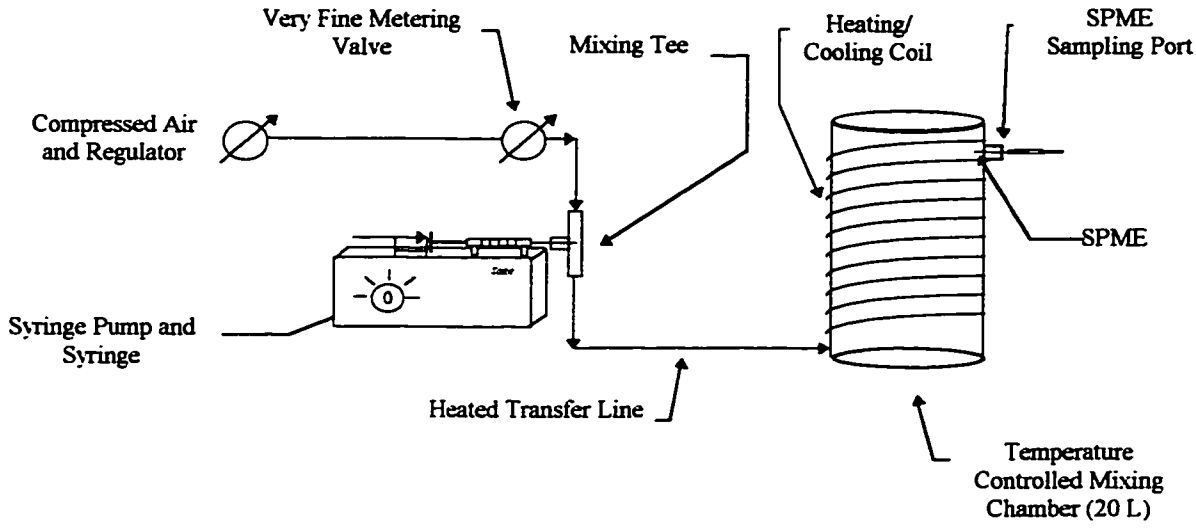

Figure 2.1: Schematic representation of the standard gas generating device.

The chamber was allowed to reach steady-state after a minimum of ten volume changes (aerodynamic residence times) after each temperature change or alteration in gas concentration. The mixing port and air line to the chamber were heated to 323 K with heat tape and controlled with a variable voltage controller. For humidification, the air was diverted through two consecutive water immersed diffusers inside sealed containers at ambient temperature.

Relative humidity (RH) in the chamber was determined by drawing air at a known flow rate directly from inside the chamber to a impinger containing dry indicating silica gel which was weighed before and after the air sample. The airborne water concentration was then

calculated and expressed in mole/L. The corresponding pressure of that concentration of water at 1 atm was calculated using the ideal gas law and this pressure was then taken as a percentage of the equilibrium vapor pressure of water at that temperature (14) resulting in % RH.

A 500 μL Hamilton gas-tight syringe was used in the syringe pump to deliver the analyte mixture. The syringe pump was calibrated for analyte delivery to 4.4 mg/hr of the analyte mixture into the mixing tee. Calibration was carried out by delivering the analyte mixture into a pre-weighed tightly capped Teflon lined vial for a known period of time, then weighed again after a specific period of time. Typical time periods for testing ranged from 1 hour to 4 hours. In addition, the balance was checked for calibration using standard weights ranging from 1 mg to 10 g. With a dilution gas air flow rate of 200mL/min, the expected *total* hydrocarbon gas concentration was 0.37 mg/L at normal temperature and pressure (NTP) and approximately 34 μg/L at NTP for an *individual* analyte. Equation 2.23 shows how the injected liquid analyte mixture forms the gas mixture of theoretical analyte concentration at the specified sampling temperature,

$$C_g\left(\frac{\mu g}{L}\right)_{(T)} = \left[\frac{\left(\mu g/hr\right)_{(mix)}}{\left(60\ \min/hr\right)} \times \frac{1}{\left(L/\min\right)_g} \times \left(\frac{\%\ Analyte}{Total}\right)\right] \qquad \text{Equation 2.23}$$

In addition, from Equation 2.23, the concentration can be converted to parts per million by volume with the molar gas volume at the specified temperature and pressure as well as the analyte molecular weight for benzene, as shown with Equation 2.24

$$C_{g(ppmv)}\left(\frac{\mu L}{L}\right) = C_{g(\mu g/L)}\left(\frac{mg}{L} \times \frac{10^3 \mu g}{mg}\right)\left(\frac{0.0821 L \times atm \times mol^{-1} \times K^{-1} \times 298K}{1 atm \times 78_g \times mol^{-1}}\right) \qquad \text{Equation 2.24}$$

The individual analyte concentration at NTP was confirmed using a standard air sampling technique. This technique is described in detail below.

2.3.4 Validation of standard gas mixture analyte concentrations

Hydrocarbons in air concentrations from the standard gas generating device at NTP were verified following National Institute for Occupational Safety and Health (NIOSH) methods 1500 and 1501 for the determination of airborne hydrocarbons. These methods require a mass flow controlled air sampling pump equipped with a very fine metering valve to draw air through small charcoal tubes at a known flow rate, in this case, 50 mL/min, which was calibrated with a bubble flow meter. The analytes were chemically desorbed from the charcoal with 1.0 mL CS_2 in Teflon capped 4 mL vials. All air samples were collected in quadruplicate and repeated after a period of 3 days in quadruplicate for confirmation. The method also requires a five-point calibration curve, with blanks, which was carried out as follows. First, 10 μL of each analyte were added to 890 μL CS_2 in a new Teflon capped 1.8 mL vial. The syringes used to transfer the individual analytes were flushed 10 times with each of three CS_2 washes, labeled 1 to 3. The CS_2 1 wash was used to clean the syringe first, then number 2 then number 3. Confirmation that this method did not result in cross contamination was verified using n-undecane as the test analyte. This was done by drawing 10 μL of n-undecane into the 10 μL syringe, then washing as indicated, followed by injection into the GC of the last 1 μL CS_2 from the last wash. The results indicated there was no observable remainder of n-undecane in the syringe. This procedure was also used with the 100 μL syringe to serially dilute 1:10 the first mixture made, until four dilutions were achieved. Finally, the GC calibration curves were developed for each of these compounds using the SPI injector interface maintained at 45 °C during the delivery of 1.0 μL of each standard mixture.

2.3.5 SPME with PDMS Sampling of Standard Gas Mixtures

Unless otherwise specified, all SPME sampling took place inside the chamber at 298 K. Each fiber was used to sample and inject the standard gases at least five times for repeatability studies, new chamber temperatures or relative humidities whereas at least nine samples were acquired for each new air concentration.

A standard gas concentration of 34 μg/L at 298 K was chosen for both intra-fiber reproducibility and inter-fiber comparisons. Ten repeats were carried out for intra-fiber reproducibility. The inter-fiber comparison was carried out with four different fibers selected from four different lots spanning six months of production. Three of the four fibers were analyzed five times and the fourth was analyzed six times. Each fiber was consecutively used to sample the standard gas mixture. The study of fiber geometry was carried out on thirteen different fibers from a number of production lots spanning 5 months of production.

Run to run carryover for one fiber was established by exposing the fiber for a given time to the standard gas then desorbing the analytes in the injector port as described. The fiber was then retracted while still in the injector then exposed for another run. Other fiber blanks included leaving the fiber retracted while covered with a new and clean silicone septum.

Appropriate fiber desorption times were established by desorbing the fibers for less than 1 minute at the injector temperature, then withdrawing the fiber from the injector and placing a silicone septum over the end, then injecting the fiber again. A 2 minute desorption time proved to be sufficient for more than 99 % removal of analytes from the fiber with an injector temperature of 225 °C.

2.3.6 Linearity and Detection Limits with PDMS

The standard gas mixture concentration was increased and decreased in the chamber by decreasing the flow rate and increasing the dilution gas air flow rate into the mixing tee, respectively. The concentration range studied was from 20 ng/L to 1,600 µg/L. Detection limits were established by analyzing eight repeats of blank fiber injections and multiplying by three the noise for the respective retention times.

2.3.7 Instrumentation and Methods for SPME and Liquid Injections

All experiments used a Varian Star computer controlled Varian 3400 *CX* gas chromatograph equipped with a carbon dioxide cooled Septum-equipped Programmable injector (SPI) and a 0.8 mm i.d. SPI insert coupled to a SPB-5 column (30m, 0.25 mm i.d., 1.0 µm film thickness) which was coupled to a flame ionization detector (FID). The injector was maintained at 225°C for SPME injections but 45°C for liquid injections which was then ramped to 225°C at 30°C/min. The column temperature program for SPME and liquid injections was 45°C for 1.50 min., 30°C/min to 175°C held for 2.67 min., then 30°C/min. to 240°C held for 2.0 min. Carrier gas velocity was 40 cm/s at 45°C for both SPME and liquid injections. The detector gas flow rates were set to 300 mL/min. for air, 30 mL/min. for nitrogen and 30 mL/min. for hydrogen and were all measured daily.

The instrument was checked daily for calibration using a liquid mid point calibration standard and any deviations in area counts greater than 15 % required re-injection of that standard and if still greater then 15 % the instrument was re-calibrated with a five point calibration. In addition, quality of peak shapes, resolution and retention times were carefully monitored to ensure all chromatography was within specification.

2.4 Results and Discussion

2.4.1 Validation of the standard gas generation device

Figure 2.2(A) shows a typical chromatogram obtained for the charcoal tube samples of the standard gas mixture containing the 11 analytes under study. These data were used to validate the concentration of the individual analytes in the gas mixture. Figure 2.2B shows the corresponding SPME with PDMS extraction of the same gas mixture. Peak assignments were confirmed with gas chromatography-mass spectrometry and single compound injection with the GC/FID. The chromatogram from Figure 2.2(B) shows an interesting trend with the analyte peak areas with increasing retention time. Recall that each analyte is present at approximately equal gas phase concentration, i.e., each are at 34 μg/L at 25 °C. This is reflected in Figure 2.2(A) in that almost all of the peaks had approximately equal areas. On the other hand, Figure 2.2(B) shows increasing peak areas with retention time, even though the system was at steady-state. This observation is thoroughly discussed in Chapter 3 where it is shown that K_{fg} increases with increasing carbon number, which can be used to accurately estimate K_{fg} from chromatographic retention indices.

Table 2.2 Column A shows the actual gas concentrations of each analyte. The theoretical gas concentration for each analyte was 34 μg/L. The data indicate there is excellent agreement between the actual standard gas concentrations and the expected analyte concentrations at 298 K (recall Equation 2.23). In addition, the standard gas mixture showed consistent day-to-day analyte concentrations, which indicated the generator was validated.

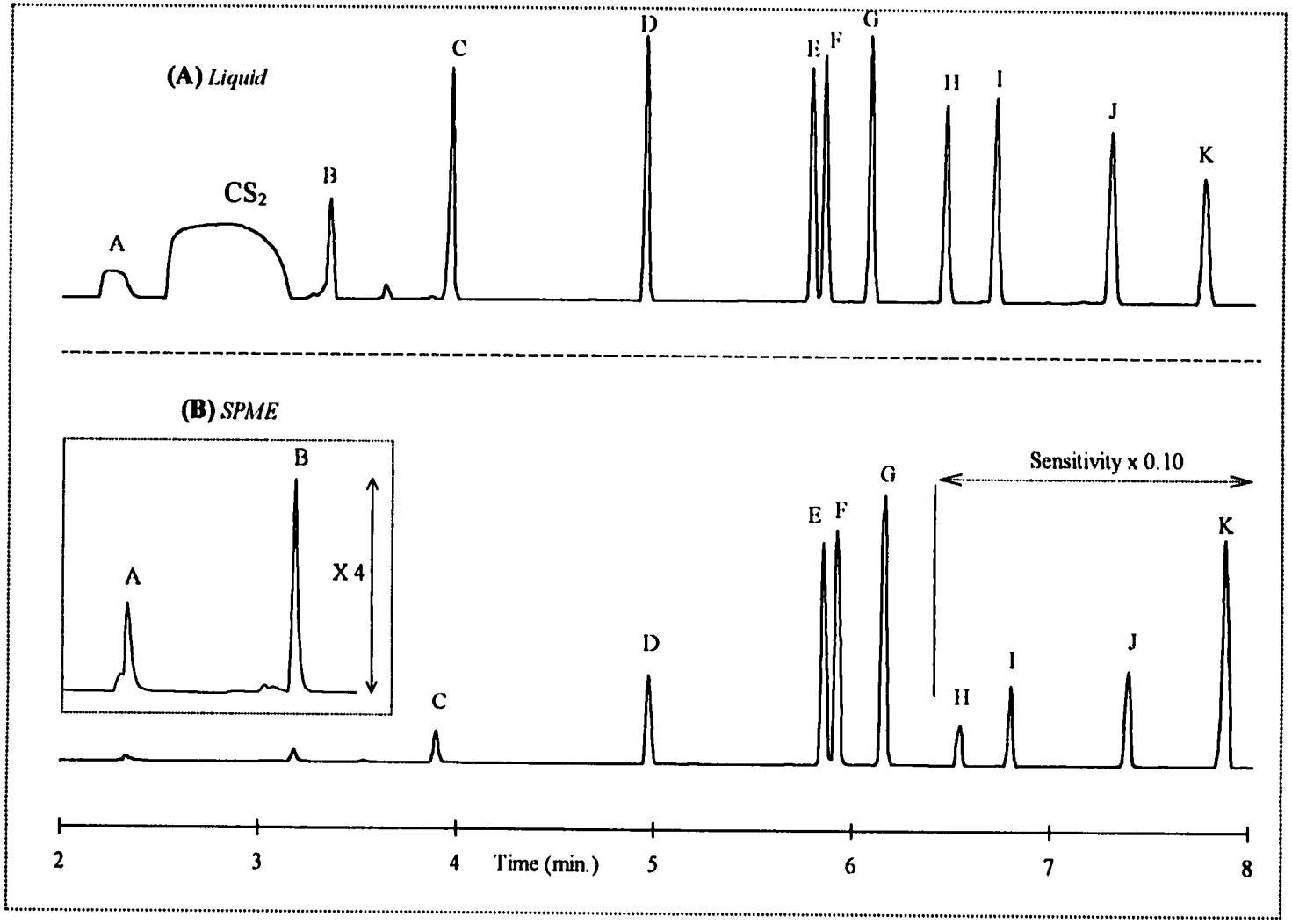

Figure 2.2: (A) Chromatograms of charcoal tube and (B) PDMS SPME extraction of the standard gas (34 μg/L @ 298 K) from the standard gas generating device. Peak identification, A) n-pentane, B) n-hexane, C) benzene, D) toluene, E) ethylbenzene, F) *p*-xylene, G) *o*-xylene, H) α-pinene, I) 1,3,5-trimethylbenzene, J) d-limonene, K) n-undecane.

Table 2.2: **Column A**: Actual analyte concentrations from the standard gas generator. The theoretical concentration was 34 µg/L at NTP.

Column B: Summary of times to reach equilibrium for 100 µm PDMS.

Column C: Summary of K_{fg} for 30 µm and 100 µm PDMS using the standard gas mixture (34 µg/L @ 298 K).

Column D: Summary of PDMS intra-fiber reproducibility for n=10 repeats (34 µg/L @ 298 K), for two different days. %RSD = relative standard deviation.

Column E: Detection limits and r^2 for 100 µm PDMS for various standard gas concentrations at 298 K. The LOD is based on three times the noise for that peak for n=8 repeats of fiber blank injections.

Analyte	A	B	C		D		E	
	µg/L	Eq (sec)	K_{fg} (30 µm PDMS)	K_{fg} (100 µm PDMS)	% RSD day 1	% RSD day 2	LOD, µg/L (NTP)	r^2
Pentane (n-)	35.7	15	100	95	6.1%	8.5%	3.3	0.99999
Hexane (n-)	36.7	45	170	150	4.7%	2.8%	1.6	0.99999
Benzene	36.8	60	260	300	2.0%	2.2%	0.72	0.99999
Toluene	34.3	60	710	880	5.1%	2.3%	0.25	0.99999
Ethylbenzene	34.2	60	2,000	2,100	2.0%	2.2%	0.096	0.99999
Xylene (*p*-)	34.2	90	2,300	2,400	2.1%	2.4%	0.090	0.99997
Xylene (*o*-)	32.9	120	3,100	3,100	2.7%	2.5%	0.072	0.99997
Pinene (α-)	33.9	160	4,300	4,500	2.4%	2.2%	0.054	0.99999
Mesitylene	33.8	150	5,900	5,800	2.2%	2.4%	0.036	0.99998
Limonene (d-)	34.3	300	10,300	10,300	2.4%	2.7%	0.024	0.99999
Undecane (n-)	34.1	450	25,000	25,000	2.7%	3.5%	0.012	0.99999

2.4.1.a Temperature and Pressure Corrections

Equation 2.25 was used to compensate for chamber temperature and pressure changes.

$$C_{g(any\ T,P)} = C_{g(@298K,1atm)}\left(\frac{T^*}{T_X}\right)\left(\frac{P_X}{P^*}\right) \qquad \text{Equation 2.25}$$

where T* and P* were the temperature and pressure at which the standard gas was calibrated and T_X and P_X were the temperature and pressure at which knowledge of the new C_g is required. This expression was used to estimate the gas concentration for a given temperature and pressure range provided the gas concentration was established at a known T* and P*. For example, from Equation 2.25, a standard gas concentration of 34 µg/L at 298 K is reduced by approximately 4% at 311 K and increased by approximately 3% at 290 K. These concentration differences were important to calibrate the standard gas generating device at different temperatures and pressures. This was specifically important to accurately describe the relationship between K_{fg} and temperature (see below).

2.4.2 Absorption time profiles for PDMS at standard gas concentrations

Absorption time profile studies were carried out to determine equilibration times for each analyte at 34 µg/L at NTP with the 100 µm PDMS. The equilibration time is generally defined as the time in the profile at which no further increases in the mass uptake are observed. Figure 2.3 shows representative absorption time profiles for a few of the test analytes and Table 2.2 Column B summarizes the equilibration times for each analyte. In comparison to previous work with similar compounds studied under static sampling, these results indicate that the time to reach equilibrium is shorter with dynamic sampling (9,11). This is logical because in both static and dynamic sampling, the time to reach equilibrium is

limited by the analyte rate of diffusion in the gas phase and the mass transport of analyte across the gas/fiber boundary layer . In a static sampling system, with the two phenomenon combined one observes an increased time to reach equilibrium in contrast to dynamic sampling. This is especially true since the diffusion layer thickness of the latter will be smaller due to aerodynamic convection. Table 2.1 shows the diffusion constants (cm^2/s) for the studied hydrocarbons. In dynamic sampling, a fresh source of analyte is constantly delivered to the fiber thus minimizing the dependence on analyte diffusion in air. Only those analytes with small diffusion coefficients and large affinities for the PDMS fiber coating are subject to longer equilibration times as evidenced by the equilibration time for n-undecane, while compounds such as n-pentane and n-hexane have short equilibration times.

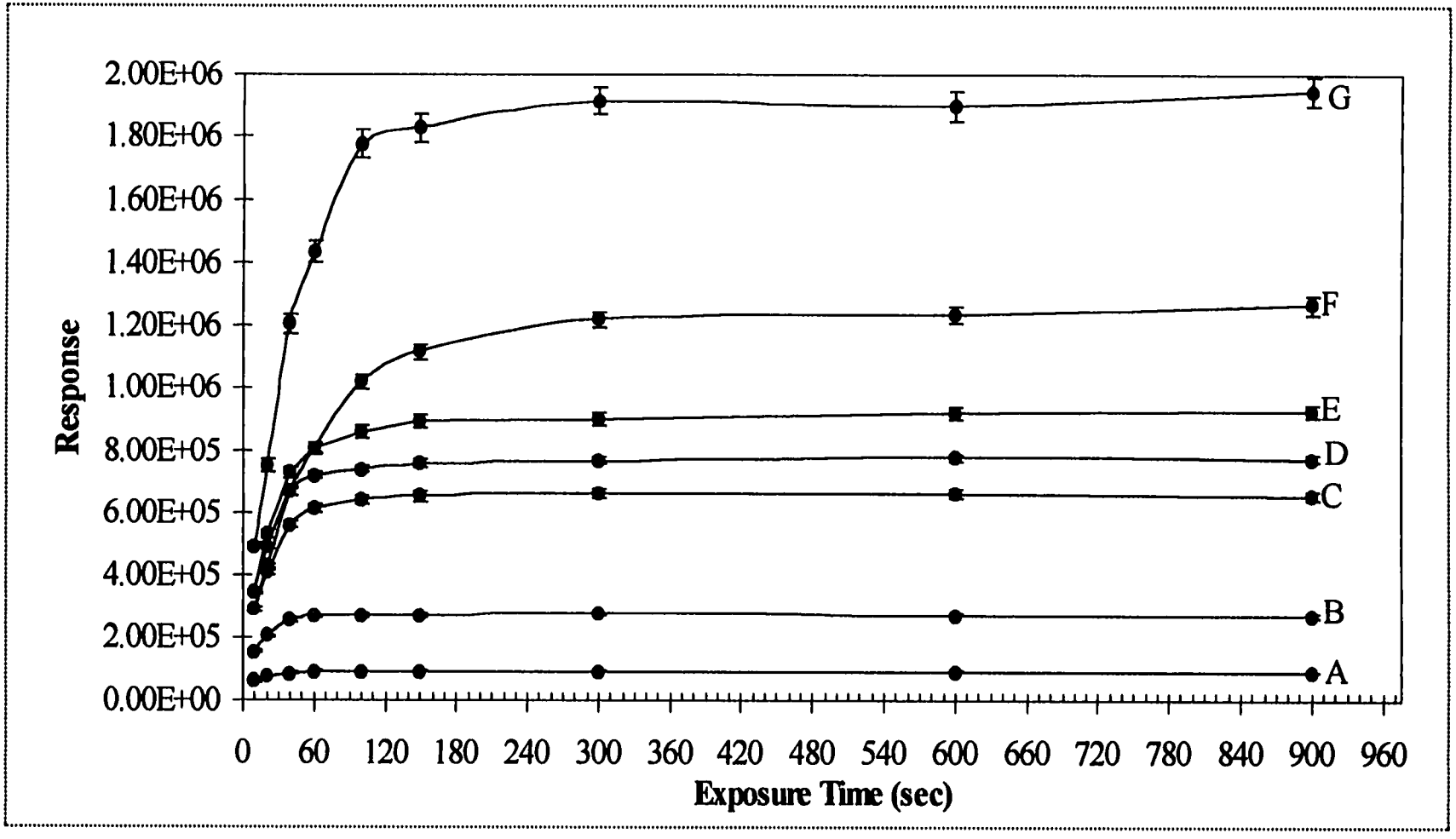

Figure 2.3: Representative absorption time profiles using PDMS SPME extraction of standard gas (34 μg/L @ 298 K) for A) benzene, B) toluene, C) ethylbenzene, D) p-xylene, E) o-xylene F) α-pinene and G) 1,3,5-trimethylbenzene (mesitylene). The lines connecting the points in no way represent a mathematical relationship.

2.4.3 Determination of analyte K_{fg} values using the standard gas generating device

Table 2.2 Column C summarizes the K_{fg} values obtained for each of the eleven analytes using both the 30 μm and 100 μm PDMS fiber, for a ten minute sampling time and under the conditions described in the previous section. The K_{fg} values were calculated using Equation 2.1 after determining the amount of absorbed analyte. The data indicate that there are some differences between K_{fg} values obtained with either fiber coating thickness but that the differences are negligible (this was not statistically validated). Recall that the K_{fg} provides a measure for the distribution of an analyte from air to PDMS as shown in Equations 1.1 and 2.1. The K_{fg} values provide a simple method to determine unknown concentrations of target analytes in air. A indicated in the Theory (Equation 2.18), K_{fg} has a temperature dependence which requires correction if the gas sampling temperature is different from the temperature at which K_{fg} was determined.

2.4.4 K_{fg} as a function of temperature

Figure 2.4 demonstrates representative curves for the linear relationship between $\log(K_{fg})$ for each analyte with PDMS and the inverse of temperature (1/K). Table 2.3 summarizes the slope (a) and y-intercept (b) values, from Equation 2.18 ($\log K_{fg} = a \times \left(\frac{1}{T}\right) + b$) and the square of the correlation coefficient (r^2) for the curves for each of the analytes studied. In addition, Table 2.3 shows the calculated a (a^L) values based on literature ΔH^v data (14) for each of the eleven analytes studied and compares the experimentally observed a values. The data indicate there is very good agreement between the calculated a^L values using literature ΔH^v and the observed a values determined using Equation 2.8. This indicates that it is possible to use literature ΔH^v to determine a values. The b values

can be determined with Equation 2.18 by determining K_{fg} for the target analyte at a specific temperature and calculating *a* with literature ΔH^v.

In order to substantiate the argument that Equation 2.18 can be used to predict K_{fg} values at different temperatures, the K_{fg} values were determined for each of the eleven analytes at 296 K, a temperature which was not used to establish the relationship between K_{fg} and temperature. The data were then compared to the estimated K_{fg} value using Equation 2.18 and are summarized in Table 2.4. The data indicate that there is good agreement between the estimated K_{fg} and actual K_{fg}.

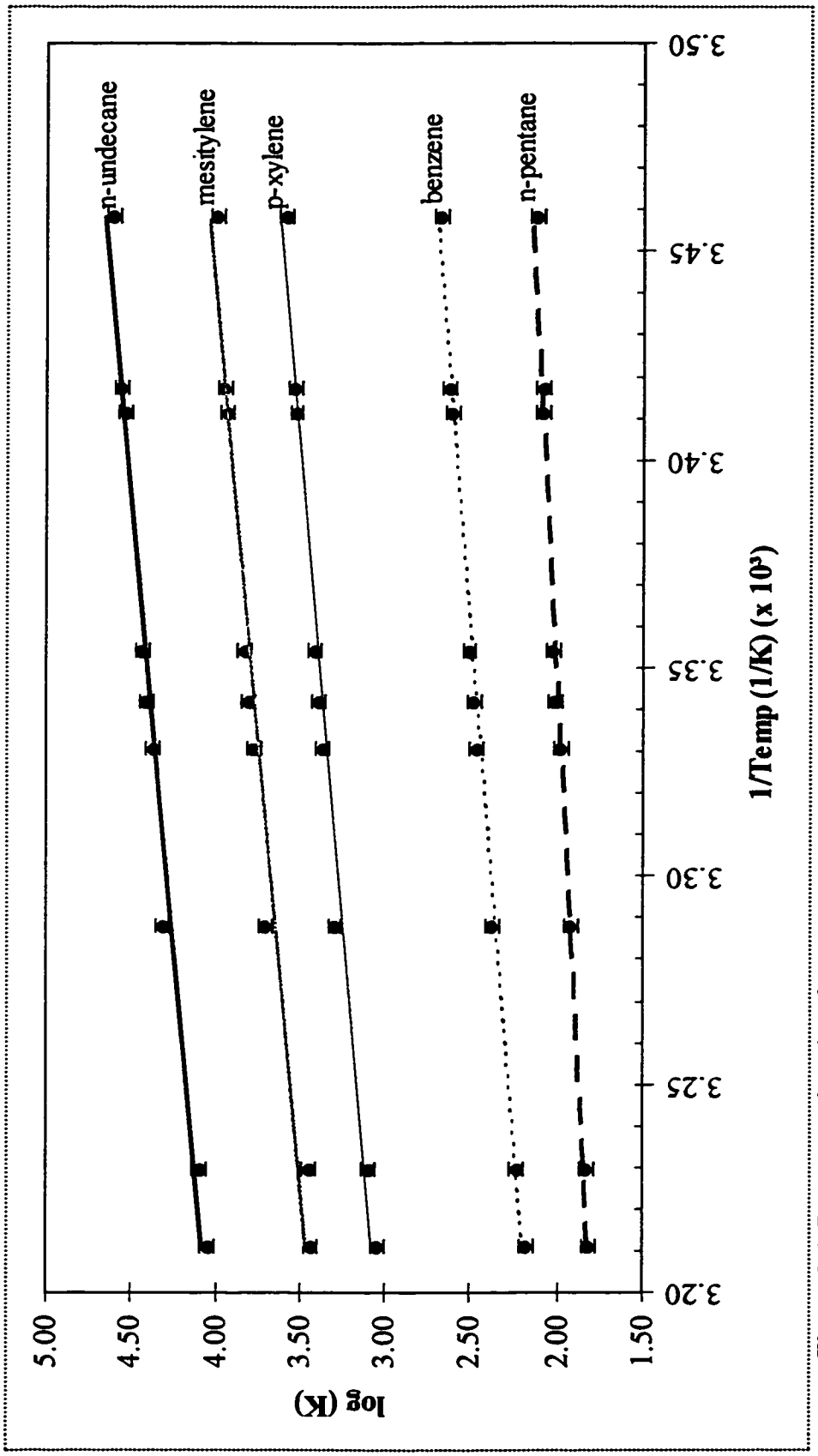

Figure 2.4: Representative plots for pentane, benzene, p-xylene, mesitylene, and n-undecane demonstrating the linear relationship between log (K_{fg}) and inverse of temperature.

Table 2.3: Summary of α and β and *a* and *b* values for each analyte from the slope and y-int of $\log(K_{fg})$ as a function of inverse temperature. See theory for a description of α, β, *a* and *b* values. Also shown are the calculated a^L values using literature ΔH^v (CRC) and the expression for *a* and *b* in equation 8.

Analyte	α	β, 298 K	*a (exp.)*	*b*	r^2	a^L *(lit)*	% Difference *a* and a^L
Pentane (n-)	1.65E+06	3.14	1278	-2.280	0.99	1441	-13%
Hexane (n-)	1.38E+06	1.99	1944	-4.324	0.98	1667	14%
Benzene	1.52E+06	0.994	2025	-4.304	0.99	2241	-11%
Toluene	1.29E+06	0.304	2189	-4.419	0.98	2047	6%
Ethylbenzene	1.12E+06	0.142	2252	-4.208	0.98	2032	10%
Xylene (*p*-)	1.12E+06	0.124	2234	-4.097	0.97	2144	4%
Xylene (*o*-)	1.12E+06	0.0962	2316	-4.283	0.97	2185	6%
Pinene (α-)	1.12E+06	0.0663	2301	-4.071	0.95	2144	7%
Mesitylene	9.89E+05	0.0514	2364	-4.127	0.96	2298	3%
Limonene (d-)	9.89E+05	0.0289	2454	-4.199	0.96	2296	6%
Undecane (n-)	7.61E+05	0.0119	2292	-3.278	0.97	2509	-9%

Table 2.4: Comparison of K_{fg} values estimated with Equation 2.18 and compared to the actual K_{fg} values determined at 296 K (100 μm PDMS fiber coating).

Analyte	Estimated K_{fg}	K_{fg} at 296 K	% Er
Pentane (n-)	110	105	5.7%
Hexane (n-)	178	174	2.2%
Benzene	351	345	1.9%
Toluene	968	967	0.1%
Ethylbenzene	2,572	2,468	4.2%
Xylene (*p*-)	2,886	2,731	5.7%
Xylene (*o*-)	3,554	3,388	4.9%
Pinene (α-)	5,151	5,500	-6.5%
Mesitylene	7,409	7,282	1.7%
Limonene (d-)	12,578	12,362	1.7%
Undecane (n-)	29,793	29,851	0.4%

2.4.5 The effect of gas flow characteristics on SPME sampling

A better understanding of how gas flow characteristics can affect analyte uptake by SPME is required so that the sampling system can be used under optimum conditions. To that end, two questions were asked about sampling gaseous analytes with SPME. The first question was whether there was a difference between sampling from a static gas versus a dynamic gas stream. The second question was to determine if there was a difference between sampling from a turbulent gas flow (Equation 2.26) versus sampling from a laminar gas flow.

To test the possible differences between static gas versus dynamic gas sampling conditions, the standard gas from the chamber was diverted into a temperature controlled 1L

gas sampling bulb (Figure 2.5A). The gas flow rate was 200 mL/min, therefore, it took 5 minutes to provide one bulb volume exchange. The setup was allowed to reach steady-state overnight. With the gas mixture flowing, the SPME samples were taken in the center of the bulb as shown in Figure 2.5A. To achieve sampling from the same gas except under static conditions, the Teflon stopcocks were closed which was followed by SPME sampling inside the bulb. The area counts obtained for each analyte following each of the sampling conditions are summarized in Table 2.5 under the column headings of Static and Laminar Flow. The data indicate that there is a small difference between the static gas sampling and dynamic gas flow sampling based on the test analytes in this study, but for compounds with K_{fg}>6000. This can be explained by considering the phenomenon that for an increasing homologous series of hydrocarbons an associated decrease in the analyte's rate of diffusion is observed (18) (Table 2.1). This suggests an increased time is required for the analyte to reach equilibrium between the air in the bulk of the sample and PDMS. This was confirmed by doubling the PDMS exposure time in the static sampling bulb and comparing the observed area counts to those from PDMS exposure to the dynamically generated standard gas. The data indicate that under these conditions there was no difference between static and dynamic sampling, only that an increased exposure time was required to reach equilibrium under static conditions compared to the same steady-state levels from dynamic conditions for those compounds with K_{fg} larger than 6000. Another problem can also arise with static sampling with PDMS for compounds with large K_{fg} when the standard gas is prepared in the gas sampling bulb and not via introduction of a steady-state concentration of analyte mixture. The problem is that some compounds can be adsorbed on the walls of the sampling bulb, thus apparently decreasing the K_{fg} (since the C_g would be lower) which would result in a lower mass loading of analyte at

equilibrium This is especially true when the analyte K_{fg} exceeds 10^5, a highly possible situation since this is the K_{fg} for tridecane.

For dynamic gas flow or laminar gas flow *versus* turbulent gas flow, the gas was sampled inside the chamber and inside the gas bulb (with gas flow) where the air flow was laminar and the gas was sampled inside the narrow diameter sampling port where the air flow was turbulent (Figure 2.5B). Laminar and turbulent flow characteristics can be defined using a dimensionless term, the Reynold's number (8). Laminar flow is achieved when the Reynold's number is less than 2,000 and turbulent flow when Re>3,000 (Equation 2.26),

$$\mathrm{Re} = \frac{2 \times R \times d \times \overline{\vartheta}}{\eta} \qquad \text{Equation 2.26}$$

where **R** is the radius of the sampling port, **d** is the density of the gas, $\overline{\vartheta}$ is the bulk velocity of the gas, and η is the absolute viscosity (8). The data in Table 2.5 indicate there is a small difference between laminar and turbulent flow, but that the difference is, overall, less than 5 %. There is no obvious explanation for this difference; however, it is possible that the SPME sampling position is the cause. Figure 2.5 B shows the SPME fiber positioned parallel to the gas flow. This position could compromise the mass uptake of analyte because the flow contour of the gas around the tip of the fiber may not provide adequate interaction with the main body of the coating due to potential changes in boundary layer thickness (8). By contrast, the experiments to test laminar gas flow characteristics involved positioning the fiber either directly inside the large chamber or perpendicular to the gas flow in the gas sampling bulb (Figure 2.5A), but never parallel to the gas flow.

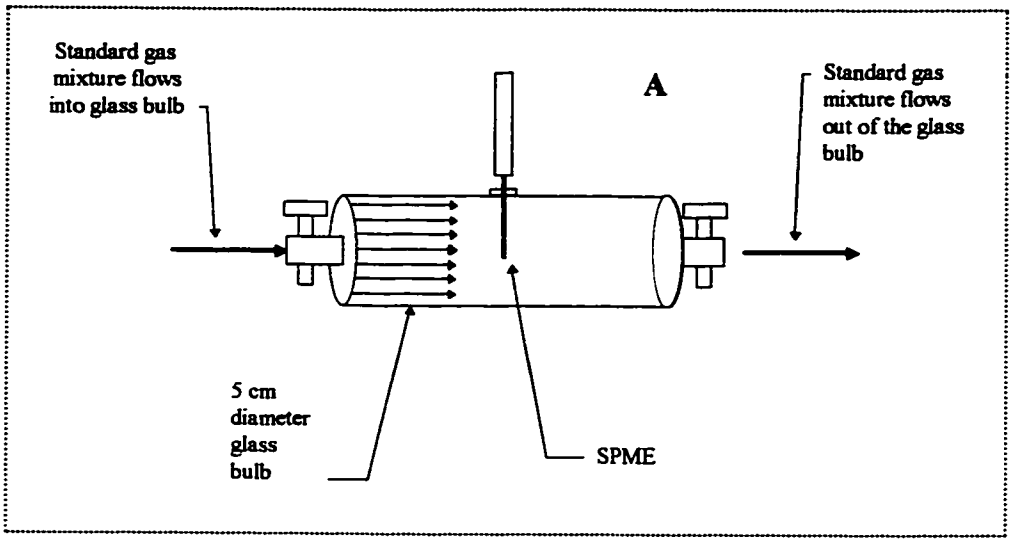

Figure 2.5: **A**: The sampling setup to compare static gas versus dynamic gas sampling. The arrows inside the bulb indicate gas flow. Not illustrated is the static sampling mode.

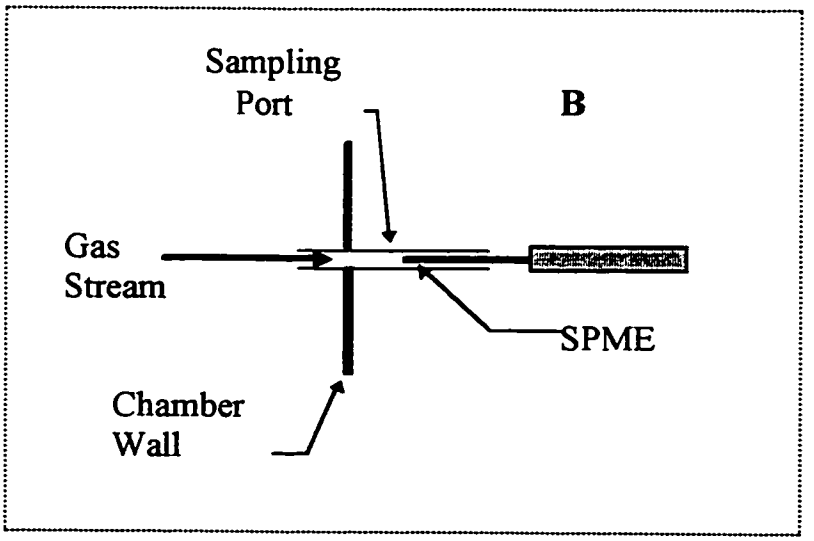

Figure 2.5: **B**: SPME sampling position to sample under turbulent flow conditions.

Table 2.5 Comparisons between static and dynamic sampling and turbulent and laminar flow (n=4 samples for each category).

	Static vs. Laminar Flow and Turbulent Flow Sampling		
	Mean Area Counts (8.5 µg/L at 297K)		
Analyte	**Static (No Flow)**	**Dynamic (Laminar) Flow**	**Turbulent Flow**
Pentane (n-)	0.508 E+04	0.513 E+04	0.504E+04
Hexane (n-)	1.02 E+04	1.05 E+04	0.979 E+04
Benzene	2.25 E+04	2.31 E+04	2.16 E+04
Toluene	6.59 E+04	6.80 E+04	6.37 E+04
Ethylbenzene	16.4 E+04	16.8 E+04	15.7 E+04
Xylene (p-)	19.5 E+04	20.0 E+04	18.4 E+04
Xylene (o-)	24.5 E+04	26.1 E+04	23.4 E+04
Pinene (a-)	32.2 E+04	33.4 E+04	31.4 E+04
Mesitylene	45.9 E+04	46.7 E+04	44.7 E+04
Limonene	76.7 E+04	77.9 E+04	74.5 E+04
Undecane (n-)	188 E+04	188 E+04	182 E+04

2.4.6 Intra-fiber reproducibility and inter-fiber comparison

An intra-fiber reproducibility study for one fiber and an inter-fiber comparison study was carried out with a standard gas concentration of 34 µg/L at 298 K.

2.4.6.a Intra-fiber and inter-fiber reproducibility

The results from the intra-fiber reproducibility are summarized in Table 2.2 Column D. The data indicate there is excellent day-to-day intra-fiber reproducibility. This shows the

SPME air sampling system can be reliably reproducible.

An inter-fiber method precision for ten different fibers yielded from approximately 3 to 9 % RSD (Table 2.6); however, the statistical accuracy of the individual fibers was questioned because of the extremely small errors in precision. This point was studied in detail by performing a statistical evaluation of three different PDMS fibers.

Table 2.6: Summary of area counts for an inter-fiber precision (ten different fibers), not corrected for fiber lengths. 34 µg/L (294 K, 10 minute sampling time, 100 µm PDMS).

Analyte	Average	Std. Dev.	%RSD
Pentane (n-)	1.91E+04	1.66E+03	8.7%
Hexane (n-)	4.49E+04	3.86E+03	8.6%
Benzene	9.66E+04	3.49E+03	3.6%
Toluene	2.74E+05	1.40E+04	5.1%
Ethylbenzene	6.68E+05	2.09E+04	3.1%
Xylene (p-)	7.34E+05	2.61E+04	3.6%
Xylene (o-)	9.78E+05	5.13E+04	5.2%
Pinene (a-)	1.35E+06	4.82E+04	3.6%
Mesitylene	1.92E+06	7.46E+04	3.9%
Limonene	3.22E+06	1.15E+05	3.6%
Undecane (n-)	7.54E+06	2.45E+05	3.3%

2.4.6.b Inter-fiber statistical comparison

In order to use the commercially available SPME 30 µm or 100 µm PDMS for air sampling, it is required to demonstrate that each similarly constructed fiber from any lot

number can yield the same concentration of analyte in air, especially since the range in fiber to fiber precision is so small. This was done by statistically evaluating the area counts obtained from the repeat analysis of a standard gas with three different fibers.

The objective was to use the t-test to compare the method accuracy of different 100 µm PDMS fibers (assuming a normal distribution of fibers). Each of three fibers from three different lots were arbitrarily labeled A, B, and C. Following this, each fiber was exposed for 10 minutes to 17 µg/L of the analyte standard gas mixture at NTP. The area counts for n=4 runs for each fiber were obtained and are presented in Table 2.6A. Also shown in Table 2.7A are the standard deviations (Equation 2.27) for each of the observed data sets (19). In Equation 2.27, X_i is a measurement, $\overline{X}$ is the mean of the measurements, and N is the total number of measurements. The F-test (Equation 2.28) (9) was used to compare the variances (S^2) of those means for each analyte since unequal variances do not allow the use of the standard two-tailed t-test (9). The data used for the inter-fiber comparisons are summarized in Table 2.7A. All variances passed the F-test at the 95 % confidence level.

$$S = \sqrt{\frac{\sum\left(X_i - \overline{X}\right)^2}{N-1}} \text{ (estimation of } \sigma) \qquad \text{Equation 2.27}$$

$$F = \frac{S_1^2}{S_2^2}, \text{ where } S_1^2 > S_2^2 \qquad \text{Equation 2.28}$$

The area counts from the three fibers were then compared with the t-test (Equations 2.29).

$$\pm t = \frac{\overline{X}_1 - \overline{X}_2}{S_p}\sqrt{\frac{N_1 N_2}{N_1 + N_2}} \qquad \text{Equation 2.29}$$

were S_p is the pooled standard deviation as shown in Equation 2.30, N_1 and N_2 are the number of measurements, and $\overline{X}_1$, $\overline{X}_2$ are the means for each data set. The equation for the pooled standard deviation is shown (Equation 3.20).

$$S_p = \sqrt{\frac{\sum(X_{i1} - \overline{X}_1)^2 + \sum(X_{i2} - \overline{X}_2)^2 + \ldots + \sum(X_{ik} - \overline{X}_k)^2}{N - k}} \qquad \text{Equation 2.30}$$

where $\overline{X}_1, \overline{X}_2 \ldots \overline{X}_k$ are the means of each of k sets of analyses and $\overline{X}_{i1}, \overline{X}_{i2} \ldots \overline{X}_{ik}$ are the individual values. $N=(N_1+N_2+\ldots N_k)$, and N-k= degrees of freedom. The results from the t-test show there is a statistically significant difference between the fiber comparisons for a number of the analytes (Table 2.7B). The reason for the failures was initially attributed to the possibility that there was a problem with the standard gas generator. A repeat of the comparison study resulted in the same findings. Therefore, in this case, it was suspected the syringe pump had been delivering very large pulses of analyte thus causing fluctuations in the standard gas concentrations. Although this possibility did not seem plausible in light of the fact all quality assurance checks were in place, the gas generator was thoroughly examined for possible failures such as the lack of appropriate temperature control, pulsing of the syringe pump, pockets of analyte mixture building up then releasing. Examination of these points did not reveal any problems with the system. Initially overlooked was the possibility the fibers themselves were to blame for these comparison failures. This did not seem possible due to the fact the fibers were reportedly given thorough quality assurance checks prior to shipment. It was found that the fiber lengths varied from one fiber to another, even within the same lot,

which resulted in different fiber coating volumes. Indeed, a detailed microscopic examination of 13 different fibers from a number of different lots demonstrated that fiber lengths ranged from 0.98 cm to 1.06 cm with an average length of 1.02 cm ± 0.30 cm. The supplier was contacted and admitted to ± 5 % tolerance of fiber lengths, consistent with our findings. When a correction for fiber lengths was applied (Table 2.7A), the differences between the individual fibers as estimated with the t-test was found statistically insignificant at the 95 % confidence level (Table 2.7C). These results indicate the fiber comparisons originally failed the *t*-tests for method accuracy due to inconsistent fiber lengths.

Table 2.7A: t-test comparison at the 95 % confidence level (t-critical=2.447) (n=4 for each fiber). Data obtained for each of the fibers (17 µg/L at 298 K, 100 µm PDMS). The column "Fiber C - corr. Length (6%)" indicates the data from the Fiber C column were adjusted upwards by 6% to normalize for fiber length.

	Fiber A		**Fiber B**		**Fiber C**		**Fiber C - corr. length (6%)**	
Analyte	Mean	Std. Dev	Mean	Std. Dev	Mean	Std. Dev	Mean	Std. Dev
Pentane (n-)	1.207E+04	1.86E+03	9.804E+03	1.340E+03	9.526E+03	1.102E+03	*1.01E+04*	*1.17E+03*
Hexane (n-)	2.283E+04	1.65E+03	2.044E+04	1.456E+03	2.038E+04	2.102E+03	*2.16E+04*	*2.23E+03*
Benzene	4.886E+04	3.01E+03	4.478E+04	1.948E+03	4.349E+04	1.908E+03	*4.61E+04*	*2.02E+03*
Toluene	1.415E+05	8.84E+03	1.329E+05	2.595E+03	1.255E+05	3.390E+03	*1.33E+05*	*3.59E+03*
Ethylbenzene	3.482E+05	2.05E+04	3.206E+05	1.432E+04	3.113E+05	1.038E+04	*3.30E+05*	*1.10E+04*
Xylene (p-)	3.846E+05	2.40E+04	3.545E+05	1.596E+04	3.411E+05	8.615E+03	*3.62E+05*	*9.13E+03*
Xylene (o-)	4.741E+05	2.94E+04	4.386E+05	1.738E+04	4.369E+05	2.622E+04	*4.63E+05*	*2.78E+04*
Pinene (a-)	7.142E+05	6.31E+04	6.566E+05	2.828E+04	6.354E+05	2.816E+04	*6.74E+05*	*2.98E+04*
Mesitylene	1.020E+06	1.02E+05	9.371E+05	4.553E+04	9.262E+05	5.381E+04	*9.82E+05*	*5.70E+04*
Limonene	1.687E+06	1.21E+05	1.565E+06	6.302E+04	1.511E+06	4.513E+04	*1.60E+06*	*4.78E+04*
Undecane (n-)	4.086E+06	2.48E+05	3.846E+06	1.505E+05	3.675E+06	1.043E+05	*3.90E+06*	*1.11E+05*

Table 2.7B: t-test comparison at the 95 % confidence level (t-critical=2.447) (n=4 for each fiber). *t*-test comparisons without correction for fiber length.

Analyte	**Pooled S Fibers A and B**	**Pooled S Fibers B and C**	**Pooled S Fibers A and C**	**t A/B**	**Pass or Fail t-Test?**	**t B/C**	**Pass or Fail t-Test?**	**t A/C**	**Pass or Fail t-Test?**
Pentane (n-)	1.62E+03	1.23E+03	1.53E+03	1.971	Pass	0.320	Pass	2.346	Pass
Hexane (n-)	1.56E+03	1.81E+03	1.89E+03	2.170	Pass	0.047	Pass	1.832	Pass
Benzene	2.54E+03	1.93E+03	2.52E+03	2.273	Pass	0.948	Pass	3.010	Fail
Toluene	6.52E+03	3.02E+03	6.70E+03	1.853	Pass	3.500	Fail	3.381	Fail
Ethylbenzene	1.77E+04	1.25E+04	1.62E+04	2.209	Pass	1.054	Pass	3.217	Fail
Xylene (p-)	2.04E+04	1.28E+04	1.80E+04	2.091	Pass	1.478	Pass	3.415	Fail
Xylene (o-)	2.41E+04	2.22E+04	2.78E+04	2.081	Pass	0.109	Pass	1.891	Pass
Pinene (a-)	4.89E+04	2.82E+04	4.89E+04	1.666	Pass	1.064	Pass	2.282	Pass
Mesitylene	7.88E+04	4.98E+04	8.14E+04	1.480	Pass	0.310	Pass	1.624	Pass
Limonene	9.63E+04	5.48E+04	9.11E+04	1.804	Pass	1.389	Pass	2.741	Fail
Undecane (n-)	2.05E+05	1.29E+05	1.90E+05	1.660	Pass	1.867	Pass	3.063	Fail

Table 2.7C: t-test comparison at the 95 % confidence level (t-critical=2.447) (n=4 for each fiber). *t*-test comparisons after the area counts obtained with fiber C were adjusted upwards by 6 % to normalize it to fibers A and B.

Analyte	**Pooled S Fibers A and B**	**Pooled S Fibers B and C**	**Pooled S Fibers A and C**	**t A/B**	**Pass or Fail t-Test?**	**t B/C**	**Pass or Fail t-Test?**	**t A/C**	**Pass or Fail t-Test?**
Pentane (n-)	1.62E+03	1.26E+03	1.55E+03	1.971	Pass	0.33	Pass	1.79	Pass
Hexane (n-)	1.56E+03	1.88E+03	1.96E+03	2.170	Pass	0.87	Pass	0.88	Pass
Benzene	2.54E+03	1.99E+03	2.57E+03	2.273	Pass	0.94	Pass	1.52	Pass
Toluene	6.52E+03	3.13E+03	6.75E+03	1.853	Pass	0.02	Pass	1.78	Pass
Ethylbenzene	1.77E+04	1.28E+04	1.64E+04	2.209	Pass	1.04	Pass	1.57	Pass
Xylene (p-)	2.04E+04	1.30E+04	1.82E+04	2.091	Pass	0.77	Pass	1.80	Pass
Xylene (o-)	2.41E+04	2.32E+04	2.86E+04	2.081	Pass	1.49	Pass	0.54	Pass
Pinene (a-)	4.89E+04	2.91E+04	4.94E+04	1.666	Pass	0.82	Pass	1.17	Pass
Mesitylene	7.88E+04	5.16E+04	8.24E+04	1.480	Pass	1.22	Pass	0.65	Pass
Limonene	9.63E+04	5.59E+04	9.18E+04	1.804	Pass	0.93	Pass	1.33	Pass
Undecane (n-)	2.05E+05	1.32E+05	1.92E+05	1.660	Pass	0.53	Pass	1.41	Pass

2.4.7 Linearity and detection limits with PDMS

Table 2.2 Column E summarizes the data obtained from the study of r^2 and limits of detection for each analyte with PDMS using the standard gas generating device at constant temperature. Figure 2.6 shows the calibration curves for benzene, ethylbenzene, α-pinene, and d-limonene. The detection limit data from Table 2.2 Column E indicate that with increasing K_{fg} there is a decreasing limit of detection. This is explained by considering that mass loading of analytes at equilibrium increases proportionally with increasing K_{fg} (Equation 1.4). For example, consider the mass loading between n-pentane and n-undecane with the 100 μm PDMS coating exposed to a standard gas of each analyte at equilibrium. The K_{fg} ratio between these two analytes is 0.0038 (pentane/undecane). Therefore, n-undecane will mass load more than 260 times more than n-pentane for equal gas phase analyte concentrations. It would be expected that n-undecane would have a 260 times lower detection limit compared to n-pentane, which was observed.

Examination of Equation 2.22 indicates that lower detection limits are possible with decreasing β due to the increase in K_{fg} with decreasing temperature. Also, Equation 1.3 indicates that a smaller fiber coating volume, such as that for the 30 μm PDMS fiber coating, will have a lower mass loading of analyte at equilibrium compared to the larger fiber coating volume for the 100 μm thick fiber when both are exposed to the same standard gas concentration. This is important because it is possible to overload the chromatographic separation with a large SPME loading of analyte. Therefore, there is flexibility in air sampling should the analyte under study have an extremely large K_{fg}, e.g., 100,000, or if it is present at very large concentrations, e.g. greater than 1 mg/L. The 30 μm fiber can be used for analytes with high K_{fg} and/or high analyte concentrations, whereas the 100 μm fiber can be used for

analytes with lower K_{fg} and/or lower analyte concentrations.

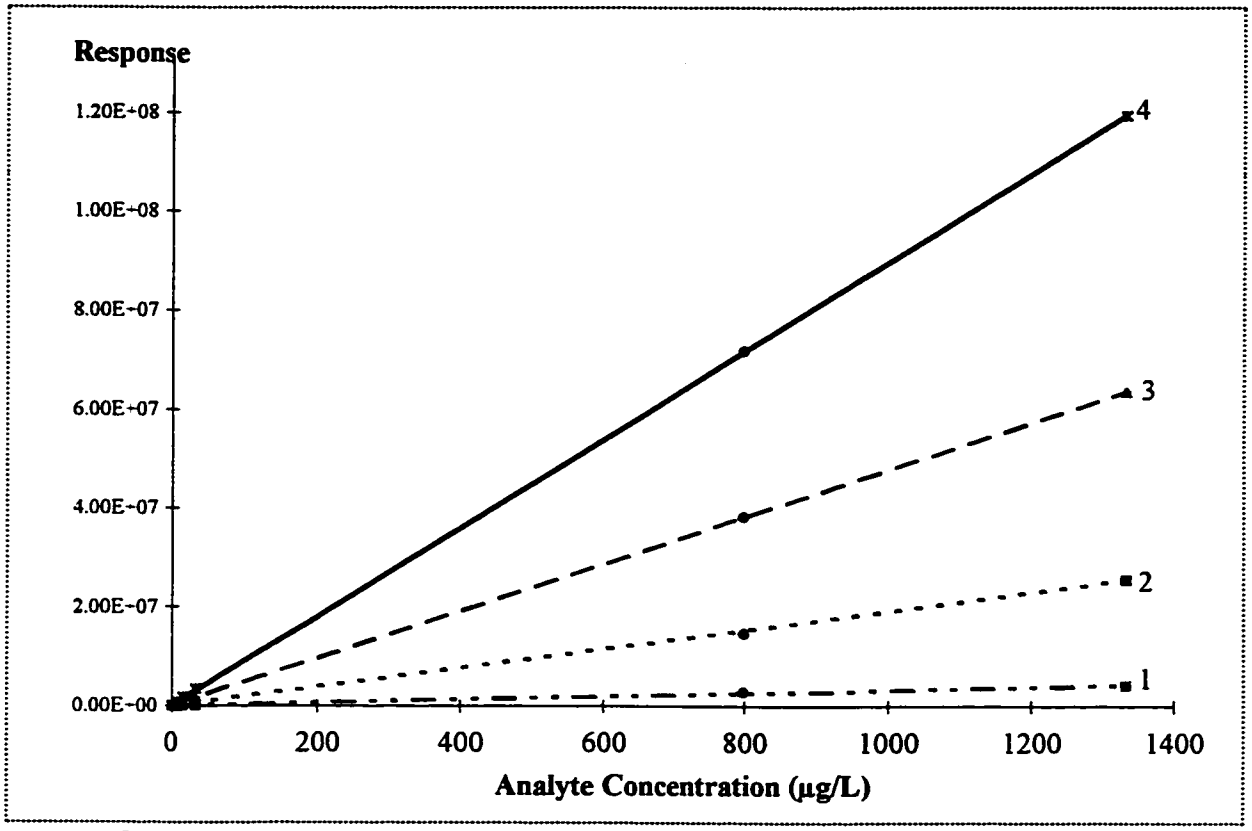

Figure 2.6: PDMS (100 µm) calibration curves for 1) benzene, 2) ethylbenzene, 3) α-pinene and 4) d-limonene for the concentration range from 0.60 µg/L to 1333 µg/L at 298 K.

Detection limits by GC/FID for conventional sampling and analysis methods for most of these analytes are reported to be from 1µg to 10 µg per sample, depending on the volume of air sampled and the analyte of interest (10). SPME with 100 µm PDMS has a conservative detection limit of 0.3 ng per sample with the same instrumental conditions, as a result of the higher signal to noise ratio and lower background noise (Chapter 1). The higher detection limits for the former are due predominantly to the chemical background of the adsorbent such as charcoal. It is marginally lower with a higher quality of charcoal and carbon disulphide (10). In addition, further examination of the detection limits with charcoal tubes indicates that

the detection limits increase significantly when these devices are used for grab sampling. For example, a one minute active grab sample with a charcoal tube at its maximum air sampling flow rate (for a total volume of 200 mL) yields a detection limit of 50 μg/L for pentane and 5 μg/L for toluene compared to 5.5 μg/L and 0.4 μg/L, respectively, by SPME with extended fiber extraction for the same time period. Therefore, SPME provides significantly better detection limits for grab sampling compared to methods using charcoal. The detection limits can be further lowered with increasing fiber lengths and/or thickness, by using more specific fiber coatings, and use of detectors more responsive to the analytes of interest.

2.4.8 Effect of humidity on air sampling with PDMS

Table 2.8 summarizes the results from the study of humidity effects on the mass uptake by the fiber. The data indicate that there is approximately a 10 % lower mass loading of analyte at greater than 90 % R.H. for the studied temperatures. This observation is consistent with other work (11). The temperature studied was 311 K with relative humidities 0 %, 30 %, 50 %, 70 % and 95 %. The high temperature was chosen to challenge the fiber at high absolute humidity. The data indicate that high humidity (greater than 90% R.H.) appears to affect the mass loading of analyte; however, studies have indicated this is due to a GC injection problem. The volume of the narrow bore insert (Figure 1.1B) is less than 50 μL. If 0.1 μL of water vapour condensed on the needle or adsorbed to the needle, and if that entire water volume was placed at 250 °C, it would expand to greater than 150 μL (at 20 p.s.i. and 523 K). The excess gaseous volume of water cannot be maintained within the body of the injector liner, thus it can backflush out of the liner and into the head of the carrier gas. It will take with it a fraction of the analytes to the septum purge line connected to the injector. This problem was corrected by turning off the septum purge gas.

Table 2.8 Effect of humidity on the analyte mass loaded on the 100 μm PDMS fiber (n=4 repeats).

	% Relative Humidity Mean Area Counts (33 μg/L at 311K)				
Analyte	**0**	**30**	**40**	**75**	**95**
Pentane (n-)	1.16E+04	1.13E+04	1.15E+04	1.11E+04	9.82E+03
Hexane (n-)	2.16E+04	2.11E+04	2.32E+04	2.12E+04	1.95E+04
Benzene	4.65E+04	4.63E+04	4.83E+04	4.69E+04	4.18E+04
Toluene	1.25E+05	1.26E+05	1.25E+05	1.22E+05	1.11E+05
Ethylbenzene	2.88E+05	2.95E+05	2.94E+05	2.92E+05	2.61E+05
Xylene (p-)	3.22E+05	3.30E+05	3.27E+05	3.38E+05	2.88E+05
Xylene (o-)	3.94E+05	4.02E+05	4.00E+05	4.27E+05	3.54E+05
Pinene (a-)	4.77E+05	4.97E+05	4.96E+05	4.81E+05	4.35E+05
Mesitylene	7.94E+05	8.22E+05	8.26E+05	7.93E+05	7.16E+05
Limonene	1.22E+06	1.27E+06	1.27E+06	1.23E+06	1.10E+06
Undecane (n-)	3.16E+06	3.25E+06	3.25E+06	3.11E+06	2.76E+06

2.5 Summary

SPME with PDMS can be used for both rapid and accurate ambient air grab sampling of target hydrocarbons. No fiber calibration curve is necessary if K_{fg} and its temperature dependence are known. If the relationship between K_{fg} and temperature is not known for an analyte, it can be estimated using the analyte's heat of vaporization and its K_{fg} at a specific temperature. Once a K_{fg} and its temperature dependence is established for the target analyte, the SPME 30 μm and/ or 100 μm PDMS fibers can be used as supplied from the

manufacturer, following a fiber length correction, given both temperature and relative humidity are monitored during sampling.

An alternate method to determine K_{fg} is presented in Chapter 3. This alternate method uses the actual chromatographic separation data to accurately estimate the K_{fg}. The method is based on the analyte's retention index value for the siloxane stationary phase, a stationary phase very similar to SPME using the PDMS fiber coating.

Finally, the work described herein strongly suggests that SPME can be used for air sampling for hydrocarbons. Chapter 6 presents the results of field sampling for airborne styrene using 100 μm PDMS with a side-by-side comparison to other air sampling methods.

2.6 References

1. Davis, M.L. and Cornwell, *Introduction to Environmental Engineering*, McGraw-Hill, Inc., 1991, Chapter 6

2. U.S.EPA Method T01 - *Method for the determination of volatile organic compounds in ambient air using Tenax adsorption and GCMS*, 1984

3. U.S.EPA Method T011 - *Determination of volatile organic compounds in ambient air using SUMMA passivated canister sampling and GC analysis*, 1988

4. Martos, P. and Pawliszyn, J., Anal. Chem., **69** (2), 1997, pp. 206-215

5. Pawliszyn, J. *Solid Phase Microextraction - Theory and Practice*, Wiley-VCH, 1997

6. McKelvey, J.M. and Hoelscher, H.E, Anal. Chem. **29** (1), 1957, page 123

7. Namiesnik, J., Journ. Chrom. **300** 1984 pp. 79-108

8. Roberson, J.A. and Crowe, C.T. *Engineering Fluid Mechanics*, 5th ed.; Houghton Mifflin Company, 1993; Chapters 4 and 10

9. Christain, G.D., *Analytical Chemistry*, 3rd ed.; John Wiley and Sons; New York, 1980; Chapter 4

10. *National Institute for Occupational Safety and Health Manual of Analytical Methods*, 1994, U.S. Department of Health and Human Services, electronic version.

11. Chai, M. and Pawliszyn, J. *Env. Sci. Technol.* **1995**, *29*, 693-701

CHAPTER 3

ESTIMATING K_{fg} FOR PDMS

3.1 Background

This chapter describes a method to estimate K_{fg} values for the PDMS fiber coating. The method is based on chromatographic parameters without the need for experimentally determining K_{fg} (1). Recall Equations 1.4a and 2.2, shown here in Equation 3.1. Equation 3.1 can be used to quantify hydrocarbons from ambient, indoor, and occupational air,

$$C_g = \frac{C_f^{\infty}}{K_{fg}} = \frac{n_f^{\infty}}{V_f} \times \frac{1}{K_{fg}} \text{ (constant T)} \qquad \text{Equation 3.1}$$

where C_g and C_f^{∞} are the analyte concentrations in the gas and fiber, respectively (at equilibrium), K_{fg} is the partition coefficient, n_f^{∞} is the analyte mass loaded on the fiber and V_f is the fiber volume. Knowledge of the K_{fg} value in Equation 3.1 provides the key to air sampling with SPME using the PDMS fiber coating without the need for fiber calibration (Chapter 2). For example, if sampling an unknown airborne concentration of analyte(s) with PDMS, the only analytically measured parameter in Equation 3.1 is the n_f where the V_f and K_{fg} are known (at a specific temperature). When the sampling temperature is different from the temperature at which K_{fg} was established, the linear relationship between $\log K_{fg}$ and inverse temperature, Equation 3.2 (Equation 2.7), can be used to correct the K_{fg} value (2),

$$\log K_{fg} = \frac{\Delta H^v}{2.303RT} + \left[\log_{10}\left(\frac{RT}{\gamma_{i\infty} p^*}\right) - \frac{\Delta H^v}{2.303RT^*} \right] \qquad \text{Equation 3.2}$$

where ΔH^v is the analyte heat of vaporization (J/mol), R is the gas constant ((L atm)/(mol K)),

T is the sampling temperature (K), p* (atm) and T* (K) are the solute vapor pressure at a known temperature, and γ_i is the solute activity coefficient. This equation can take the general form (Equation 3.3),

$$\log_{10} K_{fg} = \frac{a}{T} + b \qquad \text{Equation 3.3}$$

where $a = \frac{\Delta H^v}{2.303R}$, $b = \left[\log_{10}\left(\frac{RT}{\gamma_i \times P^*}\right) - \frac{\Delta H^v}{2.303RT^*} \right]$. By substituting Equation 3.3 into Equation 3.1 we get Equation 3.4,

$$C_g = \frac{n_f}{V_f} \times 10^{-\left(\frac{a}{T}+b\right)} \qquad \text{Equation 3.4}$$

where we can now establish the C_g for a target analyte at any temperature given the analyte's *a* and *b* values (Chapter 2). Therefore, if K_{fg} is known, Equations 3.1 or 3.4 can be used to quantify unknown concentrations of target analytes by measuring the n_f and given the actual sampling temperature.

Establishing a K_{fg} value can be a tedious and time consuming process. In those cases where there are unknown compounds of interest or of significant magnitude in a chromatogram, SPME with the PDMS fiber coating could not, until now, be used to provide an estimate of the gas concentrations. Therefore, a simple yet accurate and universally reproducible approach to establishing K_{fg} values would be highly beneficial. This Chapter shows such an approach. It is demonstrated that a general method to establish K_{fg} values for compounds of interest utilize the common retention index system which is used by chromatography experts world-wide. The retention index systems are often used to identify analytes on the basis of their retention behavior as related to standard compounds, such as the

n-alkanes. There is a linear relationship between the $\log_{10}K_{fg}$ value (for the PDMS fiber coating) and the linear temperature programmed retention index system (LTPRI). Therefore, establishing K_{fg} values with LTPRI can provide an accurate estimation of K_{fg} values for compounds in a sample as the analytes are chromatographically separated. Also, for very complex mixtures of hydrocarbons such as in gasoline, each peak from that mixture can be individually quantified based on its K_{fg} value using the LTPRI approach, and the total can be summed to provide total (airborne) petroleum hydrocarbons (TPH) (Results and Discussion). This removes the need to establish K_{fg} values for compounds before air sampling for those compounds. It also provides a means by which K_{fg} values can be accurately estimated to check on K_{fg} values reported in literature, established experimentally and/or to afford a means by which to estimate PDMS analyte detection limits. In addition, this method obviates the need to determine K_{fg} values from static gas standards (Chapter 1) or from difficult to generate dynamic gas standards (Chapter 2).

Equation 3.4 indicates it is possible to determine the concentration of an analyte in air given the mass of analyte absorbed on the PDMS fiber coating at equilibrium. The terms in brackets provide the correction for temperature thus allowing air sampling with PDMS at ambient temperatures, from 5°C to 35 °C.

3.2 Theory

In chromatography, the chemical potential at equilibrium of an analyte between the mobile phase (m) and the stationary phase (s) is expressed in Equation 3.5 (3),

$$\mu_s = \mu_m \qquad \text{Equation 3.5}$$

where $\mu_s = \mu_s^o + RT\ln\gamma' C_s$ and $\mu_m = \mu_m^o + RT\ln\gamma^* C_m$. The chemical potential of a system

can be used to describe the tendency of matter (analyte in this case), to move from a region of high chemical potential to one of low chemical potential to achieve a thermodynamic balance between the two regions (4). Therefore, when the chemical potential of an analyte distributed between the gas phase and the stationary phase are the same, that system can be considered at equilibrium. Further, if $\gamma^{'} = 1$ and $\gamma^{"} = 1$, then Equation 3.6 can be realized (3),

$$\mu_s^o + RT\ln C_s = \mu_m^o + RT\ln C_m \qquad \text{Equation 3.6}$$

where R is the gas constant, T is the temperature in K, and C_s and C_m are the solute concentrations in the stationary and mobile phases, which after rearrangement yields Equation 3.7,

$$K_{sm} = \frac{C_s}{C_m} = \exp\left(\frac{\mu_m^o - \mu_s^o}{RT}\right) = \exp\left(\frac{\Delta\mu^o}{RT}\right) \qquad \text{Equation 3.7}$$

The time necessary for a solute to pass completely through the column, i.e., the solute retention time, t_r, is a function of the time spent between the mobile and stationary phases; hence K_{sm}. Equation 3.8 describes the rate of migration through the column: (3)

$$\overline{v} = \overline{u}\left(\frac{C_m V_m}{C_m V_m + C_s V_s}\right) = \overline{u}\left(1 + \frac{C_s V_s}{C_m V_m}\right)^{-1} = \overline{u}\left(1 + K_{sm}\frac{V_s}{V_m}\right)^{-1} \qquad \text{Equation 3.8}$$

where $\overline{v}$ is the rate of migration through the column, $\overline{u}$ is the average linear velocity of the mobile phase in the column, V_m and V_s are the volumes of the mobile and stationary phases, respectively. The $\overline{v}$ is expressed as a ratio of column length L and retention time t_r (L/t_r) and if substituted into Equation 3.8 yields Equation 3.9,

$$t_r = \frac{L}{\overline{u}}\left(1 + K_{sm}\frac{V_s}{V_m}\right) = t_m\left(1 + K_{sm}\frac{V_s}{V_m}\right) \qquad \text{Equation 3.9}$$

where t_r is the peak retention time and t_m is the column dead time. By rearranging Equation

3.9 into Equation 3.10, it is obvious that the adjusted retention time (t_r') is directly proportional to the K_{sm} value.

$$t_r' = t_r - t_m = t_m K_{sm} \frac{V_s}{V_m} \qquad \text{Equation 3.10}$$

Equation 3.10 suggests that there is a relationship between K_{sm} and t_r', and that it may be used to predict analyte retention times if K_{sm} was known for a specific compound at a specific temperature and for a specific column (V_s/V_m). In addition, since the K_{sm} for a compound is constant under specific chromatographic conditions, then it could be used to assist to identify unknown compounds from a separation. If all the separations were carried out on one instrument under a strict set of separation conditions, this would be true. The problem is that t_r' will change with a GC separation system as changes occur in the column stationary phase, inaccuracies in temperature, carrier gas velocities, etc. Therefore, a system which could automatically correct for these variables would not only increase the possibility of accurately identifying an unknown peak, but would also allow other instruments (anywhere in the world) to precisely repeat the separation. This was achieved with the realization that the K_{sm} for each compound in a series of homologous compounds would all change in the same relative way with changes to temperatures, linear velocities, etc. Therefore, the K_{sm} for an unknown compound with similar physical-chemical properties as those of the same homologous series of compounds would also change in the same way. The result is the unknown compound will always elute in a relative position to some compound in the homologous series. Thus, the retention index system was developed. It is frequently used to identify compounds on the basis of their relative retention times. Historically, the Kovats retention index system has been the primary source of this procedure; however, the Kovats retention index system requires

isothermal chromatographic conditions which serves little purpose for complex mixtures of analytes spanning a broad range of boiling points (5). The linear temperature programmed retention index system (LTPRI) (Equation 3.11) is used quite extensively (5) in place of Kovats retention index to establish retention indices with the assumption the temperature program is linear and logarithms of the adjusted retention times are replaced by the retention *temperatures*, Equation 3.11,

$$LTPRI = 100 \times \left(\frac{T_{r(A)} - T_{r(n)}}{T_{r(n+1)} - T_{r(n)}} \right) + 100 \times n \qquad \text{Equation 3.11}$$

where $T_{r(A)}$ is the analyte retention temperature, $T_{r(N)}$ is the retention temperature of the n-alkane eluting directly before $T_{r(A)}$, $T_{r(n+1)}$ is the retention temperature of the n-alkane eluting directly after $T_{r(A)}$ and n is the number of carbon atoms for $T_{r(n)}$. If the increase in temperature is linear, the retention temperature is proportional to t'_r, Equation 3.12,

$$T_r = T_o + t'_r r_T \qquad \text{Equation 3.12}$$

where r_T is temperature program rate and T_o is the initial column temperature. Combining Equations 3.11 and 3.12 yields Equation 3.13 (8), for retention *times*,

$$LTPRI = 100 \times \left(\frac{t_{r(A)} - t_{r(n)}}{t_{r(n+1)} - t_{r(n)}} \right) + 100 \times n \qquad \text{Equation 3.13}$$

where $t_{r(A)}$ is the analyte retention time, $t_{r(n)}$ is the retention time of the n-alkane eluting directly before $t_{r(A)}$, $t_{r(n+1)}$ is the retention time of the n-alkane eluting directly after $t_{r(A)}$ and n is the number of carbon atoms for $t_{r(n)}$ (5). LTPRI values are easily established with Equation 3.13 or are alternatively readily available from a considerable number of published sources. There are a number of advantages to the use of LTPRI in favor of Kovats retention indices; predominantly, the former does not require measurement of t_m (which is not necessarily simple

to establish), and it does not suffer from problems associated with isothermal chromatography. For example, the Kovats retention index for the same compound often yields different values depending on the temperature chosen, most probably due to peak broadening making it more difficult to accurately determine retention times (6,7).

Of importance is the finding from recent work (8) which has demonstrated that solute activity in PDMS is ostensibly identical to the solute activity in the siloxane capillary stationary phase thus suggesting that parameters used in chromatography can be used to describe properties of PDMS.

The relationship between the retention volume of an analyte and carbon number within a homologous series has long been known, Equation 3.14 (7),

$$\ln V_g(C^n) = a' + b'(C^n) = a' + b'(n) \qquad \text{Equation 3.14}$$

where V_g is the retention volume, C^n is the carbon number, a' and b' are the slope and y-intercept of the curve, respectively. The K_{sm} for a given solute is related to its V_g and the stationary phase density, ρ (Equation 3.15) (3),

$$V_g = \frac{K_{sm}}{\rho} \qquad \text{Equation 3.15}$$

Substituting Equation 3.15 into Equation 3.14 for V_g we get Equation 3.16,

$$\ln \frac{K_{sm}}{\rho} = \ln K_{sm} - \ln \rho = a' + b'(n) \qquad \text{Equation 3.16}$$

The density of the PDMS stationary phase is approximately 1, by observing that $100n$ is LTPRI, and that the activity of an absorbed hydrocarbon in PDMS is identical to that in the siloxane stationary phase, Equation 3.16 can be modified to provide the relationship between K_{fg} and retention index as shown in Equation 3.17 (where the a and b terms now include

2.303).

$$\log_{10} K_{fg} = a + b(LTPRI) \qquad \text{Equation 3.17}$$

Therefore, a linear relationship between $\log K_{fg}$ and LTPRI is expected for a homologous series of carbon atoms with the PDMS fiber coating, providing a simple and accurate approach to estimating K_{fg} values for any compound when its LTPRI is known. In fact, a linear relationship was observed as will be shown in the Results and Discussion. Retention index data can be found in Sadtler (6) references, or can be determined from chromatographic separation.

We can further understand the relationship between $\log_{10} K_{fg}$ and LTPRI by considering the slope in Equation 3.17 with the following parameters described with Equation 3.18,

$$b = \frac{\Delta \log_{10} K_{fg}}{\Delta LTPRI} = \frac{\log_{10} K_{fg(n+1)} - \log_{10} K_{fg(n)}}{100(n+1) - 100n} \qquad \text{Equation 3.18}$$

where $\log_{10} K_{fg(n)}$ and $\log_{10} K_{fg(n+1)}$ are the logarithms of the K_{fg} for an n-alkane and the next n-alkane in the series which bracket the analyte of interest, and n is the n-alkane carbon number. These constants can be related to physicochemical properties of the PDMS fiber coating. The K_{fg} value is related to the partial molar free energy of solution (ΔG_s) as follows:

$$\Delta G_s = -2.303RT \log_{10} K_{fg} \qquad \text{Equation 3.19}$$

where R is the gas constant and T is the temperature in Kelvin at which the K_{fg} value was obtained. Equation 3.18 can also be rewritten in terms of the partial free energy of solution by substituting the logarithms of K_{fg} for the consecutive n-alkane values with Equation 3.19. In addition, the difference in LTPRI for two adjacent alkanes will always be 100 and therefore Equation 3.18 can be expressed as shown in Equation 3.20,

$$\frac{\Delta \log_{10} K_{fg}}{\Delta LTPRI} = \frac{-\Delta G_{s_{(n+1)}} + \Delta G_{s_{(n)}}}{2.303RT \times 100}$$ Equation 3.20

It can be assumed the difference in the partial free energy of solution for two adjacent n-alkanes equals the free energy of solution of a methylene group, $\Delta G_s(CH_2)$, and that $\Delta G_s(CH_2)$ is independent of chain length and further that $\Delta G_s(CH_2) \cong \Delta G_s(CH_3)$ (Equation 3.21) (9),

$$\frac{\Delta \log_{10} K_{fg}}{\Delta LTPRI} = -\frac{\Delta G_s(CH_2)}{230.3RT}$$ Equation 3.21

This assumption is valid for the nonpolar solute/nonpolar stationary phase system studied for the sampling of hydrocarbons with PDMS but is not valid in cases where the solute and stationary phases differ significantly in polarity (9). In addition, the partial molar free energy of solution for any hydrocarbon is related to the free energy of solution for a methylene group (Equation 3.22),

$$\Delta G_s = \Delta G_s(CH_2)\frac{LTPRI}{100}$$ Equation 3.22

Equation 3.17 relating $\log K_{fg}$ to LTPRI may be expressed in terms of a thermodynamic parameter as given in Equation 3.23 (10,11),

$$\log_{10} K_{fg} = -\frac{\Delta G_s(CH_2)}{2.303RT} \times \frac{LTPRI}{100} + C$$ Equation 3.23

where C is the y-intercept $= \left(\log_{10} K_{fg(n)} - b \times \frac{LTPRI_{(n)}}{100} \right)$ and is -0.188 for PDMS, $K_{fg(n)}$ is n-alkane with n carbon atoms and $LTPRI_{(n)}$ is the retention index corresponding to that n-alkane. The $-\frac{\Delta G_s(CH_2)}{2.303RT}$ term is constant at a given temperature and can be replaced by a

constant, B. Equation 3.23 can be rewritten to give Equation 3.24:

$$\log_{10} K_{fg_{(i)}} = B \times \frac{LTPRI_{(i)}}{100} + \left(\log_{10} K_{fg(n)} - b \times \frac{LTPRI_{(n)}}{100} \right) \qquad \text{Equation 3.24}$$

where $K_{fg(i)}$ and $LTPRI_{(i)}$ are the PDMS fiber coating/gas partition coefficient and the corresponding LTPRI for the hydrocarbon of interest, in that order.

3.2.1. LTPRI and waterborne analytes

An interesting development from the relationship in Equation 3.24 is that it is now possible to extend the relationship to one which includes the dimensionless Henry's law coefficient, as given in Equation 3.25,

$$H_C = \frac{C_g^{\infty}}{C_w^{\infty}} \qquad \text{Equation 3.25}$$

where C_g^{∞} and C_w^{∞} are the gas phase and water phase concentration of a dilute analyte distributed between the two phases in a closed system, at equilibrium. Consider then, that Equation 3.25 can be related to terms described with PDMS as shown with Equation 3.26,

$$H_C = \frac{K_{fw} C_f^{\infty}}{K_{fg} C_f^{\infty}} = \frac{K_{fw}}{K_{fg}} \qquad \text{Equation 3.26}$$

where K_{fw} is the distribution coefficient realized for a direct two phase equilibrium established between PDMS and a waterborne analyte, while the remainder of terms are familiar. Therefore, with Equation 3.26 and with Equation 3.24, we can realize Equation 3.27 which allows for the determination of K_{fw} for PDMS and waterborne analytes (12)

$$\log_{10} K_{fw_{(i)}} = b \times \frac{LTPRI_{(i)}}{100} + \left[\left(\log_{10} K_{fg(n)} - b \times \frac{LTPRI_{(n)}}{100} \right) + \log_{10} K_{aw_{(i)}} \right] \qquad \text{Equation 3.27}$$

In addition, it can be seen from Equation 3.27 that the slope for the $\log K_{fw}$ as a function of

LTPRI should be the same as that slope for the $\log_{10}K_{fg}$ as a function of LTPRI (Equation 3.17) because the formation of a solution between the solute and the PDMS fiber coating is independent of the matrix being sampled, whether it is ideal air or ideal water. Finally, Equation 3.27 can be expanded to Equation 3.28 by combining the equation shown in Figure 3.1, $\log_{10} K_{fg} = 0.00415 LTPRI - 0.188$, with Equation 3.26 (13),

$$\log_{10} K_{fw} = 0.00415 LTPRI - 0.188 + \log_{10} K_{Hc} \qquad \text{Equation 3.28}$$

Therefore, it is possible to obtain K_{fw} values from the values of K_{fg}. As a result of finding the relationship between $\log_{10}K_{fg}$ and LTPRI, it is now possible to estimate the K_{fw} for target analytes given the analyte's Henry's Constant and its retention index value, for the series of general hydrocarbons. This aspect of retention indices for waterborne analytes will not be discussed further in this dissertation.

3.3 Experimental

3.3.1 Chemicals and Materials

3.3.1.a Chemicals

Certified Alphagaz PIANO isoparaffins calibration standard and Alphagaz PIANO aromatics calibration standard were obtained from Supelco (Mississauga, Ontario). Toluene and carbon disulphide were from Caledon Laboratories, Ltd. (Georgetown, Ontario). Pentane, hexane, heptane, octane, nonane, decane, undecane, dodecane, tridecane and tetradecane were from Sigma-Aldrich (Milwaukee, WI).

3.3.1.b Materials

For the Varian 3400 *CX* gas chromatograph, nitrogen, helium, and hydrogen gases were from

Praxair (Waterloo, Ontario) and compressed air was generated from an air generator from Balston (Mississauga, Ontario). For the Hewlett Packard 5890 Series II gas chromatograph, helium, hydrogen, and air were from Canox (Guelph, Ontario). SPME devices with 100μm, 30μm and 7 μm PDMS coated fiber assemblies were from Supelco (Mississauga, Ontario), as well as the 1.0 L gas sampling bulb. The ten microliter syringes were from Hamilton.

3.3.2 Preparation of analyte mixtures

A standard mixture of toluene in carbon disulphide (CS_2) was prepared by diluting 8660 μg of toluene to 1.00 mL CS_2 in an EPA approved Teflon capped vial. The mixture was then thoroughly mixed and serially diluted to 0.866 μg/mL. The resulting calibration curve was used to calculate the mass of analyte loaded on the fiber. A 10.0 % w/w standard mixture of n-alkanes comprised of pentane, hexane, heptane, octane, nonane, decane, undecane, dodecane, tridecane and tetradecane was prepared by adding 1.00 g of each analyte, starting with n-tetradecane, into a Teflon capped vial. The mixture was then thoroughly mixed and transferred to 1.8 mL Teflon capped vials leaving no headspace. This mixture was used in a standard gas generation system previously described and used to determine K_{fg} values as discussed below (2). The system was allowed to reach steady-state at a concentration of 15 μg/L for each n-alkane at 25.0 °C. The concentration of each n-alkane was verified with a standard method (National Institute of Occupational Safety and Health 1500) (14).

3.3.3 SPME with PDMS Sampling of Isoparaffinic and Aromatic Standard Gas Mixtures

A mixture of standard gases was prepared by adding 1.0 μL of neat isoparaffins or aromatics to the 1.0 L gas sampling bulb (with the half hole septum covered with Teflon tape). All SPME overnight extractions were carried out with a 100 μm PDMS for the

isoparaffins and 30 μm PDMS for the aromatics at 298 K. The standard gas generating device could not be used for these standards due to the fact that only 100 μL of each mixture was available for the experiments.

3.3.4 Instrumentation and Methods for SPME and Liquid Injections

3.3.4.a Establishing K_{fg} values for n-alkanes

A Star software (Varian) computer controlled Varian 3400 *CX* gas chromatograph (without electronic pressure control) equipped with a carbon dioxide cooled Septum-equipped Programmable Injector (SPI) and an 0.8 mm i.d. SPI insert coupled to a pre-column (1m long, 0.25 mm i.d.) and an SPB-5 column (30m, 0.25 mm i.d., 1.0 μm film thickness) which was coupled to a flame ionization detector (FID) was used for the research. The injector was maintained at 225°C for SPME injections, and at 45°C for liquid injections, followed by a temperature increase to 225°C at 30°C/min. The column temperature program for SPME and liquid injections was 45°C for 1.50 min., 30°C/min to 175°C held for 2.67 min., then 30°C/min. to 240°C and held for 2.0 min. Helium, the carrier gas, was set to 40 cm/s at 45°C for both SPME and liquid injections. The detector gas flow rates were set to 300 mL/min. for air, 30 mL/min. for nitrogen and 30 mL/min. for hydrogen and were all measured daily.

3.3.4.b Establishing retention times for n-alkanes, retention indices and K_{fg} values for isoparaffins and aromatics with constant carrier gas velocity

All experiments to establish retention indices and K_{fg} values for isoparaffins and aromatics used a computer controlled Hewlett Packard 5890 Series II gas chromatograph equipped with electronic pressure controlled (EPC) split/splitless injection port (250 °C) coupled to a deactivated fused silica pre-column (1 m, 0.32 mm i.d.) and Hewlett Packard PONA column (50 m, 0.20 mm i.d., 0.50 μm film thickness) followed by flame ionization

detection (FID) (250 °C). A narrow bore insert (0.75 mm i.d.) was used for all SPME experiments and a wide bore glass wool packed insert was used for all HP 7673A autosampler liquid injections performed to establish the FID response to toluene for a five point calibration. The purge valve was initially set off, and turned on after 1.0 min. for both SPME and liquid injections. Helium, the carrier gas, was set to 28 cm/s and was automatically maintained at that velocity with the EPC. The initial column temperature was 35°C for 0.50 min., ramped to 220°C at 1 °C/min and then held for 8.0 min., for a total run time of 193.5 min.. The detector gas flow rates were set to 375 mL/min. for air, 30 mL/min. for helium (make-up gas) and 20 mL/min. for hydrogen and were all measured daily.

The instruments were checked daily for calibration using a liquid mid-point calibration standard. Any deviations in area counts greater than 15 % required re-injection of that standard. If the deviation was still greater then 15 %, the detector response as a function of amount injected was re-established. In addition, quality of peak shapes, resolution and retention times were carefully monitored to ensure all chromatography was within specifications.

3.3.5 Analysis of airborne gasoline with SPME

Regular unleaded gasoline was purchased and transferred into 4 mL standard amber vials cleaned according to U.S. E.P.A. protocols and capped with Teflon. This gasoline was injected to a standard gas generating device (described above) and allowed to reach steady-state for four weeks. Gasoline was injected at a rate of 4 mg/hr with an air stream dilution of approximately 200 mL/min. yielding a total volatile organic carbon concentration of 247 µg/L ± 10 µg/L (25 °C) as determined with NIOSH Method 1501. The 100 µm PDMS was chosen to analyze the airborne gasoline mixture due to the anticipated low mass loading of

compounds with known small distribution coefficients. The fiber was exposed to the air mixture for 30 minutes thus allowing equilibration of all gasoline components.

3.4 Results and Discussion

3.4.1 Relationship between $\log K_{fg}$ for n-alkanes and LTPRI

When the data of $\log K_{fg}$ for PDMS as a function of LTPRI were plotted (Figure 3.1), a linear relationship was observed. The equation for the relationship for the studied n-alkanes ranging from n-pentane to n-tetradecane, inclusive, is shown in Figure 3.1, and given here, $\log_{10} K_{fg} = 0.0042\,LTPRI - 0.188$, with the predicted linear relationship between $\log K_{fg}$ and LTPRI shown with Equation 3.17. Table 3.1 summarizes the retention times, the K_{fg}, and the $\log K_{fg}$ for the n-alkanes from n-pentane to n-tetradecane, inclusive.

The data in Table 3.1 were used to establish the LTPRI data shown in Tables 3.2 and 3.3, which is discussed below. Additionally, from Table 3.1, there is a linear relationship between t_r and LTPRI for the n-alkanes ranging from octane to tetradecane (r^2=0.9996) thus providing agreement with literature findings (9).

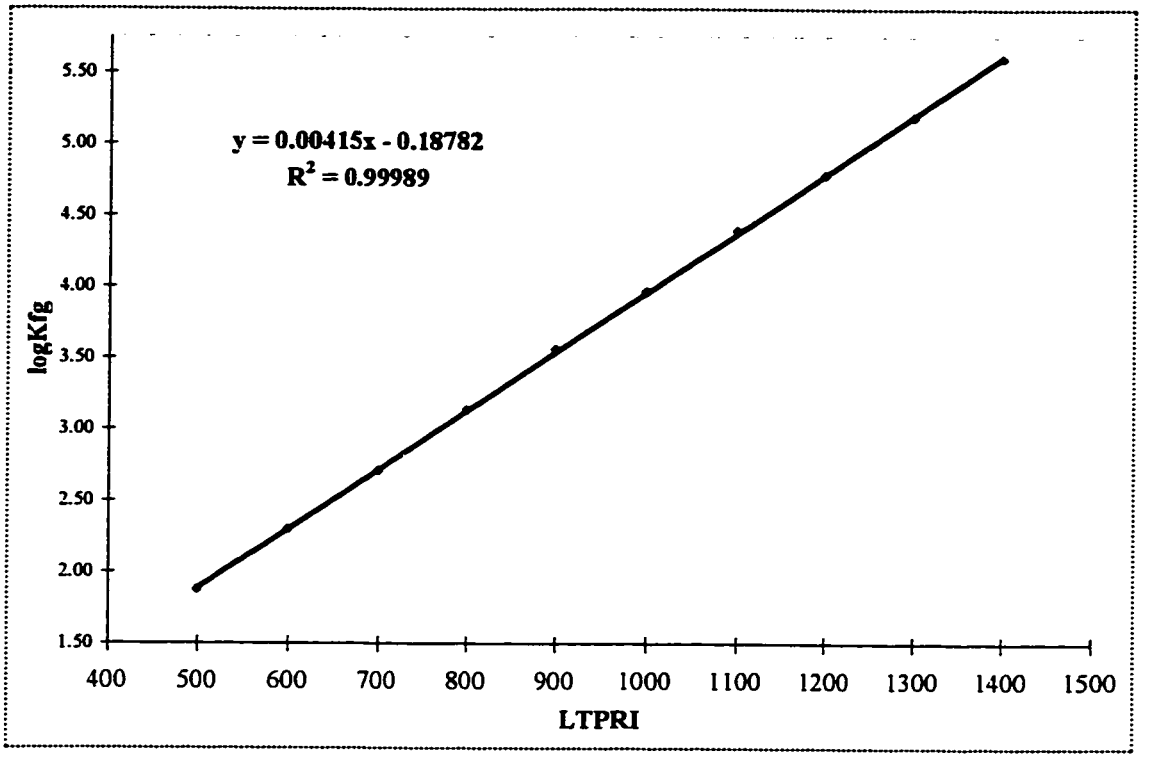

Figure 3.1: $\log_{10}K_{fg}$ for PDMS/air as a function of LTPRI for n-alkanes at 25 °C.

Table 3.1: Summary of data for the series of n-alkanes studied.

n-alkane	LTPRI	tr (min.)	K_{fg} (25 °C)	$\log_{10}(K_{fg})$
pentane	500	4.508	9.5E+01	1.97
hexane	600	6.868	1.5E+02	2.18
heptane	700	11.948	5.1E+02	2.71
octane	800	20.957	1.4E+03	3.14
nonane	900	33.643	3.7E+03	3.56
decane	1000	47.924	9.3E+03	3.97
undecane	1100	62.599	2.5E+04	4.40
dodecane	1200	76.879	6.1E+04	4.78
tridecane	1300	90.501	1.6E+05	5.19
tetradecane	1400	103.39	4.0E+05	5.61

Figure 3.2 shows the chromatogram obtained from the SPME sampling of the standard gas mixture of equal concentrations (37 μg/L each) of n-alkanes described above. This figure shows that n-tetradecane has a significantly larger mass loaded on the fiber compared to n-pentane, thus reflecting the fact that K_{fg} values increase with increasing carbon number, and with increasing retention time, as was observed and described in Chapter 2. Typical relative standard deviations (RSD) of retention times for repeat injections yielded no more then 0.30 % RSD. The K_{fg} values for each of the n-alkanes were determined using a 20 L standard gas generating device described in Chapter 2, thus eliminating the problems associated with establishing K_{fg} values obtained from small sampling vessels (Chapter 1) (12).

Another interesting finding is that there is a linear relationship from the plot of ΔH^v of each n-alkane from a series of n-alkanes as a function of their carbon number (therefore, by definition, their retention index values when n is multiplied by 100). Figure 3.3 shows the plot, with the linear relationship between the ΔH^v and carbon number. It should be noted the relationship appears to posses a sinusoidal relationship; however, no explanation, other than experimental error, can be attributed to this observation. This relationship corroborates the one from Chapter 2 where a linear relationship was observed between $\log K_{fg}$ and 1/T with the slope = $\Delta H^v/R$ which therefore means there should be a linear relationship between ΔH^v. Also, from Chapter 2, Figure 2.1, the K_{fg} for PDMS increased with increasing analyte chromatographic retention time. Therefore, the linear relationship between ΔH^v and carbon number could have been predicted. As such, this finding provides another method to predict LTPRI and K_{fg}.

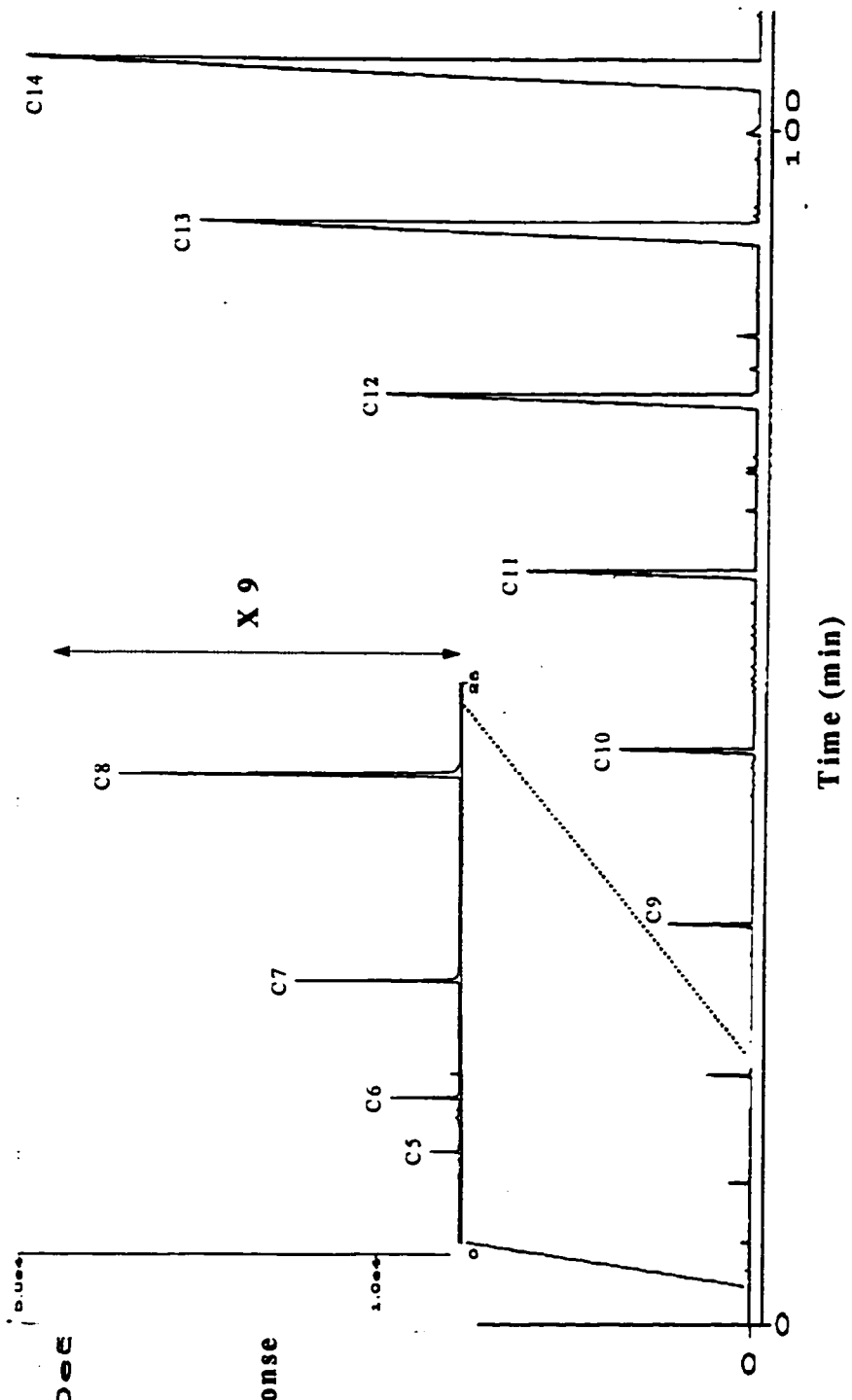

Figure 3.2: Chromatogram of n-alkanes (Conditions: See Text). The 7 µm PDMS fiber was used (lower mass loading) to properly determine the retention times for those compounds with large peak widths at half height.

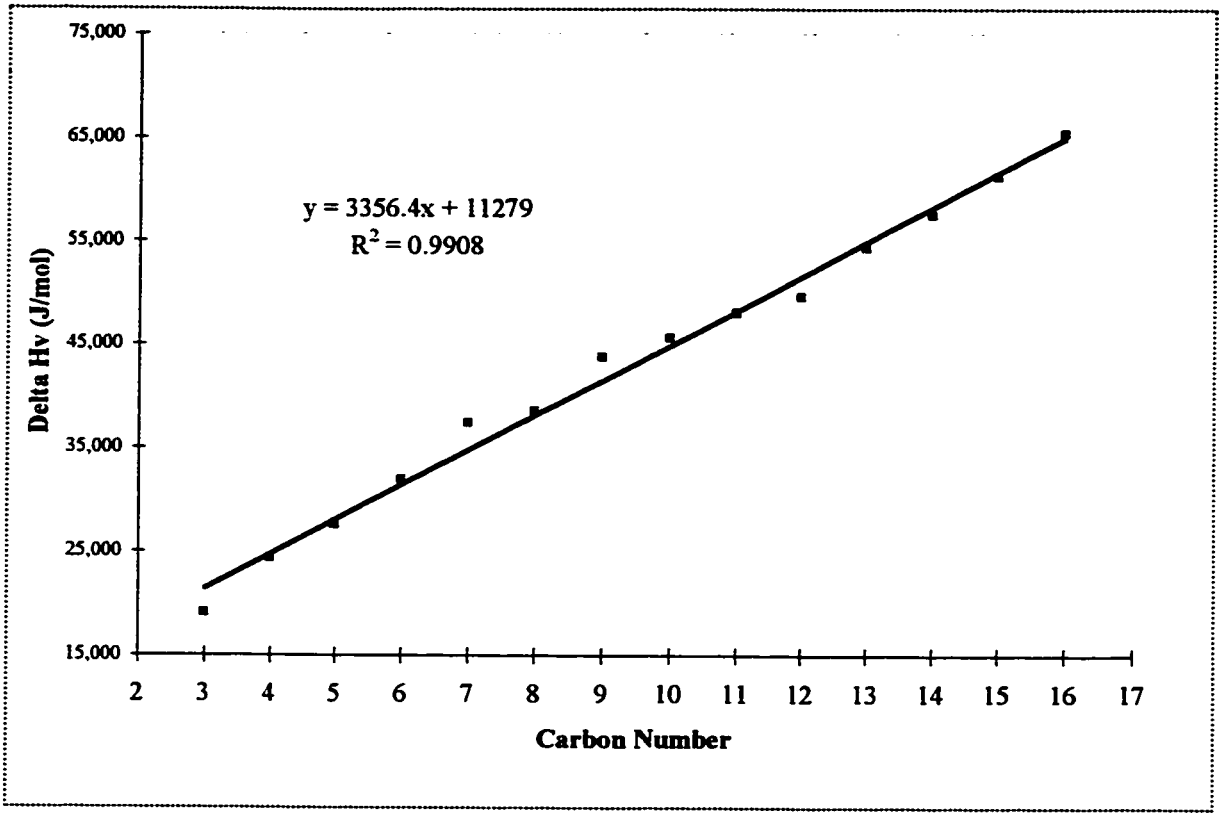

Figure 3.3: Plot of the ΔH^v (J/mol) as a function of carbon number for the series of n-alkanes from propane to hexadecane, inclusive (CRC).

3.4.2 Estimation of K_{fg} values from literature and experimentally determined LTPRI and comparison to directly determined K_{fg} values with SPME

Using the n-alkane retention times provided in Table 3.1, LTPRI for the studied isoparaffinic and aromatic compounds, Equation 3.17, were calculated. The isoparaffinic compounds ranged in retention indices from 576.8 to 971.6 and from 640.7 to 1247.2 for the aromatics. Table 3.2 summarizes the data for the isoparaffins and Figure 3.4 shows the chromatogram obtained. Table 3.3 summarizes the data for the aromatic compounds and Figure 3.5 shows the chromatogram obtained. The group of isoparaffins was bracketed by n-pentane to n-decane, inclusive, while the group of aromatics was bracketed by n-hexane to n-dodecane, inclusive. Columns A and B in both tables summarize the LTPRI provided with

the standard mixtures and literature LTPRI, respectively. Column C shows the calculated LTPRI (Equation 3.13) based on the analyte retention times shown in column D. It should be noted that except for a few compounds for which literature values were not readily available, all data in column C agree very well with those in columns A and B and fall within reported ranges (9,8,13). Once the LTPRI values were established for each compound, a K_{fg} value was estimated using $\log K_{fg} = 0.0042 LTPRI - 0.188$, the results of which are presented in column E. Column F shows the K_{fg} value, as calculated with Equation 1.6, directly obtained from the exposure of SPME fiber coated with 100 μm PDMS from a standard gas mixture of the isoparrafins (29 compounds) and 30 μm PDMS from a standard gas mixture of the aromatics (33 compounds). Finally, column G shows the percent relative error (% Er) between columns E and F. The data in column G clearly demonstrate that, except for a few compounds, the %Er were well below 10%, thus substantiating the validity of the method to estimate K_{fg} values for SPME. Figures 3.4 and 3.5 show the SPME chromatograms for the isoparaffinic and aromatic compound mixtures with the 100 μm PDMS fiber and the 30 μm PDMS fiber, respectively. Both chromatograms show by peak height that there is increasing mass loaded on the fiber with increasing retention time, similar to the phenomenon presented in Figure 3.2. It should be noted there are some peaks which do not appear to follow the trend observed in Figure 3.2 because the standard gas mixtures for the isoparrafins and aromatics were not made up of equal amounts of each analyte; however, the same trend as in Figure 3.2 was observed when the peak areas for the isoparrafins and aromatics were normalized for the amount of analyte in the mixture.

There is an error of approximately 3% in the K_{fg} value for a window of ± 3 LTPRI units which can be considered insignificant. With the methods previously described (3) and

presented in this chapter, air concentrations of any analyte can be established at any temperature without experimentally calibrating the fiber. Conversely, we can verify directly determined K_{fg} values using this approach thus providing a measure of the accuracy of the experimental K_{fg} value. Finally, other homologous series can be studied using this method thus further extending this fundamental relationship.

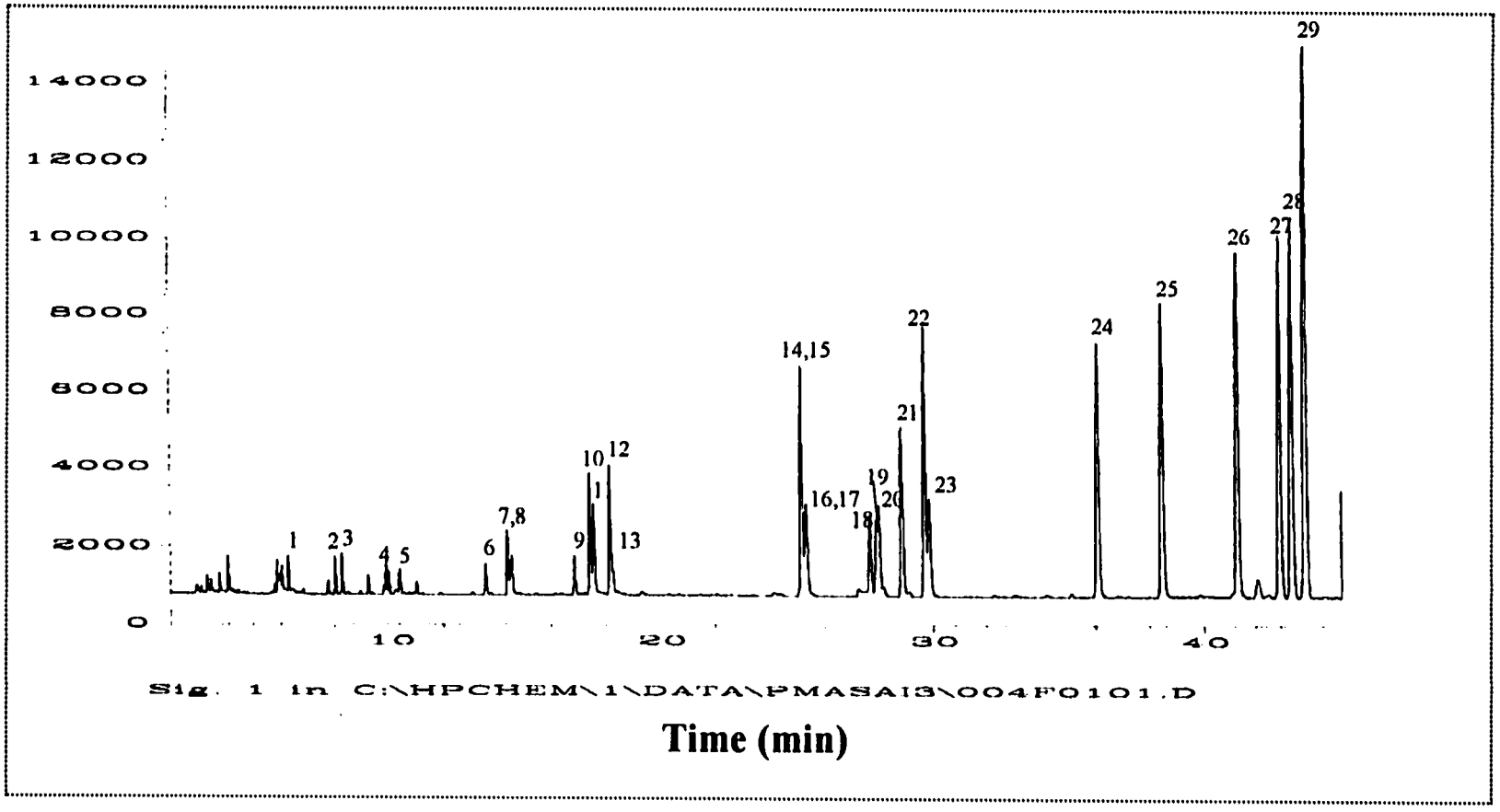

Figure 3.4: Chromatogram for the isoparaffins (Conditions: See Text). 1) 3-Methylpentane, 2) 2,4-Dimethylpentane, 3) 2,2,3-Trimethylbutane, 4) 2-Methylhexane, 5) 2,3-Dimethylpentane, 6) 2,2-Dimethylhexane, 7) 2,5-Dimethylhexane, 8) 2,2,3-Trimethylpentane, 9) 2,3-Dimethylhexane, 10) 2-Methylheptane, 11) 4-Methylheptane, 12) 3-Methylheptane, 13) 3-Ethylhexane, 14) 2,5-Dimethylheptane, 15) 3,5-Dimethylheptane (D), 16) 3,3-Dimethylheptane, 17) 3,5-Dimethylheptane, (L) 18) 2,3-Dimethylheptane, 19) 3,4-Dimethylheptane (D), 20) 3,4-Dimethylheptane (L), 21) 2-Methyloctane 22) 3-Methyloctane, 23) 3,3-Diethylpentane, 24) 2,2-Dimethyloctane, 25) 3,3-Dimethyloctane, 26) 2,3-Dimethyloctane, 27) 2-Methylnonane, 28) 3-Ethyloctane, 29) 3-Methylnonane.

Table 3.2: Summary of data for the isoparaffinic compounds.

Peak	Compound	A LTPRI Stand.	B LTPRI Lit.	C LTPRI Cal.	D tr (min.)	E K_{fg} LTPRI	F K_{fg} SPME	G % Er (K_{fg})
1	3-Methylpentane	571.1	577.2	576.8	6.320	157	159	0.94%
2	2,4-Dimethylpentane	620.3	624.2	623.1	8.042	246	262	6.4%
3	2,2,3-Trimethylbutane	624.7	629.0	628.1	8.295	258	280	8.2%
4	2-Methylhexane	656.9	661.2	659.6	9.898	351	387	10%
5	2,3-Dimethylpentane	658.5	662.8	661.7	10.00	358	412	15%
6	2,2-Dimethylhexane	717.0	719.3	717.9	13.565	616	673	9.2%
7	2,5-Dimethylhexane	726.9	728.7	726.9	14.375	672	587	-13%
8	2,2,3-Trimethylpentane	726.9	729.7	726.9	14.375	672	569	-15%
9	2,3-Dimethylhexane	754.1	756.7	754.5	16.862	877	968	10%
10	2-Methylheptane	761.1	763.0	761.0	17.440	933	993	6.4%
11	4-Methylheptane	762.5	764.6	762.5	17.579	947	1,055	11%
12	3-Methylheptane	768.7	771.0	769.0	18.167	1,009	1,090	8.1%
13	3-Ethylhexane	769.7	772.0	770.1	18.265	1,019	985	-3.3%
14	2,5-Dimethylheptane	827.4	837.0	833.3	25.177	1,876	1,970	5.0%
15	3,5-Dimethylheptane (D)	827.4	NA	833.3	25.177	1,876	1,955	4.2%
16	3,3-Dimethylheptane	828.6	835.4	834.6	25.345	1,901	2,086	9.8%
17	3,5-Dimethylheptane (L)	828.6	NA	834.6	25.345	1,901	2,096	10%
18	2,3-Dimethylheptane	846.5	857.5	853.1	27.692	2,273	2,385	4.9%
19	3,4-Dimethylheptane (D)	848.3	NA	855.0	27.928	2,314	2,420	4.6%
20	3,4-Dimethylheptane (L)	849.2	NA	855.7	28.025	2,331	2,616	12%
21	2-Methyloctane	856.3	864.6	862.3	28.865	2,485	2,603	4.7%
22	3-Methyloctane	863.4	872.2	869.6	29.788	2,666	2,893	8.5%
23	3,3-Diethylpentane	864.3	873.6	870.6	29.919	2,693	2,609	-3.1%
24	2,2-Dimethyloctane	920.3	918.7	917.6	36.156	4,239	4,322	2.0%
25	3,3-Dimethyloctane	939.3	936.0	934.4	38.553	4,985	5,046	1.2%
26	2,3-Dimethyloctane	958.8	954.8	953.9	41.345	6,022	6,096	1.2%
27	2-Methylnonane	968.6	965.2	964.8	42.890	6,686	6,692	0.09%
28	3-Ethyloctane	971.3	968.4	967.9	43.335	6,890	6,974	1.2%
29	3-Methylnonane	974.2	971.6	971.7	43.878	7,148	7,098	-0.69%

A) The LTPRI provided with the certified standard.
B) The literature LTPRI. (13)
C) The calculated LTPRI by using the experimentally obtained retention times (column D) for the individual hydrocarbons. The $\log K_{fg}$ vs. LTPRI calibration curve ranged from pentane to decane for the isoparaffins. The slope and y-int were 0.00420 and -0.224 respectively.
D) The retention time for the individual isoparaffins.
E) The K_{fg} values as determined by the $\log K_{fg}$ versus LTPRI (column C) relationship.
F) The K_{fg} values determined experimentally by using Equation 3.1.
G) The relative error between the K_{fg} values in columns E and F.

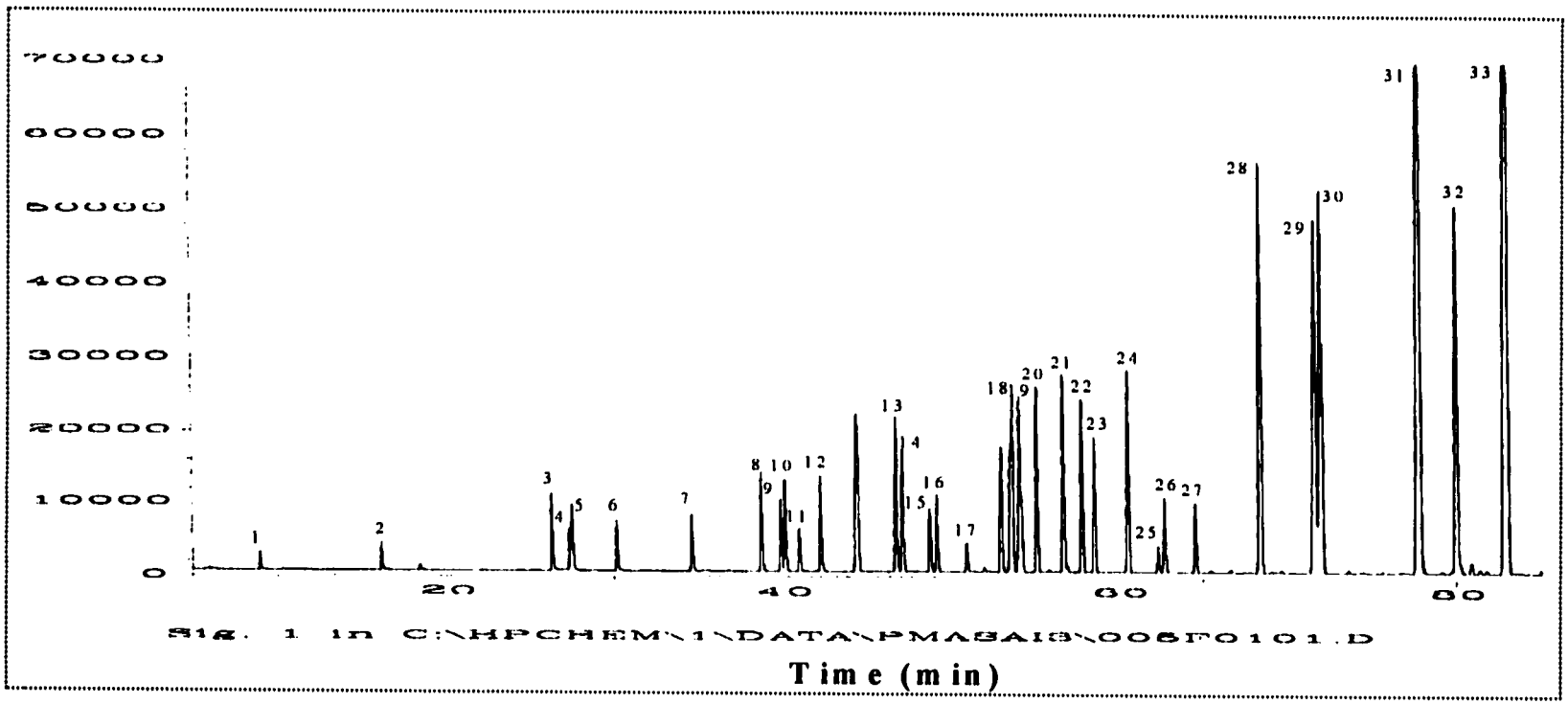

Figure 3.5: Chromatogram for aromatics (Conditions: See Text). 1) Benzene, 2) Toluene, 3) Ethylbenzene, 4) m-Xylene, 5) p-Xylene, 6) o-Xylene, 7) Isopropylbenzene ,8) n-Propylbenzene, 9) 1-Methyl-3-Ethylbenzene, 10) 1-Methyl-4-Ethylbenzene, 11) 1,3,5-Trimethylbenzene, 12) 1-Methyl-2-Ethylbenzene, 13) Isobutylbenzene, 14)sec-Butylbenzene, 15) 1-Methyl-3-Isopropylbenzene, 16) 1-Methyl-4-Isopropylbenzene, 17) 1-Methyl-2-Isopropylbenzene, 18) 1-Methyl-3-n-Propylbenzene, 19) 1,3-Dimethyl-5-Ethylbenzene, 20) 1-Methyl-2-n-Propylbenzene, 21) 1,4-Dimethyl-2-Ethylbenzene, 22) 1,2-Dimethyl-4-Ethylbenzene, 23) 1,3-Dimethyl-2-Ethylbenzene, 24) 1,2-Dimethyl-3-Ethylbenzene, 25) 1,2,4,5-Tetramethylbenzene, 26) 2-Methylbutylbenzene, 27) tert-1-Butyl-2-Methylbenzene, 28) n-Pentylbenzene, 29) t-1-Butyl-3,5-Dimethylbenzene, 30) t-1-Butyl-4-Ethylbenzene, 31) 1,3,5-Triethylbenzene, 32) 1,2,4-Triethylbenzene, 33) n-Hexylbenzene

Table 3.3: Summary of data for the aromatic compounds.

Peak	Compound	A LTPRI Stand	B LTPRI Lit.	C LTPRI Cal.	D tr (min)	E K_{fg} LTPRI	F K_{fg} SPME	G % Er (K_{fg})
1	Benzene	638.6	642.0	640.7	8.934	296	301	1.7%
2	Toluene	747.1	749.0	746.5	16.141	815	818	0.39%
3	Ethylbenzene	836.1	844.7	841.7	26.244	2,023	2,066	2.1%
4	*m*-Xylene	844.6	853.4	850.2	27.321	2,194	2,088	-4.8%
5	*p*-Xylene	845.7	854.8	851.3	27.460	2,217	2,500	13%
6	*o*-Xylene	867.9	NA	872.3	30.126	2,710	2,904	7.1%
7	Isopropylbenzene	907.9	909.6	907.2	34.670	3,784	3,876	2.4%
8	n-Propylbenzene	942.1	938.2	935.4	38.700	4,955	5,036	1.6%
9	1-Methyl-3-Ethylbenzene	950.4	946.9	943.2	39.816	5,339	4,753	-11%
10	1-Methyl-4-Ethylbenzene	952.2	948.9	945.1	40.087	5,437	6,225	15%
11	1,3,5-Trimethylbenzene	964.1	954.7	958.0	41.920	6,147	6,484	5.5%
12	1-Methyl-2-Ethylbenzene	966.4	963.7	959.9	42.199	6,262	6,584	5.1%
13	Isobutylbenzene	992.7	996.8	991.3	46.682	8,454	8,355	-1.2%
14	sec-Butylbenzene	994.7	NA	994.1	47.053	8,680	8,589	-1.0%
15	1-Methyl-3-Isopropylbenzene	1005.9	1007.8	1005.2	48.689	9,655	10,139	5.0%
16	1-Methyl-4-Isopropylbenzene	1008.6	1010.9	1008.1	49.109	9,923	10,182	2.6%
17	1-Methyl-2-Isopropylbenzene	1022.7	1023.9	1020.4	50.917	11,163	12,026	7.7%
18	1-Methyl-3-n-Propylbenzene	1037.5	1037.8	1034.5	53.659	12,776	13,186	3.2%
19	1,3-Dimethyl-5-Ethylbenzene	1041.3	1044.2	1041.9	54.070	13,708	15,008	9.5%
20	1-Methyl-2-n-Propylbenzene	1052.5	1052.7	1048.9	55.100	14,659	14,891	1.6%
21	1,4-Dimethyl-2-Ethylbenzene	1063	1063.1	1059.6	56.675	16,242	15,906	-2.1%
22	1,2-Dimethyl-4-Ethylbenzene	1070.3	1070.7	1067.1	57.768	17,441	17,434	-0.04%
23	1,3-Dimethyl-2-Ethylbenzene	1075.7	1076.4	1072.1	58.504	18,297	18,104	-1.1%
24	1,2-Dimethyl-3-Ethylbenzene	1088.4	1090.0	1085.8	60.510	20,850	19,984	-4.2%
25	1,2,4,5-Tetramethylbenzene	1101.2	1101.8	1097.9	62.285	23,406	24,703	5.5%
26	2-Methylbutylbenzene	1102.1	1104.8	1100.7	62.697	24,046	24,112	0.27%
27	tert-1-Butyl-2-Methylbenzene	1117.2	NA	1113.4	64.509	27,147	26,194	-3.5%
28	n-Pentylbenzene	1143.1	1144.3	1140.9	68.443	35,323	34,489	-2.4%
29	t-1-Butyl-3,5-Dimethylbenzene	1164.0	1165.0	1163.6	71.675	43,854	45,586	3.9%
30	t-1-Butyl-4-Ethylbenzene	1169.4	NA	1165.9	72.015	44,863	43,657	-2.7%
31	1,3,5-Triethylbenzene	1205.7	1207.9	1207.6	77.925	66,785	67,323	0.81%
32	1,2,4-Triethylbenzene	1225.2	1226.1	1223.2	80.090	77,570	75,573	-2.6%
33	n-Hexylbenzene	1247.2	1247.2	1245.2	83.132	95,731	90,091	-5.9%

A) The LTPRI provided with the certified standard.

B) The literature LTPRI (13).

C) The calculated LTPRI by using the experimentally obtained retention times (column D) for the individual hydrocarbons. The $\log K_{fg}$ vs. LTPRI calibration curve ranged from hexane to dodecane for the aromatics.

D) The retention time for the individual aromatics. The slope and y-int were 0.00415 and -0.1875.

E) The K_{fg} values as determined by the $\log K_{fg}$ versus LTPRI (column C) relationship.

F) The K_{fg} values determined experimentally with Equation 3.1.

G) The relative error between the K_{fg} values in columns E and F.

Note: For n-hexylbenzene, the K_{fg} value was adjusted upwards by 1.3 % to compensate for the extraction of this compound.

3.4.3 Estimating SPME detection limits with K_{fg}

A method to estimate detection limits (LOD) for C_g with PDMS without experimentation would be useful. In Chapters 2 and 3, relationships between K_{fg} and temperature as well as LTPRI provide a flexible method to using PDMS for air sampling without calibration. Those relationships can also be used to estimate detection limits. This is done by calculating the K_{fg} from LTPRI data. Once the K_{fg} is estimated, its temperature dependence can also be estimated (Chapter 2). The estimated detection limit of an airborne analyte with PDMS will be related to the minimum amount of which that analyte can be detected on a mass basis. Equation 3.29 combines the aforementioned points.

$$C_{g(LOD)} = \frac{n_{f(LOD)}}{V_f} \times \frac{1}{K_{fg}} \text{ (constant T)} - \frac{n_{f(LOD)}}{V_f} \times \frac{1}{\left(10^{\frac{a}{T}+b}\right)} \text{ (other T)} \qquad \text{Equation 3.29}$$

where $n_{f(LOD)}$ is the lowest mass of analyte which can be detected from the SPME, with the other terms as familiar. The equation indicates that as K_{fg} increases, the $C_{g(LOD)}$ will decrease correspondingly because the instrument detection limit is relatively constant for compounds of similar chemical properties, such as the hydrocarbons. This equation will be used in Chapter 6.

3.4.4 Analysis of airborne gasoline with SPME and comparison to active sampling with charcoal tubes for a total petroleum hydrocarbon value

An airborne mixture of gasoline sampled with PDMS fiber coatings and analyzed by GC/FID is shown in Figure 3.6. The objective was to obtain a total (airborne) petroleum hydrocarbon (TPH) value or also termed Total Volatile Organic Carbon (TVOC). This parameter is extensively used in environmental air sampling (15). The K_{fg} value for each peak in this chromatogram was determined with its LTPRI from the equation shown in Figure 3.1,

provided here, $\log K_{fg} = 0.0042 LTPRI - 0.188$. The amount on the fiber (n_f) for each peak was determined from the peak's area count (based on a toluene equivalent, assuming a constant response factor for each peak). The air concentration, Equation 3.1, was calculated for each peak, then summed providing a TPH in air concentration of 262 ± 13 µg/L at 25°C compared to the airborne TPH value of 247 ± 10 µg/L obtained by air sampling the same gas mixture with charcoal tubes. This small difference is explained by considering the interference presented by carbon disulphide which is used to chemically desorb charcoal adsorbed analytes (Figure 2.2A, Chapter 2 has an example of this).

These results further indicate an extremely promising use of SPME for air sampling. No external calibration procedures are required. The analyst needs only to calibrate the FID with standard liquid injections, acquire the air sample with PDMS (at constant temperature), then quantify the analyte concentrations directly from the chromatogram via the retention times and the relationship between $\log K_{fg}$ and LTPRI. Finally, a faster ramp rate can be used to reduce analysis time without contributing a significant error to the overall result.

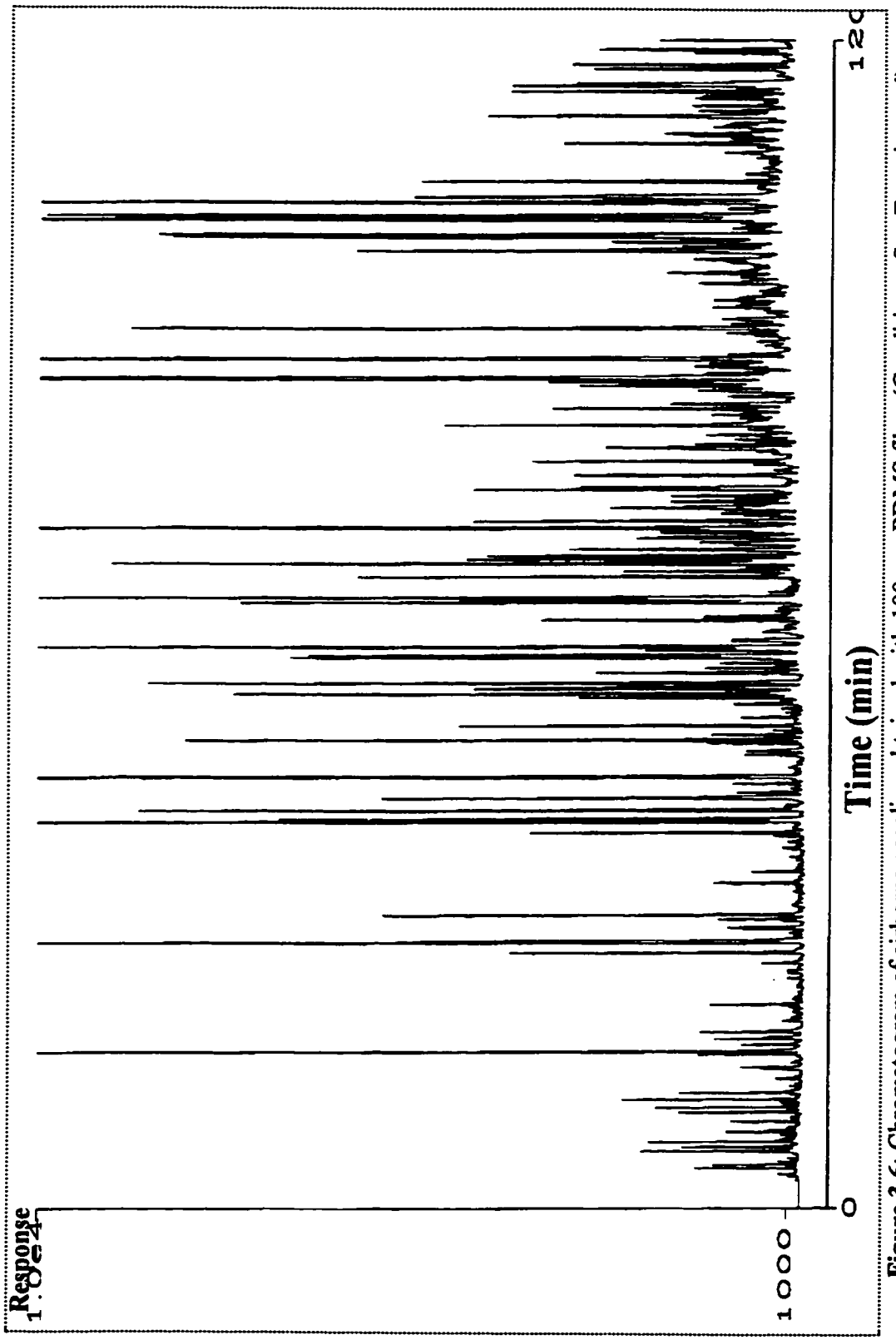

Figure 3.6: Chromatogram of airborne gasoline obtained with 100 µm PDMS fiber (Conditions: See Experimental)

3.5 Summary

LTPRI can be applied to establish partition coefficients for airborne analytes to SPME fibers coated with PDMS, based on the linear relationship between $\log K_{fg}$ and LTPRI for a homologous series of compounds such as the n-alkanes. A number of advantages can be realized with this application, namely obviating the necessity for the analyst to experimentally determine K_{fg} values, a way to estimate airborne analyte detection limits given K_{fg} and C_g (Equation 3.29), and finally quantifying airborne analytes without an external calibration curve.

Very complex mixtures of unknown airborne organics could not be quantified, until now, by SPME due to the fact the K_{fg} value for each of the peaks were difficult or impossible to determine, especially if no standard was available. Using the method presented herein, the unknown compound's LTPRI can be used to establish its K_{fg} for SPME. Once the K_{fg} value is known for that compound, its air concentration can be determined and summed with all the other components from the mixture providing a total volatile organic concentration in air, which is an excellent marker of air quality (Chapter 1) (15). In addition, the analysis of air samples for airborne TPH using SPME can be simplified with the use of a post-run macro which could calculate each peak's LTPRI and the corresponding K_{fg}, convert the peak areas to mass loaded on the fiber, calculate the air concentration for that peak based on Equation 3.1, and sum up all individual peak concentrations thus providing airborne total organic concentration. There is an excellent agreement between the results obtained by sampling and analysis of an air stream containing gasoline with SPME fiber coated with PDMS and charcoal tube samples which proves the method described can be used for quantitation of individual

compounds, known or unknown (given approximately similar response factors). A pre-screen of the air sample in question with GC/mass spectrometry can provide information whether halogenated organics, or other substituted organics, are present. If the air sample is predominantly non-halogenated, then GC/FID can be safely used for the quantification.

In cases where the solutes and the stationary phase differ significantly with respect to the chemical character of the calibration retention index standard (e.g., n-alkanes on polar phases), other homologous series instead of the n-alkanes should be used. For example, appropriate methyl esters of linear saturated fatty acids can be used as the standard for the determination of methyl esters of unsaturated fatty acids (8). In fact, this method was recently used to quantify airborne long-chain esters and proved successful (16).

3.6 References

1. Martos, P., Saraullo, A., and Pawliszyn, J., Anal. Chem. **69** (3), 1997, pp. 402-408

2. Martos, P. and Pawliszyn, J., Anal. Chem., **69** (2), 1997, pp. 206-215

3. Laub, R.J. and Pecsok, R.L, *Physicochemical Applications of Gas Chromatography*, John Wiley and Sons: New York, 1978, Chapter 2

4. Castellan, G.W., *Physical Chemistry*, 3rd edition, Addison-Wesley Publishing Company, 1983, Chapter 11

5. Pacáková, V. and Ladislav F., *Chromatographic Retention Indices*, , Ellis Horwood Ltd., England, 1992; pp 21-22

6. *The Sadtler Capillary GC Standard Retention Index Library and Data Base*, Sadtler Research Laboratories, Philadelphia, USA.

7. Poole, C.F. and Schuette, S.A., *Contemporary Practice of Chromatography*; Elsevier Science; New York, 1984; page 24.

8. Zhang, Z. and Pawliszyn, J.; *J. Physical Chemistry*, **1996**, *100*, 17648-17654

9. Rotzsche, H. *Stationary Phases in Gas Chromatography*; Elsevier Science Publishing Company Inc.: New York,1990; Chapter 4.

10. Golovnya, R.V. and Arsenyev, Yu. N. *Chromatographia* **1971**, *4*, 250-258

11. Golovnya, R.V. and Misharina, T.A. *Chromatographia* **1977**, *10*, 658-660

12. Saraullo, A., Martos, P., and Pawliszyn, J., Anal. Chem., **69**, 1997, pp.

13. Pawliszyn, J. *Solid Phase Microectraction - Theory and Practice*, Wiley-VCH, 1997

14. *National Institute for Occupational Safety and Health Manual of Analytical Methods*, 1994, U.S. Department of Health and Human Services, electronic version.

15. Batterman, S. and Peng, C., Am. Ind. Hyg. Assoc. J., **56** 1995 pp. 55-65

16. Górecki, T. personal communication

CHAPTER 4

SAMPLING FORMALDEHYDE WITH SPME

4.1 Background

The previous chapters presented how the PDMS coating can be used for air sampling hydrocarbons based on physical-chemical properties of the coating. That coating is not suitable to sample a large range of other important compounds, such as the aldehydes, in particular, formaldehyde (HCHO). The 100 μm PDMS coating cannot mass load a sufficient quantity of HCHO and HCHO is not, without derivatization, sufficiently detectable with chromatographic detectors. This chapter presents the development of a novel method to sample airborne HCHO using SPME with on-fiber derivatization.

HCHO is a ubiquitous airborne contaminant in our environment as a result of its use in plywood and particle board (1), medium density fiberboard, adhesives used for tiling, cosmetic products, from ozone generators (2), carpeting, fuel-burning appliances and fire place exhaust (3), tobacco smoke (4,5), as a preservative in some paints, insulation (6), to add permanent-press qualities to clothing and draperies, as specimen preservatives in hospitals, laboratories, mortuaries, and others (7,8,9).

HCHO is a colorless gas with a pungent odor detectable at approximately 1 ppmv; however, its toxicity in humans can be observed at concentrations significantly less than 1 ppmv. HCHO is a probable human carcinogen according to the U.S.E.P.A. while NIOSH and OSHA recognize it is a known animal carcinogen, and the American Conference of Governmental Industrial Hygienists recognizes HCHO as a suspected human carcinogen (10,11). At concentrations marginally greater than 100 ppb_v, HCHO can cause watery eyes,

itching skin, burning sensations in mucous membranes (eyes), nausea, difficulty breathing, and of concern, sensitization in a percentage of the population who are chronically, and sometimes acutely, exposed to it. Acceptable concentrations of formaldehyde in ambient air are reported to range from 80 to 100 ppb_v (12).

Sensitive sampling and analysis methods for formaldehyde at these levels presents a number of analytical problems specifically related to the difficulty in detecting HCHO. The sampling and analysis methods can be generally categorized as colorimetric, polarographic, gas and liquid chromatographic (GC and HPLC) (13). In addition, the methods can be further divided according to whether detection of HCHO is required below 100 ppb_v, i.e., ambient air levels (in contrast to levels observed in occupational settings). For detection of ambient HCHO concentrations, there are standard methods which use active air sampling over solid adsorbent cartridges coated with dinitrophenyl hydrazine (DNPH) followed by analysis with HPLC (14). A method which can be used to sample HCHO concentrations above 100 ppb_v (15) makes use of active air sampling over a solid sorbent coated with hydroxymethyl piperidine (HMP) and analysis by GC. There are a number of other methods which can be used to sample HCHO at concentrations above 100 ppb_v (16). It is clear that there is a requirement for better sampling and analysis methods for HCHO for large concentration ranges as demonstrated by the fact there are a number of recent methods which attempt to increase analytical sensitivity while undertaking to reduce the analysis time and simplifying the overall method (17,18,19,20). Rapid yet sensitive measurements of HCHO levels during the manufacture of materials such as food and cosmetics can provide enhanced process control (21). Therefore, a sampling and analysis method for airborne or headspace levels of HCHO, which is simple to use yet yields high sensitivity and is extremely cost effective, is required and

would be of extreme benefit.

Until now, no method employing SPME for sampling HCHO has been successful. Shown in this chapter is a novel sampling method for gaseous HCHO employing SPME and on-fiber derivatization with *o*-(2,3,4,5,6-pentafluorobenzyl)-hydroxylamine (PFBHA). Also shown in this chapter is the proposed physical-chemical and kinetic relationship between sorbed PFBHA and reaction with gaseous HCHO forming the stable PFBHA-HCHO oxime. It is not possible to sample and analyze HCHO with SPME and GC/FID without derivatization. As stated in Chapter 1, sampling gaseous phases for target analytes with SPME provides a significant advantage over traditional methods, both active sampling and whole air sampling. SPME requires no sampling pumps, is easy to deploy, re-usable and amenable to automation.

In addition, derivatization sampling for HCHO realizes a number of advantages over techniques not employing derivatization: 1. provides analyte specificity based on key functional groups, 2. allows for detection with conventional detectors (for those compounds which do not yield a response), 3. can provide for sampling based on first order rate kinetics, and 4. can act as a method for confirmation that the compound of interest is present in the sample.

This new sampling method can be used to sample HCHO in air and the off-gassing of HCHO from materials. In addition, it can be used to monitor ambient air levels of HCHO while maintaining the flexibility to quantify high HCHO concentrations. The sampling method is rapid, highly reproducible, and can utilize an empirically obtained 1st order rate constant for quantitation without the need for interpolation from calibration curves; however, the latter is possible if required. Data are also included on the use of SPME to sample HCHO under a

number of different conditions such as temperature, a large range of HCHO concentrations and static gas sampling versus dynamic gas sampling. In this chapter, it is emphasized the exposed fiber position is used to sample HCHO (Chapter 1).

4.2 Theory

There are four steps to consider in describing the overall rate of formation of PFBHA-carbonyl oxime as a function of gaseous carbonyl. Shown below are the individual steps in the sampling system for PFBHA loaded onto the SPME coating, PDMS/DVB, with exposure to carbonyl.

(Step A) $PFBHA + S \xrightarrow{k_1} PFBHA*S$ (adsorption)

$PFBHA*S \xrightarrow{k_{-1}} PFBHA + S$ (desorption)

(Step B) $Carbonyl + S \xrightarrow{k_2} Carbonyl*S$ (adsorption)

$Carbonyl*S \xrightarrow{k_{-2}} Carbonyl + S$ (desorption)

(Step C) $Carbonyl + PFBHA*S \xrightarrow{K^*} Oxime*S$ (reaction)

(Step D) $Oxime*S \xrightarrow{k_{-3}} Oxime + S$ (desorption)

Also, $K_A = \frac{k_1}{k_{-1}}$ and $K_B = \frac{k_2}{k_{-2}}$. It is assumed that loading of PFBHA (Step A) is ostensibly irreversible (based on experimental results), that the number of available sites for sorption of other compounds may occur, (Step B), that the reaction rate K^* (Step C) is rate limiting (in contrast to the analyte rate of diffusion) and finally, that the rate of desorption of the product (Step D) does not occur to any significant degree at ambient temperature due to the strong

affinity of the PFBHA-Carbonyl oxime for the sorbent, i.e., $k_{-3} = 0$. Finally, the PFBHA aromatic moiety is assumed to provide the majority of the adsorption to the polymer while the hydroxyl amine moiety is free to react with an approaching carbonyl compound.

Based on the nature of the sampling system, the Langmuir-Rideal mechanism for the process is assumed (22). This mechanism is assumed because the Langmuir-Rideal theory accounts for a reaction between an adsorbed molecule and a gas phase molecule, which is precisely the case for the sampling system employing adsorbed PFBHA onto PDMS/DVB followed by exposure to gaseous carbonyl. When there are two molecules, such as PFBHA and HCHO, which can bind to any of the sites on the PDMS/DVB porous polymer, there can be competitive adsorption; however, because PFBHA ostensibly saturates all of the PDMS/DVB sites *prior* to exposure to HCHO (based on experimental evidence), the polymer acts as the surface and PFBHA is the adsorbed molecule, as required by the Langmuir-Rideal theory. Nevertheless, considering the possible binding of the carbonyl to the PDMS/DVB facilitates a better description of the reaction kinetics for those instances when there are carbonyl compounds which may have significantly larger binding affinity constants than that for PFBHA.

If θ is the fraction of surface covered by PFBHA and θ' is the fraction of the surface covered by the carbonyl, HCHO in this case, then $1-\theta-\theta'$ is the fraction of the surface remaining unoccupied. The overall rate of adsorption/desorption of PFBHA is given by Equation 4.1,

$$\frac{\theta}{1-\theta-\theta'} = \frac{k_1}{k_{-1}} C_{PFBHA \cdot S} = K_A C_{PFBHA \cdot S} \qquad \text{Equation 4.1}$$

where K_A represents the rate of adsorption and desorption of PFBHA from the fiber. The

same can be shown for the binding of HCHO to the fiber without reaction (Equation 4.2)

$$\frac{\theta'}{1-\theta-\theta'} = \frac{k_2}{k_{-2}} C_{HCHO} = K_B C_{HCHO} \qquad \text{Equation 4.2}$$

Equation 4.2 can be rearranged to solve for θ' (Equations 4.2a to 4.2d, inclusive),

$$\theta' = K_B C_{HCHO} - \theta K_B C_{HCHO} - \theta' K_B C_{HCHO} \qquad (4.2a)$$

$$\theta' + \theta' K_B C_{HCHO} = K_B C_{HCHO} - \theta K_B C_{HCHO} \qquad (4.2b)$$

$$\theta'(1 + K_B C_{HCHO}) = K_B C_{HCHO} - \theta K_B C_{HCHO} \qquad (4.2c)$$

$$\theta' = \frac{K_B C_{HCHO} - \theta K_B C_{HCHO}}{1 + K_B C_{HCHO}} \qquad (4.2d)$$

this equation can be replaced for θ' into Equation 4.1, yielding Equation 4.3, which, upon rearrangement, yields Equation 4.4,

$$\frac{\theta}{1-\theta-\frac{K_B C_{HCHO} - \theta K_B C_{HCHO}}{1 + K_B C_{HCHO}}} = K_A C_{PFBHA \bullet S} \qquad \text{Equation 4.3}$$

$$\theta = K_A C_{PFBHA \bullet S} - \theta K_A C_{PFBHA \bullet S} - \frac{K_A C_{PFBHA \bullet S} K_B C_{HCHO} - \theta K_A C_{PFBHA \bullet S} K_B C_{HCHO}}{1 + K_B C_{HCHO}} \qquad (4.3a)$$

$$\theta = K_A C_{PFBHA \bullet S} - \theta K_A C_{PFBHA \bullet S} - \frac{K_A C_{PFBHA \bullet S} K_B C_{HCHO}}{1 + K_B C_{HCHO}} - \frac{\theta K_A C_{PFBHA \bullet S} K_B C_{HCHO}}{1 + K_B C_{HCHO}} \qquad (4.3b)$$

$$\theta = K_A C_{PFBHA \bullet S} - \theta(K_A C_{PFBHA \bullet S} - \frac{K_A C_{PFBHA \bullet S} K_B C_{HCHO}}{1 + K_B C_{HCHO}}) - \frac{K_A C_{PFBHA \bullet S} K_B C_{HCHO}}{1 + K_B C_{HCHO}} \qquad (4.3c)$$

$$K_A C_{PFBHA \bullet S} - \frac{K_A C_{PFBHA \bullet S} K_B C_{HCHO}}{1 + K_B C_{HCHO}} = \theta + \theta(K_A C_{PFBHA \bullet S} - \frac{K_A C_{PFBHA \bullet S} K_B C_{HCHO}}{1 + K_B C_{HCHO}}) \qquad (4.3d)$$

$$K_A C_{PFBHA \bullet S} - \frac{K_A C_{PFBHA \bullet S} K_B C_{HCHO}}{1 + K_B C_{HCHO}} = \theta(1 + K_A C_{PFBHA \bullet S} - \frac{K_A C_{PFBHA \bullet S} K_B C_{HCHO}}{1 + K_B C_{HCHO}}) \qquad (4.3e)$$

$$\theta = \frac{K_A C_{PFBHA \bullet S} - \frac{K_A C_{PFBHA \bullet S} K_B C_{HCHO}}{1 + K_B C_{HCHO}}}{1 + K_A C_{PFBHA \bullet S} - \frac{K_A C_{PFBHA \bullet S} K_B C_{HCHO}}{1 + K_B C_{HCHO}}} \tag{4.3f}$$

$$\theta = \frac{K_A C_{PFBHA \bullet S} - \frac{K_A C_{PFBHA \bullet S} K_B C_{HCHO}}{1 + K_B C_{HCHO}}}{1 + K_A C_{PFBHA \bullet S} - \frac{K_A C_{PFBHA \bullet S} K_B C_{HCHO}}{1 + K_B C_{HCHO}}} \times \frac{1 + K_B C_{HCHO}}{1 + K_B C_{HCHO}} \tag{4.3g}$$

$$\theta = \frac{K_A C_{PFBHA \bullet S} + K_A C_{PFBHA \bullet S} K_B C_{HCHO} - K_A C_{PFBHA \bullet S} K_B C_{HCHO}}{1 + K_A C_{PFBHA \bullet S} + K_B C_{HCHO} + K_A C_{PFBHA \bullet S} K_B C_{HCHO} - K_A C_{PFBHA \bullet S} K_B C_{HCHO}} \tag{4.3h}$$

$$\theta = \frac{K_A C_{PFBHA \bullet S}}{1 + K_A C_{PFBHA \bullet S} + K_B C_{HCHO}} \qquad \text{Equation 4.4}$$

Now, if the available surface is almost completely covered with PFBHA before exposure to HCHO, and then when gaseous HCHO approaches the PFBHA coated surface of the fiber, a reaction between the two is much more likely to occur before HCHO can bind to the surface. Recall the fraction of the surface covered by PFBHA is given in Equation 4.1. Also, the model indicates the reaction rate is proportional to the concentration of gaseous analyte (HCHO), the number of sites occupied by PFBHA, in addition to the reaction rate between PFBHA and HCHO, yielding Equation 4.5,

$$v = C_{HCHO} K^* \theta \qquad \text{Equation 4.5}$$

By substituting the fraction of sites occupied by PFBHA, θ, from Equation 4.4 into Equation 4.5 yields Equation 4.6 for the rate of reaction,

$$v = \frac{K^* K_A C_{PFBHA \bullet S} C_{HCHO}}{1 + K_A C_{PFBHA \bullet S} + K_B C_{HCHO}} \qquad \text{Equation 4.6}$$

Equation 4.6 can be rearranged, isolating v and C_{HCHO}, which ultimately yields Equation 4.7 (Equations 4.7a to 4.7c, inclusive),

$$\frac{1}{v} = \frac{1 + K_A C_{PFBHA \bullet S} + K_B C_{HCHO}}{K^* K_A C_{PFBHA \bullet S} C_{HCHO}} \quad (4.7a)$$

$$\frac{1}{v} = \frac{1}{K^* K_A C_{PFBHA \bullet S} C_{HCHO}} + \frac{K_A C_{PFBHA \bullet S}}{K^* K_A C_{PFBHA \bullet S} C_{HCHO}} + \frac{K_B C_{HCHO}}{K^* K_A C_{PFBHA \bullet S} C_{HCHO}} \quad (4.7b)$$

$$\frac{1}{v} = \frac{1}{K^* K_A C_{PFBHA \bullet S} C_{HCHO}} + \frac{1}{K^* C_{HCHO}} + \frac{K_B}{K^* K_A C_{PFBHA \bullet S}} \quad (4.7c)$$

$$\frac{1}{v} = \frac{1}{C_{HCHO}} \left(\frac{1}{K^* K_A C_{PFBHA \bullet S}} + \frac{1}{K^*} \right) + \frac{K_B}{K^* K_A C_{PFBHA \bullet S}} \quad \text{Equation 4.7}$$

A plot of $1/v$ as a function of $1/C_{HCHO}$ would yield a linear relationship where the slope would be $\left(\frac{1}{K^* K_A C_{PFBHA \bullet S}} + \frac{1}{K^*} \right)$ and the y-intercept would be $\frac{K_B}{K^* K_A C_{PFBHA \bullet S}}$ (Equation 4.7). In addition, consider that when $K^* << K_A C_{PFBHA \bullet S}$, Equation 4.7 can be reduced to Equation 4.8,

$$\frac{1}{v} = \frac{1}{C_{HCHO}} \frac{1}{K^*} + \frac{K_B}{K^* K_A C_{PFBHA \bullet S}} \quad \text{Equation 4.8}$$

The slope in Equation 4.7 contains terms for the rate of reaction between gaseous HCHO and the PFBHA loaded on the SPME fiber as well as the K_A and the surface concentration of PFBHA on the fiber; however, the slope in Equation 4.8 is dependent only on the rate of reaction. This condition is easily satisfied when the loss of PFBHA (following reaction and/or desorption) from the sorbent is negligible (Results and Discussion). The inverse of the slope yields an apparent 1st order rate constant, K^*, when the amount of sorbed PFBHA consumed during the reaction is negligible, $\frac{weight}{C_{HCHO} \bullet time}$. The conclusion is that quantitation of unknown HCHO concentrations is possible using the 1st order rate constant when the amount of PFBHA is negligibly consumed, i.e., during short sampling times for high [HCHO] and/or longer sampling times when the [HCHO] is low. In addition, with increasing

sampling temperature, K^* increases, but conversely, K_A and thus $C_{PFBHA\text{-}S}$ decreases, thereby reducing the apparent rate of product formation (see text). This was confirmed from experimentally obtained data. Finally, when $K_B << K_A$, i.e., the binding affinity of the analyte is negligible compared to that for PFBHA, then the equation can be reduced to Equation 4.9

$$\frac{1}{v} = \frac{1}{C_{HCHO}} \frac{1}{K^*} \qquad \text{Equation 4.9}$$

indicating the direct relationship between the velocity of the reaction and the reaction rate as a function of the analyte concentration,

$$v = C_{HCHO} K^* \qquad \text{Equation 4.10}$$

Therefore, if the velocity of the reaction is in weight/time of product formation while the C_{HCHO} is in ppb_v, K* will be a first order rate constant, $\frac{weight}{C_{HCHO} \bullet time}$, as mentioned in the aforementioned text.

4.3 Experimental

4.3.1 Chemicals and Materials

4.3.1.a Chemicals

The reagents, *o*-(2,3,4,5,6-pentafluorobenzyl)-hydroxylamine hydrochloride (PFBHA.HCl) and hexane were purchased from Sigma-Aldrich (Toronto, Canada). Formaldehyde, 37 % stabilized with methanol, was from Fisher Scientific (Nepean, Canada)

4.3.1.b Materials

All solid phase microextraction fibers, holders, 40 mL, 4 mL and 2 mL amber vials with Teflon faced silicone septa, the SPB-5 GC column (30 m, 0.25 mm i.d., 1.0 μm film

thickness), syringes, charcoal scrubber, bubble flow meter, 1 L gas sampling bulb, charcoal filter and molecular sieve were purchased from Supelco (Supelco-Sigma-Aldrich, Canada). The stirrer, Teflon stir bars, and NIST traceable timer were from VWR (Canada). The 3 mL conical vials were from Kontes. The balance was from Sartorious and shown to be linear from 1 mg to 10 grams. Hydrogen (for the flame ionization detector) and compressed nitrogen (for the standard gas generator) were purchased from Praxair (Waterloo, Ontario). Air and nitrogen for the flame ionization detector generated with gas generators purchased from Balston.

A Kin-Tek (Texas City, Texas) standard gas generating device, Model 491-B, was equipped with a mass flow-controlled dilution gas system and temperature-controlled holding zone. NIST traceable certified HCHO permeation tubes were also from Kin-Tek. The N_2 was scrubbed with a molecular sieve followed by a charcoal scrub.

4.3.2 Headspace loading of the SPME fibers with PFBHA

A solution of PFBHA.HCl (17 mg/mL) in formaldehyde free water was placed in 4 mL amber Teflon capped vials with a 1 cm stir bar. The solution was stirred at 1800 rpm which resulted in the formation of a vortex. Then, the SPME fiber was placed in the headspace above the vortex.

4.3.3 Synthesis of PFBHA-HCHO Oxime and Standard Solutions in Hexane

The oxime formed from the reaction between PFBHA and HCHO (Figure 4.1) was synthesized using a modified literature method (23). Table 4.1 summarizes the ratios of formaldehyde and PFBHA.HCl used to synthesize approximately 160 mg of PFBHA-HCHO oxime.

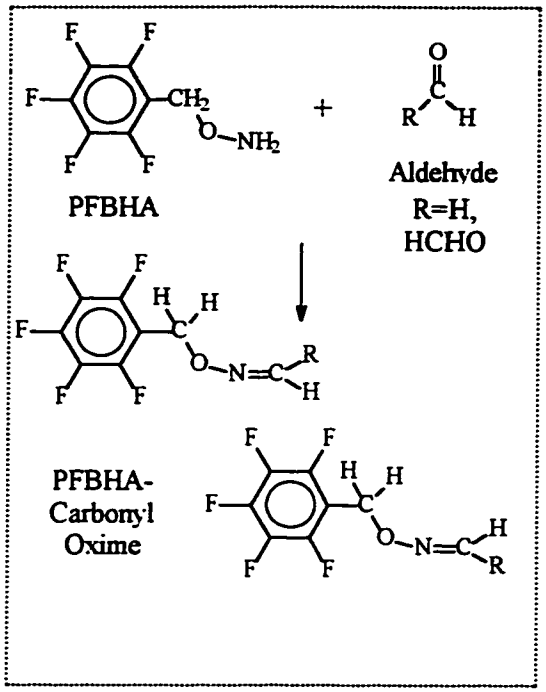

Figure 4.1: Reaction between PFBHA and HCHO (R=H) forming the PFBHA-HCHO oxime. Note that when R is not H, there are syn- and anti-isomers of the oxime, which was also observed for the PFBHA oxime products of n-valeraldehyde and acrolein (23).

Table 4.1: Amounts of PFBHA for the reaction which originates from the PFBHA.HCl salt.

Aldehyde	Aldehyde Volume (μL) / (mmols)	Reaction Vessel Size	Mass of PFBHA.HCl (mg) / (mmols of PFBHA)	Water Volume (mL)	PFBHA.HCl / Aldehyde Molar Ratio
Formaldehyde (HCHO)	70.0 / 0.930	16 X 120 mm	272.1 / 0.930	10	1.0

Once the PFBHA aqueous solution was prepared by exposure to ultrasonic frequencies to enhance the solubility of PFBHA.HCl, the aldehyde was added slowly while shaking. The solution immediately turned cloudy upon addition of HCHO to the PFBHA solution. After all of the HCHO was added, the solution was vigorously shaken, then heated for 5 seconds. The solution was then cooled on an ice bath and centrifuged for five minutes. The centrifuge holders were cooled to ~5°C before centrifugation. When the tubes were cold, the HCHO oxime appeared as a solid layer at the bottom, but turned liquid upon warming to room temperature. The upper layer was removed with a disposable transfer tube. The bottom layer (the PFBHA-HCHO oxime) was extracted with three 900 μL portions of hexane and pooled into pre-weighed conical vials. The hexane extract was evaporated to constant weight with a stream of nitrogen. In addition, the upper aqueous layer was extracted with three 900 μL portions of hexane, and pooled into a 3 mL graduated V-vial, then dried down with N_2, but a negligible amount of the product was recovered. The PFBHA-HCHO oxime (a liquid at room temperature) was stored in the conical vial, wrapped with aluminum foil. The density of the PFBHA-HCHO oxime was determined to be 1.431 g/mL. This oxime was then used to calibrate the GC/FID after solutions were prepared. Injection of this oxime into the GC/FID showed the product was better than 99 % pure (based on FID response). Standard PFBHA-HCHO oxime solutions were prepared and ranged from to 0.143 ng/μL to 14,300 ng/μL. The synthesis of the oxime not only provided detector calibration which was then used to calculate the amount of product formed on the fiber, but also confirmed, with GC/MS, the identity of the PFBHA-HCHO oxime product (Figure 4.2 and Table 4.2).

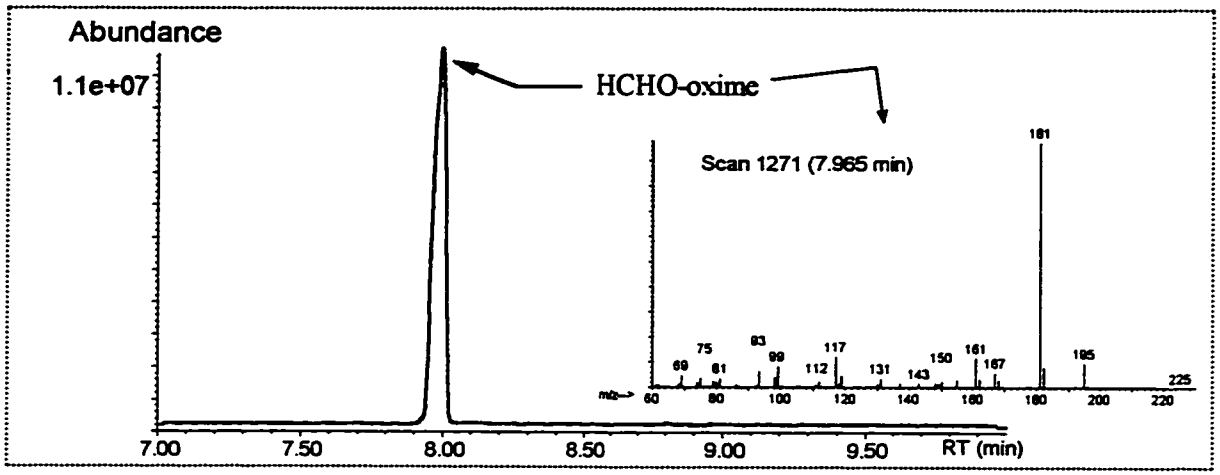

Figure 4.2: GC/MS of 1.8 μL of 143 ng/μL PFBHA-HCHO oxime in hexane. The insert shows the mass spectrum of the peak. The mass spectral data are summarized in Table 4.2.

Table 4.2: Mass spectral information of PFBHA-formaldehyde oxime. The literature data for PFBHA-HCHO oxime are compared to those obtained from the synthesized oxime. The data in italics are the m/e, the data in bold are percent of base peak observed, m/e 181, and finally the literature reported percent of base peak are presented for comparison.

HCHO	**FW**	***181***	***195***	***161***	***117***	***182***	***99***	***167***	***93***
Lit.	225	100	11	10	9	7	7	5	5
Obs.	225	100	12	10	9.9	6.7	9.6	5.4	6.3

4.3.4 Instrumentation and methods for SPME and liquid injections of PFBHA-HCHO Oxime

All experiments used a Varian Star computer controlled Varian 3400 gas chromatograph equipped with a carbon dioxide cooled Septum-equipped Programmable injector (SPI). The column effluent was split with a Y-connector and coupled to an FID and

an electron capture detector. The connection from the Y-connector to the detectors was facilitated with two identical lengths of deactivated 0.25 mm i.d. pieces of fused silica tubing. Confirmation that 50 % of the column eluant entered the FID was achieved by injecting a standard without the Y-connector and with the Y-connector. The ECD was used to confirm the retention time of the PFBHA-HCHO oxime from liquid injections. The injector was maintained at 210 °C for SPME injections but 70°C for hexane liquid injections which was then ramped to 250°C at 300°C/min. The column temperature program for SPME and hexane liquid injections was 45°C for 1.00 min., 30°C/min to 200 °C then 50°C/min. to 290°C held for 4.0 min. The column head pressure was set to 26 psi hydrogen which resulted in a flow rate of 1.7 mL/min and a carrier gas velocity of approximately 58 cm/sec. The detector gas flow rates were set to 300 mL/min. for air, 30 mL/min. for nitrogen and 30 mL/min. for hydrogen and were all measured daily. The instrument was checked daily for calibration using a liquid mid point calibration standard and any deviations in area counts greater than 10 % required re-injection of that standard and if still greater then 10 % the instrument was re-calibrated with a six point calibration. In addition, quality of peak shapes, resolution and retention times were carefully monitored to ensure all chromatography was within all required specifications.

4.3.5 Sampling the HCHO standard gas

The HCHO standard gas effluent was directed into a one liter gas sampling bulb equipped with a sampling port from which the SPME device could be exposed to the gas. The bulb was maintained at 25 °C for all experiments except for the temperature study. All sampling times were accurately measured with a NIST traceable timer.

4.3.6 Analysis of headspace samples of hair gel, particle board, biological material, and coffee grounds

Approximately three grams of hair gel known to contain formaldehyde (according to the manufacturer's label) were placed in a 40 mL vial and allowed to reach equilibrium for one minute before sampling. Approximately three grams of four year old particle board were placed in 40 mL vials and allowed to reach equilibrium. For the hair gel, the PFBHA loaded SPME fiber was introduced into the headspace for 10 seconds, and then analyzed. New samples were prepared and the process repeated for other sampling times. For the particle board sample, the PFBHA loaded SPME fiber was exposed to the headspace for two minutes, then the fiber was analyzed. This was repeated on the same sample after the vial was heated for 15 seconds in a microwave oven on high until moisture was observed to condense on the inside of the vial. A 3 cm^2 of a deciduous plant material was placed in a 40 mL Teflon capped vial. The leaf contents were permitted to reach equilibrium with the vial headspace. Two minute sampling of the headspace took place at room temperature. Finally, the lid from 1 kg container of fresh coffee grounds was opened and the PFBHA loaded SPME fiber was inserted into the headspace for 15 seconds and then analyzed as before.

4.4 Results and Discussion

4.4.1 Selection of a carbonyl specific derivatization reagent suitable for loading onto SPME fiber coatings

The first objectives of the work were to obtain a carbonyl specific derivatization reagent which could be reversibly loaded onto selected SPME fibers, in addition to the requirement that the product of the reaction between the derivatization reagent and the carbonyl compound be stable and amenable to analysis with conventional chromatographic

equipment and detectors, such as GC/FID. When reacted with the aldehyde, the derivatization reagent should yield a thermally stable product thus allowing for ambient temperature storage conditions so that samples could be field acquired and then analyzed in the laboratory. Other requirements were that the derivatization reagent should be preferably non toxic, insensitive to light, heat and air.

The commercially available derivatization reagents selected for study were DNPH, HMP and PFBHA; however, of these three derivatization reagents, only PFBHA was found to satisfy all of the aforementioned criteria for the study. For example, after loading various PDMS and PDMS/DVB fibers with each of the three selected derivatization reagents, only PFBHA on either coating yielded a chromatogram showing only one GC peak associated with the derivatization reagent and another peak from the product of the reaction between PFBHA and formaldehyde (see below). In contrast, both DNPH and HMP loaded on either fiber types yielded a significant number of peaks from which the product of the reaction could not be identified. The use of PFBHA is also highly desirable due to the fact it is water soluble thus allowing a highly controlled loading of the free amine onto various SPME fibers via headspace extraction from aqueous solutions. Experiments also showed that PFBHA was better than 97 % desorbed from the PFBHA loaded SPME fibers following a one minute desorption at 210 °C, and that an extremely reproducible amount of PFBHA could be loaded onto the fiber even after twenty injections. In addition, the PFBHA-HCHO oxime is a halogenated aromatic compound which allows for specific detection with ECD and photo ionization detection, and the compound yields characteristic electron impact fragmentation patterns having base peak daughter ions at m/z 181 and it shows an excellent response with FID (see below). The electronegative fluorine atoms stabilize the ring structure rendering PFBHA,

and its reaction products, stable under a large range of conditions, such as exposure to water and elevated temperatures. Therefore, based on the aforementioned points, PFBHA was selected as the derivatization reagent for HCHO, but what was next required was an SPME fiber coating best suited for loading PFBHA and sampling HCHO.

4.4.2 Fiber selection for loading PFBHA

A number of different SPME fiber coatings were examined to establish one, or more, which would provide the highest loading and stability of PFBHA and oxime retention characteristics. The studied fibers were PDMS, PDMS/DVB for GC (65 μm), Carbowax/DVB, PDMS/DVB for HPLC (60 μm) and Carboxen/PDMS (CXN/PDMS).

The first screening was based on the extent to which the fiber would load PFBHA and the carryover following one desorption step. Each of the fibers were consecutively exposed to an aqueous headspace of a PFBHA solution (10 mg/mL), in random order, assuring at least three extractions per fiber type. The largest mass loading of PFBHA was on the CXN/PDMS fiber. This was followed by the PDMS/DVB fibers (the GC and HPLC types) and Carbowax/DVB fibers each having similar mass loading, yet only half of that observed for the CXN/PDMS fiber. The lowest mass loading was observed for the PDMS fiber coating, approximately half of the that observed for the PDMS/DVB fibers. The CXN/PDMS fiber coating would have been selected for the remainder of the studies were it not for the fact that the optimum desorption temperature for this fiber was found to be approximately 310 °C, with a two minute desorption time to overcome low desorption yields which then resulted in significant peak tailing. Attempts to reduce the observed peak tailing then required cryofocussing the injection band, and/or changing the column. Both were attempted, with the latter proving unsuccessful and the former approach being dismissed due to the desire to

maintain the analysis method as simple as possible. In addition, given the mass loading of PFBHA on the CXN/PDMS fiber coating was only approximately two times that observed for the PDMS/DVB fiber, there was no advantage to using CXN/PDMS given its problems. Each of the other fiber coatings showed significantly less peak tailing compared to the CXN/PDMS coating.

The next criterion for fiber selection was to select a coating which would retain the largest amount of PFBHA with time. This was examined by loading the PFBHA on each of the fibers for a given time and exposing the fibers to aldehyde free air for 10 minutes and then comparing the amount of remaining PFBHA to the amount of PFBHA without exposure to the air. The results showed that PDMS lost more than 90 % of the PFBHA while the Carbowax/DVB and the different PDMS/DVB fibers only showed a loss of approximately 30 %. Increasing the time to 30 minutes resulted in essentially no further loss in PFBHA for the PDMS/DVB and Carbowax/DVB fiber coatings, while the PDMS fiber coating retained approximately three percent of the original amount. In addition, the stability study was carried out by placing PFBHA loaded fibers, with the coating retracted into the needle, overnight in clean air and at room temperature. The finding was that the PDMS fiber lost more than 70 % of the PFBHA while the other fibers only lost approximately 15 %. Therefore, the results indicated that Carbowax/DVB and the two PDMS/DVB fibers could be used to load PFBHA. Finally, the PFBHA solution pH was increased with the addition of Na_2CO_3 which resulted in a significantly larger mass loading of PFBHA on all the fibers, but which also resulted in higher background; however, no further enhancements in loading PFBHA were required since an appropriate level of method sensitivity was achieved without it.

The Carbowax/DVB fiber coating was ultimately not selected due the fact that the coating proved to be less rugged than either of the PDMS/DVB fiber coatings. The PDMS/DVB fiber coating for GC was selected over the one designed for HPLC because the former showed greater reproducibility from one lot to another even though the latter was structurally more rugged than the former. With care, the PDMS/DVB fiber for GC could be used for more than 200 loading and desorption steps without failure. An important point to consider at this time is that the PDMS/DVB fiber was considered saturated with PFBHA prior to exposure to HCHO. This was a result of the finding that increasing the PFBHA aqueous concentration from 17 mg/mL to 60 mg/mL did not yield an increase in mass loading of PFBHA on the PDMS/DVB. Following the selection of the PDMS/DVB fiber coating for GC, the PFBHA loaded fibers were exposed to standard concentrations of HCHO.

4.4.3 Exposure of PFBHA loaded PDMS/DVB fibers to HCHO standard gases

Figure 4.3 shows the typical GC/MS data obtained following exposing PFBHA loaded PDMS/DVB fibers to approximately 650 ppb$_v$ HCHO for 10 minutes, with comparative chromatograms showing the fiber blank and the PFBHA loaded fiber alone.

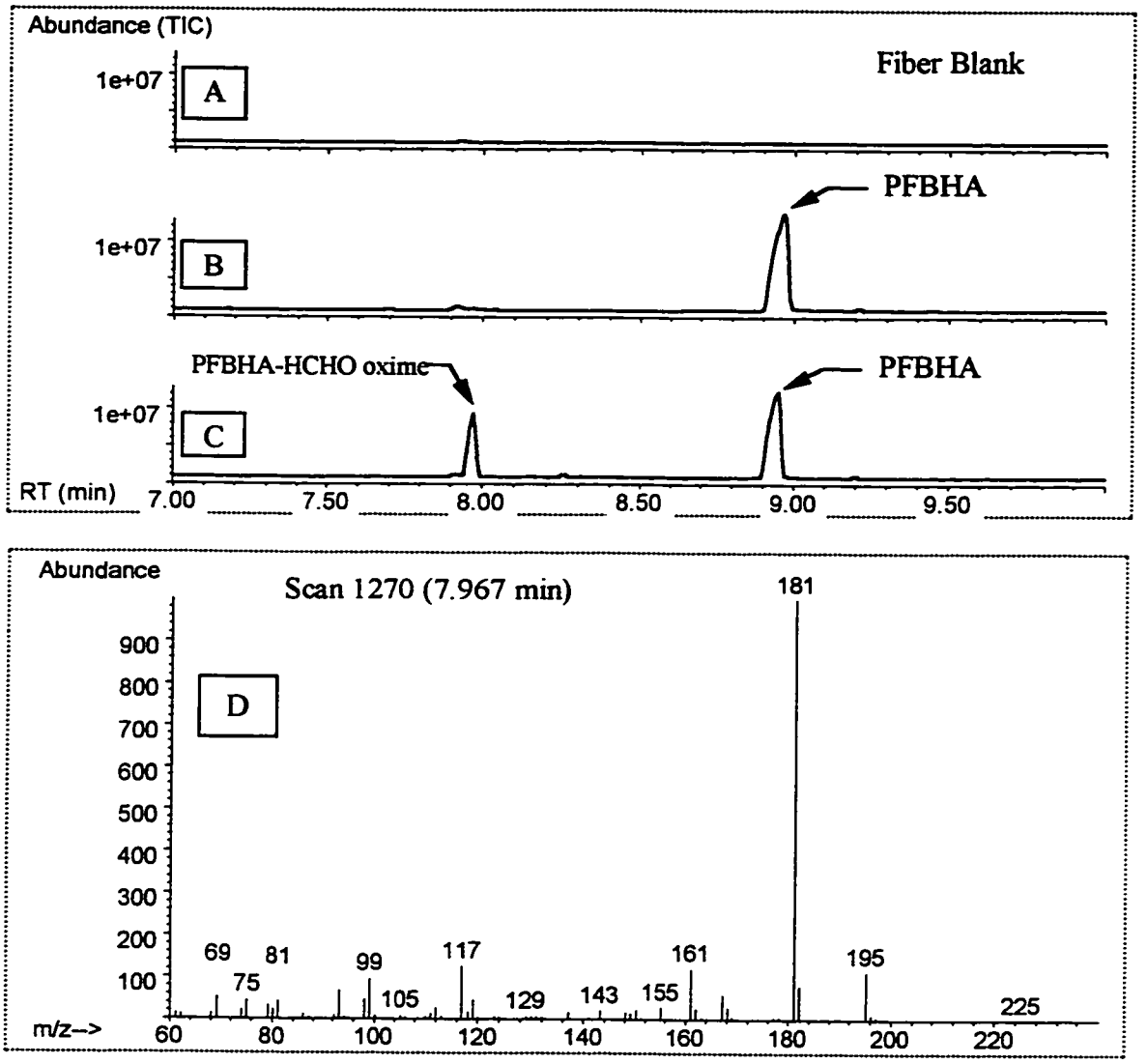

Figure 4.3: GC/MS of PFBHA loaded PDMS/DVB fibers (65 μm) with and without exposure to 650 ppb_v HCHO. A. PDMS/DVB fiber blank. B. PFBHA loaded on PDMS/DVB. C. PFBHA loaded PDMS/DVB fibers followed by exposure to 650 ppb_v for 10 minutes. D. Mass spectrum of the peak at approximately 8 minutes. The chromatographic conditions here were the same as those for the data shown in Figure 4.2.

Figure 4.3A shows the PDMS/DVB fiber blank while Figure 4.3B shows the chromatogram from the PFBHA loaded PDMS/DVB fiber and Figure 4.3C shows the chromatogram with the PFBHA-HCHO oxime and unreacted PFBHA. Figure 4.3D shows

the mass spectrum of the PFBHA-HCHO oxime, which is ostensibly identical to that obtained from the injection of pure PFBHA-HCHO oxime (Figure 4.2). Therefore, the identity and retention time of the PFBHA-HCHO oxime was confirmed.

4.4.4 Calibration of FID with PFBHA-HCHO Oxime

Figure 4.4 shows the calibration curve obtained from the FID response as a function of the liquid injection of PFBHA-HCHO oxime stock solutions. The amounts injected ranged from 0.14 ng to 1430 ng. The equation shown, Y=2630X+1640, was used to quantify the amount of PFBHA-HCHO oxime formed between gaseous HCHO and sorbed PFBHA..

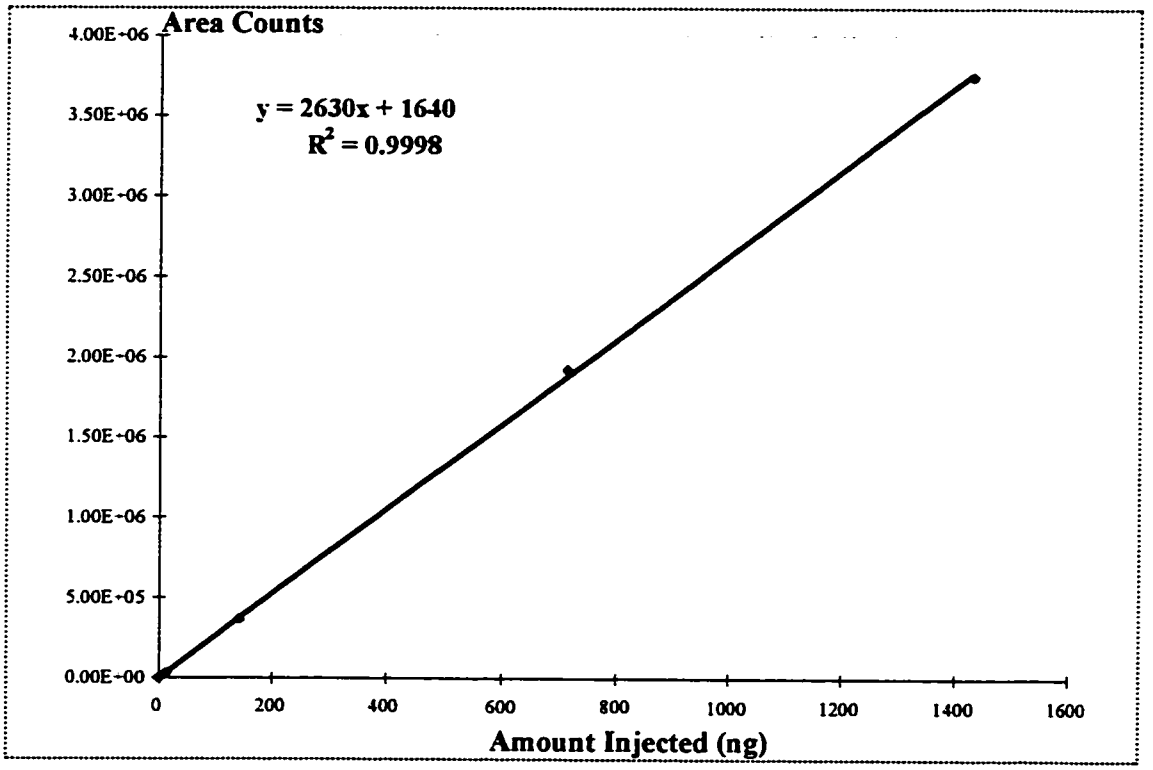

Figure 4.4: Calibration curve data for FID response as a function of amount of PFBHA-HCHO oxime injected. See Experimental for GC conditions.

4.4.5 Exposure Time Profiles

Exposure time profiles were determined for 636, 229, 45, and 15 ppb_v HCHO concentrations (25°C). Figure 4.5 shows the time profiles obtained for 636 and 229 ppb_v HCHO. The ordinate depicts the mass of PFBHA-HCHO oxime formed as a function of time.

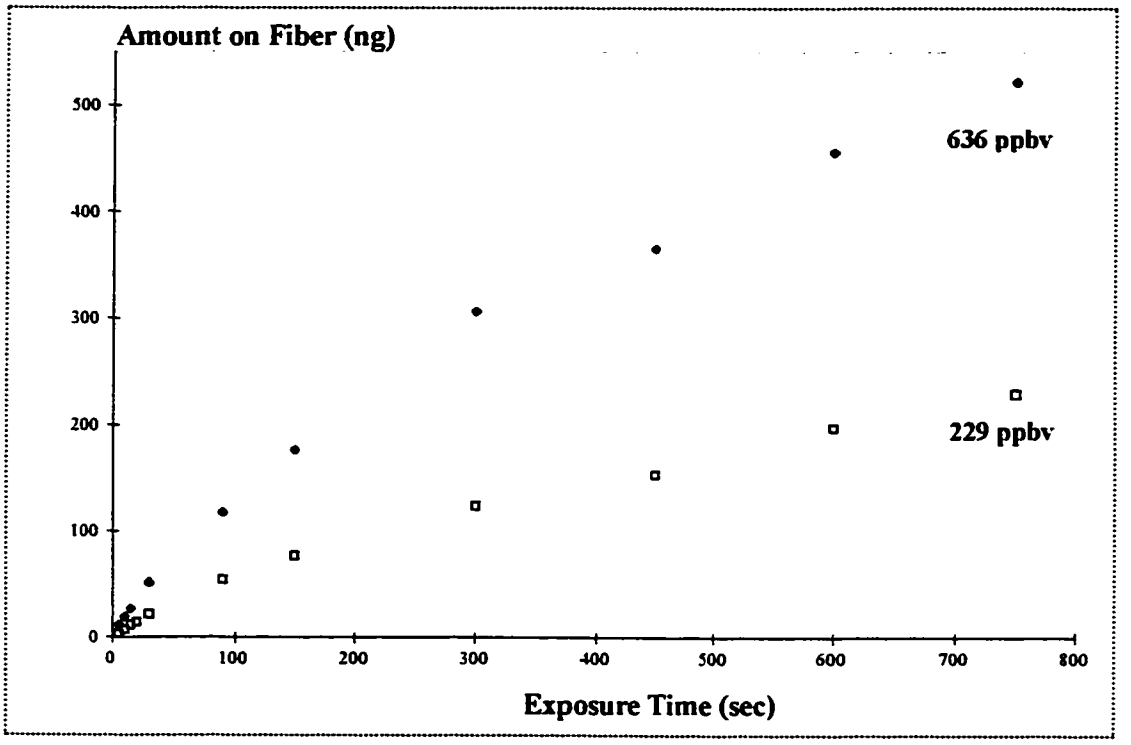

Figure 4.5: Representative exposure time profiles for PFBHA loaded PDMS/DVB fibers (65 μm) for 636 ppb_v and 229 ppb_v HCHO. Not shown are those for 45 and 15 ppb_v HCHO.

The data indicate that a steady-state level of product formation was not observed even after 12 minute extraction times, and was not dependent on the gas velocity (see below). The data also showed an increase in the rate of reaction with increasing concentration of formaldehyde, a point consistent with the requirement of the kinetic model for the Langmuir-Rideal mechanism for the reaction between a gaseous analyte and a sorbed compound. In

addition, there is a linear range for each exposure time profile starting from ten seconds to approximately sixty seconds which increases with decreasing HCHO concentration. This is consistent with the point that the reaction is pseudo first order in this region due to the fact that the derivatization reagent, PFBHA, is in significant excess to the amount of PFBHA-HCHO oxime formed and the concentration of HCHO. This point was exploited in establishing the 1st order rate constant for the reaction which would allow a quantitative description of the dependence of the velocity of the reaction between PFBHA and the HCHO concentration.

4.4.6 Establishing the apparent 1st order rate constant for the reaction between PFBHA loaded onto PDMS/DVB fibers and HCHO

Figure 4.6 shows the plots of the inverse of amount of HCHO oxime formed as a function of the inverse of exposure time, the slopes of which represent the inverse of the reaction velocity, sec/ng, of PFBHA-HCHO oxime product formation from the reaction between PFBHA and HCHO. A plot of the slope of each curve as a function of the inverse of the HCHO concentration yields a curve where the inverse of the slope is the actual apparent 1st order rate constant for the reaction (Figure 4.7), 0.00297 $^{ng}/_{(ppb,\,sec)}$, and is described in section 4.2. It is this apparent 1st order rate constant which can be used to quantify unknown concentrations of airborne HCHO with the SPME sampling method. The amount of HCHO oxime product formed following a given exposure time, e.g., 10 seconds, for an unknown HCHO concentration is divided by the 1st order rate constant, the result being the unknown HCHO concentration. In this way, no SPME fiber calibration curve is required for quantification, provided the sampling time is accurately known and that the amount of derivatization reagent consumed does not exceed approximately 5% of the original amount.

This first order rate constant was confirmed with calibration curve data shown in the next section.

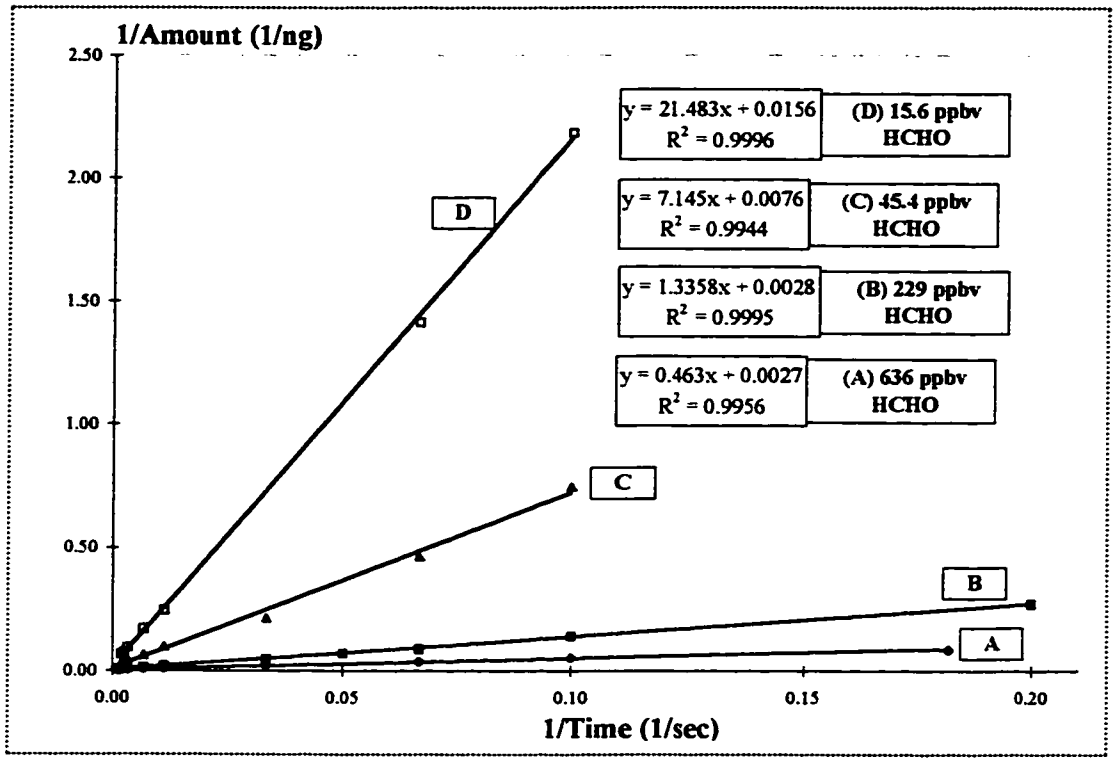

Figure 4.6: Plots of the inverse of amount of PFBHA-HCHO oxime formed (1/ng) as a function of the inverse of time (1/sec). The equations for each of the curves are presented on the chart with its associated formaldehyde concentration (ppb_v).

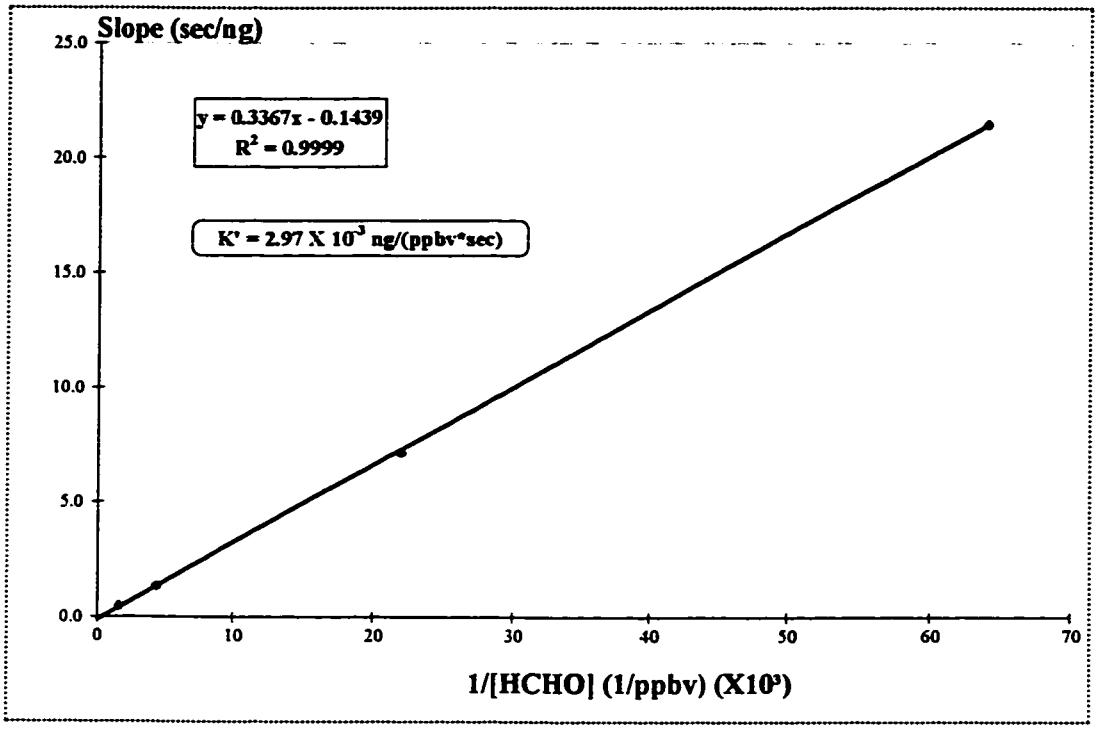

Figure 4.7: Plot of the slope for each of the curves from Figure 4.6 as a function of the inverse formaldehyde concentration (1/[HCHO]). The equation for the line is presented as well as the inverse of the slope which represents the overall 1st order rate constant.

4.4.7 SPME fiber calibration curve data for HCHO

Plots for the amount of HCHO oxime formed for 10 seconds and 300 seconds sampling times for various concentrations of HCHO are provided in Figure 4.8. The data show that, as expected, long sampling times result in a larger mass of product formed compared to shorter sampling times, i.e., 300 seconds versus 10 seconds. The slopes of the two curves indicate that sampling for 300 seconds results in approximately sixteen times greater sensitivity compared to sampling for 10 seconds which is consistent with the concept that an increased exposure time will result in an increased amount of product formed.

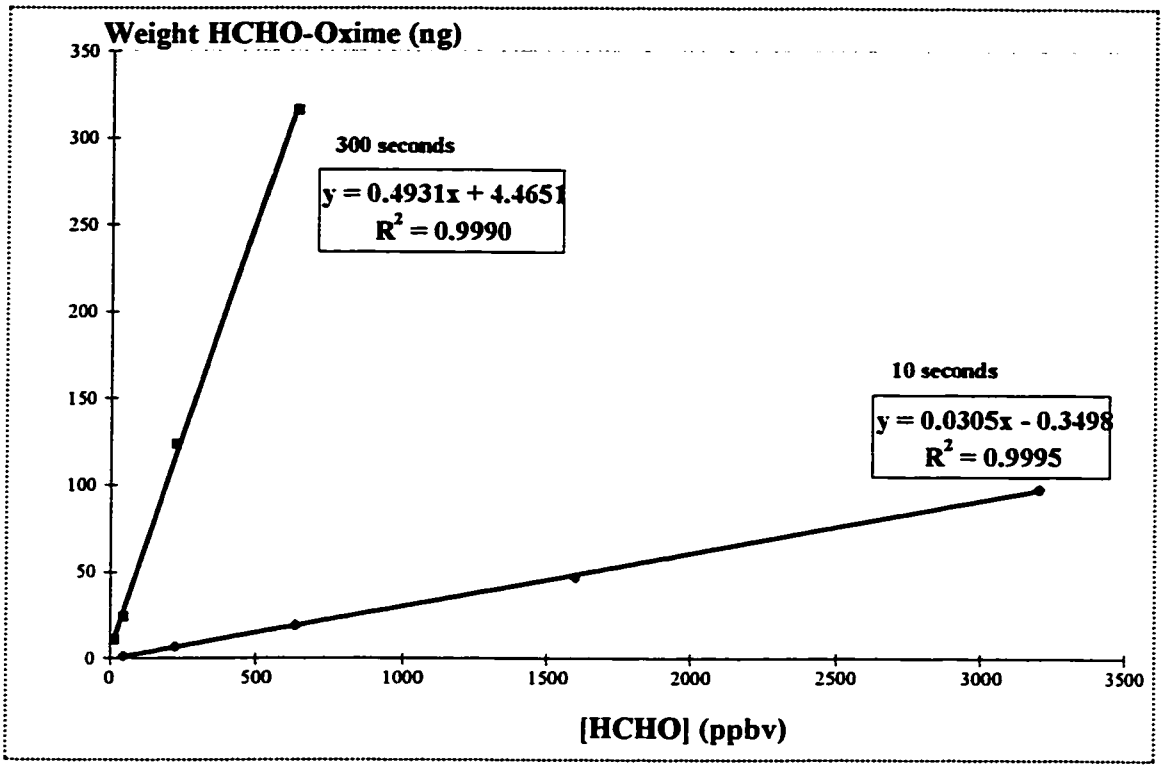

Figure 4.8: Amount of PFBHA-HCHO oxime formed at 10 and 300 seconds sampling times as a function of various [HCHO] (ppb_v). The equations for the curves are presented. Note that the slope for the 300 second sampling time is approximately 16 times larger than that observed for the 10 second sampling time. Also note that the slope of the curve obtained from the 10 second sampling times is essentially identical to that obtained from the inverse of the slope from the plot shown in Figure 4.7.

Of particular interest is that the slope from the curve obtained for ten second sampling of the various HCHO concentrations is 0.0305 $\frac{ng}{ppbv \times 10\,sec}$ yielding an apparent 1st order rate of 0.00305 $\frac{ng}{ppbv \times sec}$. This is significant because it independently confirms the 1st order rate constant reported in the previous section where the two values differ by less than three percent. Finally, these data indicate that it should be possible to obtain 1st order constants for

other PFBHA carbonyl reactions by simply exposing the PFBHA loaded SPME fibers to various concentrations of the carbonyl compounds of interest for very short times where the slopes represent the apparent 1st order rate constant.

4.4.8 Temperature dependence

Figure 4.9 shows the dependence of amount of HCHO oxime formed as a function of the inverse of temperature for a given HCHO concentration. The data indicate that as temperature increases, one finds a corresponding decrease in the amount of HCHO oxime formed for a fixed sampling time.

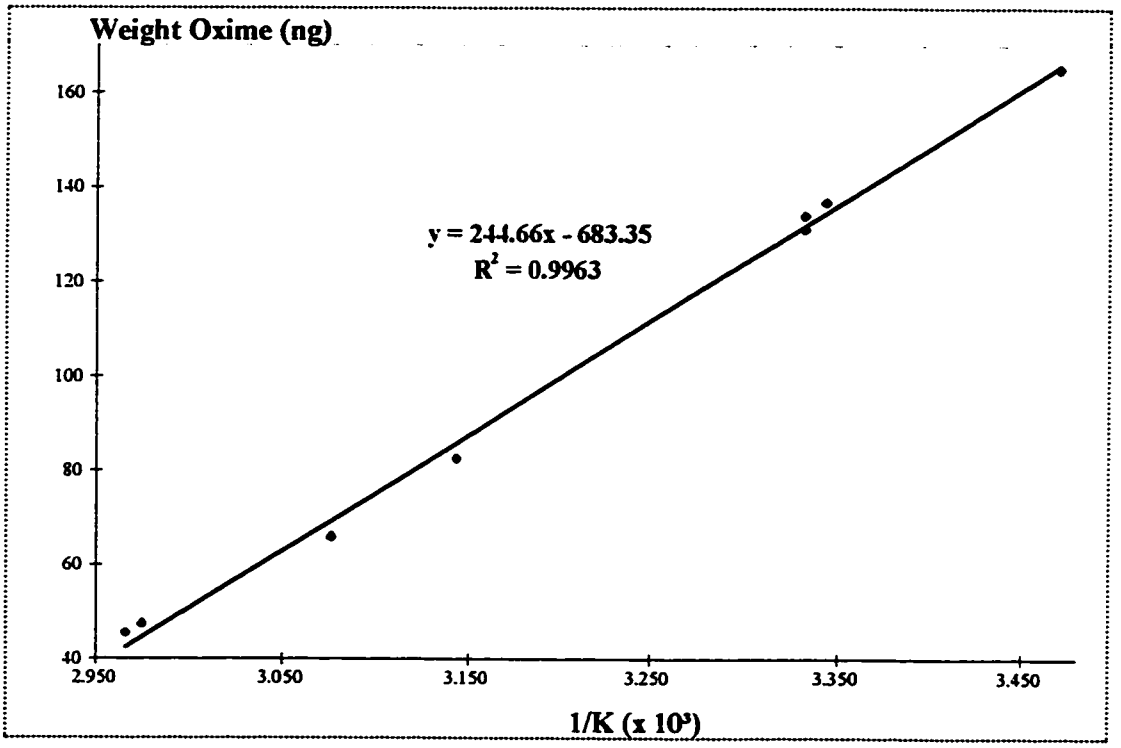

Figure 4.9: Dependence of the amount of PFBHA-HCHO oxime formed as a function of the inverse of temperature (1/K) for a 300 second sampling time and a fixed [HCHO] of 650 ppb_v.

Increasing temperature results in an increase in the rate of reaction between the

PFBHA and HCHO but the increase in temperature also decreases the binding affinity of the PFBHA and PFBHA-HCHO oxime to the PDMS/DVB fiber coating and is described in the Theory. Of significance is that a temperature variation of ± 5 °C from 25 °C does not significantly affect the amount of PFBHA-HCHO oxime detected thus potentially reducing the requirement to correct for sampling temperature; however, the option to correct for sampling temperature is available if required.

4.4.9 Sampling formaldehyde from a static gas mixture versus the same dynamic gas mixture

The question as to whether there was a difference between sampling HCHO from a dynamic gas flow from the standard gas generator and sampling while the same gas was static was addressed. First, one concentration of HCHO standard gas was dynamically sampled with the PFBHA loaded PDMS/DVB fibers. Second, the same HCHO standard gas concentration was sampled under static conditions with the same PDMS/DVB fibers loaded with fresh PFBHA (recall Figure 2.5A). The data indicate that there is no difference between the two sampling methods, i.e., the amount of PFBHA-HCHO oxime formed for a given sampling time was identical for each sampling type, presumably due to the fact that the reaction rate between the PFBHA on the fiber and HCHO is much slower than the diffusion rate of HCHO. In addition, these data indicate that sampling HCHO under static conditions should yield highly accurate determinations of HCHO concentrations.

4.4.10 Precision of overall method

The overall method precision, comprising loading PFBHA onto the PDMS/DVB fibers, exposure for fixed times to various standard HCHO concentrations and GC/FID analyses, was established to be less than 7 % RSD for 15 ppb_v HCHO and better than 2 %

RSD for 3200 ppb_v. The data indicate that the method of loading the derivatization reagent, sampling and analysis is highly reproducible. It is this excellent precision which allows the method to achieve very low detection limits for 300 second sampling times.

4.4.11 Method detection limits

Table 4.3 summarizes the data obtained from a two-tailed *t*-test of eight replicate analyses carried out at 15 ppb_v. The data estimate an overall method detection limit (MDL) of approximately 2 ppb_v for 300 seconds sampling and 40 ppb_v for 10 seconds, MDL values equal to or better than all other rapid sampling methods for HCHO.

Table 4.3: Summary of data obtained from the method detection limit study of PFBHA loaded PDMS/DVB fiber coatings. The study was carried out with 8 repeats at 10 times the expected method detection limit, yielding 7 degrees of freedom. A two-tailed *t*-test of the data was carried out where t=2.998. A five minute exposure, at 25 °C, to 15 ppb_v HCHO.

Run Number	PFBHA-HCHO Oxime (ng)
1	10.5
2	11.8
3	11.1
4	12.1
5	10.4
6	10.6
7	9.9
8	10.7
Average	10.9
Std. Dev.	0.73
% RSD	6.7
MDL (ppb_v)	2.1

4.4.12 Inter-fiber reproducibility

The use of a number of different PDMS/DVB fibers during the course of the study raised questions regarding the possible fiber to fiber variations. Four different fibers from a number of different production lots were used to consecutively load PFBHA then sample 640 ppb_v HCHO for 300 seconds. The results indicate that there was no difference in the amount of HCHO oxime formed for any of the fibers. These data indicate there is good reproducibility of PDMS/DVB fibers for this new sampling method and that PDMS/DVB fibers are highly reliable for this new sampling method for HCHO.

4.4.13 Specificity of the method for HCHO

Given that acrolein has been reported to interfere with the uptake of formaldehyde with a sampling system using DNPH on a solid sorbent (9), the possibility of interference from other reactive aldehydes with this new sampling method was addressed. Table 4.4 summarizes the data from this study. First, PFBHA loaded PDMS/DVB fibers were exposed to 46,000 ppb_v *n*-valeraldehyde (1) for 20 seconds then to 75,000 ppb_v acrolein (2) for 20 seconds then to 640 ppb_v HCHO (3) for 60 seconds, followed by analysis. These data were compared to those when the fiber was exposed to each aldehyde alone then analyzed. The data indicate that the sampling system can still sample for HCHO even when the fiber is exposed to one hundred times higher concentrations of other very reactive aldehydes.

Finally, the possibility that humid air can affect the reaction between gaseous HCHO and sorbed PFBHA for large relative humidities was addressed by sampling 3,000 ppb_v HCHO from a static bulb with 0, 8.6 and 86% relative humidity. The findings were that there was less than 4 % difference in the PFBHA-HCHO oxime rate of formation for the low versus high humidity levels, within the margins of experimental error.

Table 4.4: Specificity of the sampling method for HCHO with and without exposure to high concentrations of reactive aldehydes. The numbers to the right of the specified aldehyde indicate the order of exposing the PFBHA loaded PDMS/DVB fiber to the aldehyde, with exposure to HCHO occurring last.

Aldehyde	Exposure Time (sec)	[Aldehyde] (ppbv)	Consecutive Exposure (Area Counts)	Individual Exposure (Area Counts)	% of Original AC
HCHO (3)	**60**	**640**	**2.19E+05**	**2.42E+05**	**91%**
Acrolein (2)	*20*	*72000*	*9.86E+04*	*1.31E+05*	*75%*
n-Valeraldehyde (1)	*20*	*45000*	*4.41E+05*	*4.87E+05*	*90%*

4.4.14 Real samples with the method

The proposed method was tested on a number of materials. The materials were chosen to reflect potentially common applications of the sampling method. The materials were a hair gel suspected of containing formaldehyde, 4 year old particle board which was expected to be devoid of residual formaldehyde. Also chosen were plant material and freshly ground coffee beans.

Figure 4.10 shows the chromatograms obtained from the GC/FID analysis of HCHO oxime formed after PFBHA loaded PDMS/DVB fibers were exposed to hair gel known to contain HCHO according to the list of ingredients. The results indicate that HCHO was indeed present in the headspace of the hair gel, thus presenting an additional source of potential exposure of HCHO to those individuals in the vicinity on whom the hair gel may be applied. In fact, it is estimated that exposure to off-gassed HCHO from this amount of hair gel would be equivalent to a personal exposure similar to a daily HCHO exposure at the recommended indoor air quality level. Therefore, the method proposed can be potentially used as a method for estimating exposure to HCHO from cosmetics.

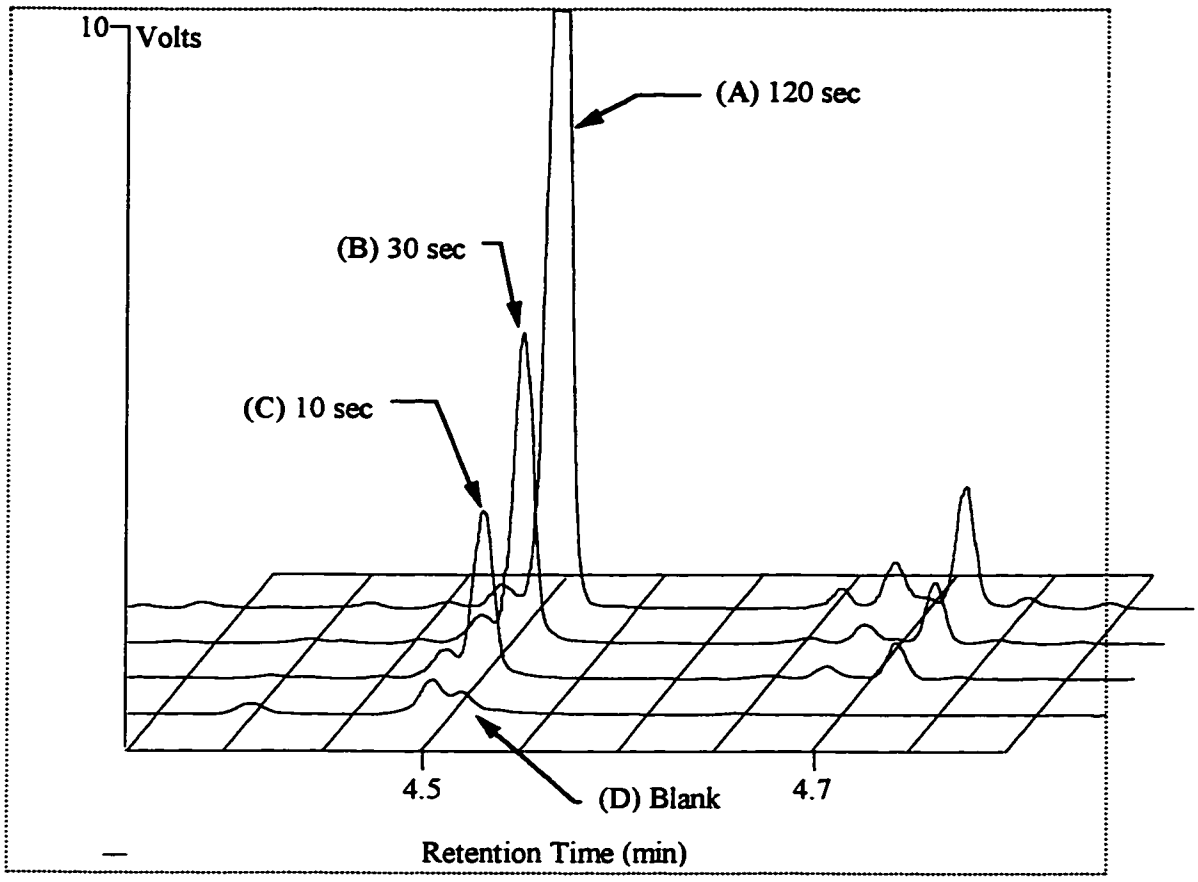

Figure 4.10: Exposure of PFBHA loaded PDMS/DVB fibers (65 μm) to the headspace of approximately 3.5 g hair gel. The various times presented are different sampling times.

Figure 4.11 shows the chromatogram obtained from the sampling of HCHO from four year old laminated particle board. The data indicate that HCHO emissions from this material are still occurring, even after four years, and that with heating a significant amount of HCHO is further released.

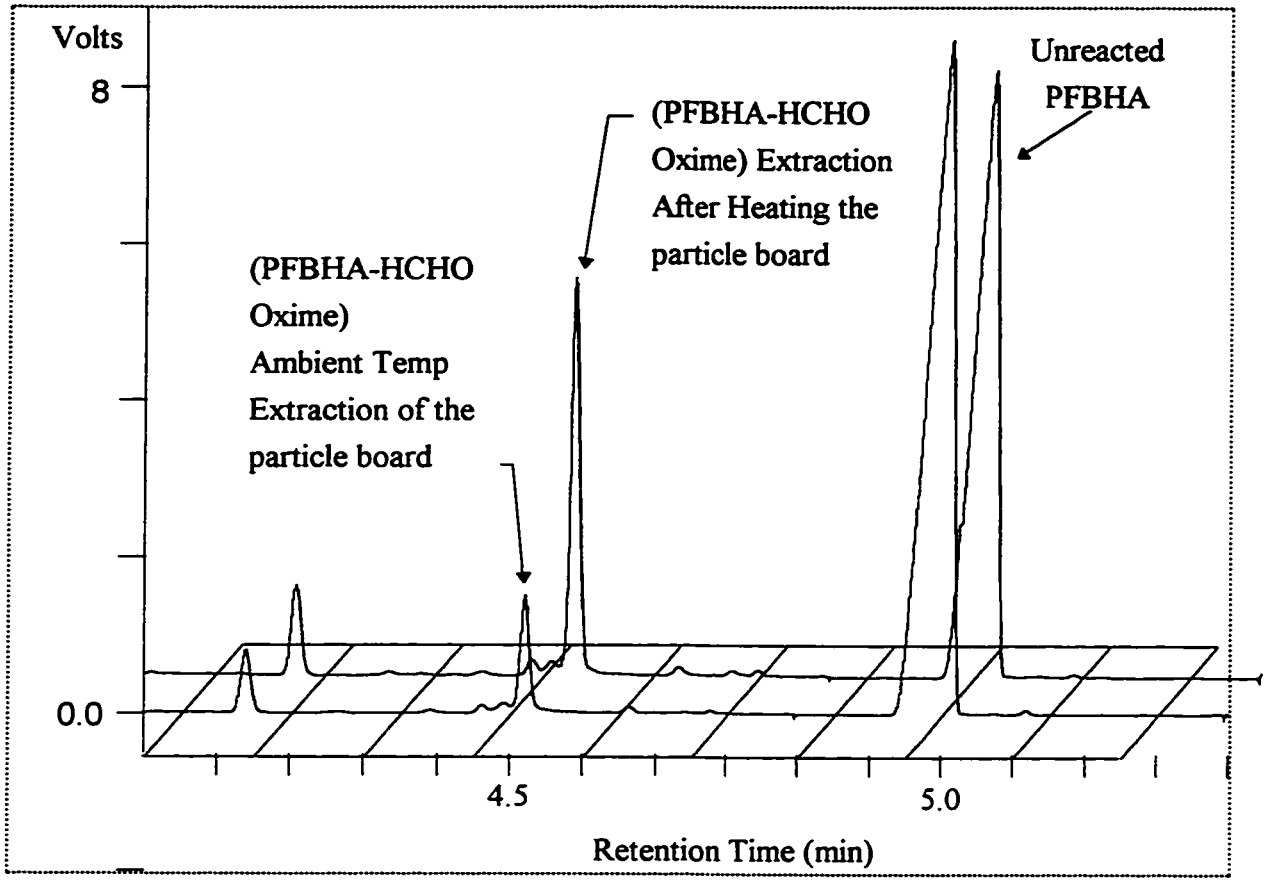

Figure 4.11: Exposure of PFBHA loaded PDMS/DVB fibers (65 μm) to the headspace of approximately 3 g of four year old particle board before and after heating.

Figure 4.12 shows the chromatogram obtained from the exposure of the PFBHA loaded PDMS/DVB fibers to the headspace of a deciduous plant located in our laboratory. The finding was that there are a large number of carbonyl compounds originating from the leaf. Therefore, it should be possible to sample headspace carbonyl compounds from biological materials.

Finally, Figure 4.13 shows the chromatogram obtained from the headspace extraction of coffee grounds. The large number of peaks formed to the right of the PFBHA peak represent PFBHA reaction products with the carbonyls in the headspace. The chromatogram

obtained from the direct extraction of coffee grounds headspace compared to the one obtained after the same fiber was exposed to PFBHA then to the coffee grounds headspace indicates the method allows for selectivity of sampling carbonyl compounds.

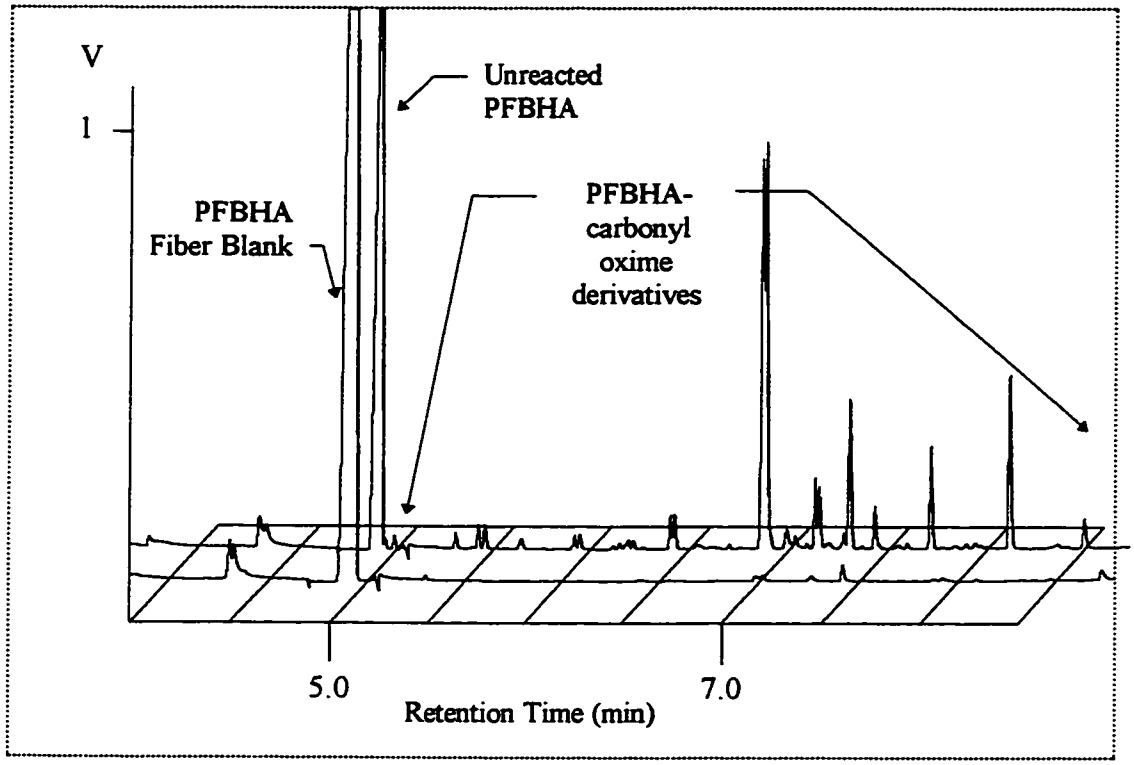

Figure 4.12: Exposure of PFBHA loaded PDMS/DVB fibers (65 μm) to the headspace of a deciduous leaf.

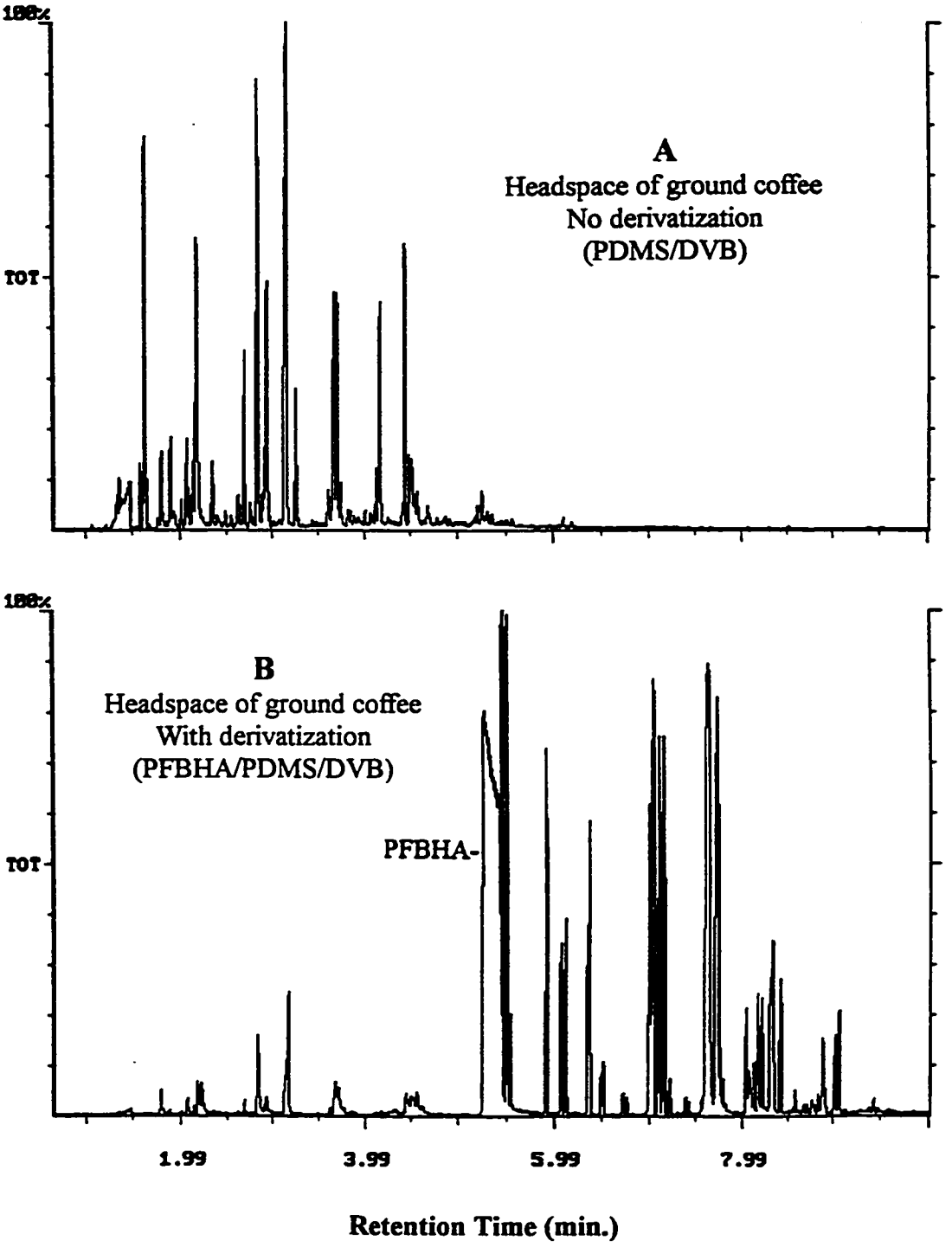

Figure 4.13: Exposure of PFBHA loaded PDMS/DVB fibers to the headspace of fresh coffee grounds. A - PDMS/DVB headspace extraction without derivatization. B - PFBHA/PDMS/DVB headspace extraction with derivatization products to the right of unreacted PFBHA.

4.5 Summary

This new formaldehyde sampling method can be used for accurate grab sampling. The method allows for easy sampling of formaldehyde, and other carbonyl compounds, from a wide range of matrices. The PFBHA-HCHO oxime is not reactive, does not spontaneously decompose, is not sensitive to moisture and light, is therefore extremely stable which allows for field sampling and transportation of the fiber following sampling without special methods for preservation (Chapter 6).

The small size of the sampler lends itself to personal monitoring and/or easy placement in the home, office, school, industry, or government facility. The extraordinary feature of this device is its flexibility for use as both a grab sampling device to allow for an estimate of the instantaneous concentration of HCHO and as a time-weighted average sampling device for HCHO. This latter system is discussed in detail in Chapter 5.

4.6 References

1. Tichenor, B.A.; Mason, M.A. *J. Air Pollut. Control Assoc.* **1988** *38* 264-268

2. Boeniger, M.F. *Am. Ind. Hyg. Assoc. J.* **1995** *56* 590-598

3. Lipari, F., Dasch, J.M., and Scruggs, W.F. **1984** *18* 326-329

4. Godish, T. *Am. J. Public Health* **1989** *79* 1044-1045

5. Risner, C.H.; *J. Chrom. Science* **1995** *33* 168-176

6. Milton, D.K., Walters, M.D., Hammond, K., and Evans, J.S. *Am. Ind. Hyg. Assoc. J.* **1996** *57* 889-896

7. Bennett, J.S., Feigley, C.E., Underhill, D.W., Drane, W., Payne, T.A., Stewart, P.A.; Herrick, R.F., Utterback, D.F., and Hayes, R.B. *Am. Ind. Hyg. Assoc. J.* **1996** *57* 599-609

8. Carlier, P., Hannachi, H., and Mouvier, G.; *Atmos. Environ.* **1986** *20*, 2079-2099

9. Otsen, R. and Felin, P. *Gaseous Pollutants: Characterization and Cycling*, John Wiley & Sons, **1992** 335-421

10. American Conference of Governmental Industrial Hygienists, *Threshold Limit Values for Chemical Substances and Physical Agents*, **1996** 23

11. Bernstein, R.S., Stayner, L.T., Elliott, L.J., Kimbrough, R., Falk, H., and Blade, L., Am. Ind. Hyg. Assoc. J., **45** (11) 1984 pp. 778-785

12. Sittig, M; *Handbook of Toxic and Hazardous Chemicals and Carcinogens*, 3rd edition, **1991**

13. Otsen, R. and Fellin, P. *The Science of the Total Environment*, **1988** *77* 95-131

14. Method TO-11, EPA-600/4-89-017, *Compendium of Methods for the Determination of Toxic Organic Compounds in Air*, U.S. Environmental Protection Agency, Research Triangle Park, NC, **1988**

15. NIOSH Method 2541, *NIOSH Manual of Analytical Methods*, Electronic Version, 1994

16. Goelen, E., Lambrechts, M. and Geyskens, F. *Analyst*, **1997** *122* 411-419

17. Lange, J., Eckhoff, S., and *Fresnius J. Anal. Chem.* **1996** *356* 385-389

18. Luong, J., Sieben, L., Fairhurst, M., and de Zeeuw, J.; *J. High Resol. Chromatogr.* **1996** *19* 591-594

19. Shi, Y. and Johnson, B.J.; *Analyst*, **1996** *121* 1507-1510

20. Chan, W.H. and Huang, H.; *Analyst*, **1996** *121* 1727-1730

21. Tashkov, W.; *Chromatographia*, **1996** *43* 11-12

22. Laidler, K.J. *Chemical Kinetics*, McGraw-Hill Book Company, **1965** Chapter 6

23. Cancilla, D.A., Chou, C., Barthel, R.m and Que Hee, S.S., *J. of AOAC International*, **1992** *75* 842-854

CHAPTER 5

INTEGRATED (TIME-WEIGHTED AVERAGE) SAMPLING WITH SPME

5.1 Background

The previous chapters have been devoted to grab sampling airborne analytes with SPME (less than five minute samples). Both the PDMS and PDMS/DVB fiber coatings were used to grab sample air; however, it is often necessary to describe the concentration of an analyte averaged over a long sampling period, such as eight hours. There are two ways in which this can be achieved. The first way is to take a large number of grab samples during the time period of interest, then average the concentrations. The second way is to acquire one sample which mass loads the analyte of interest in direct proportion to the gaseous analyte concentrations over the sampling time period. This chapter shows how SPME can be used as an integrated sampler. Using SPME as an integrated sampler provides significant advantages over other methods, such as its low cost due to its re-usability, portability, and large selection of organic phases to sample a large range of airborne analytes. This chapter shows how SPME with the PDMS and PDMS/DVB fiber coatings are suitable for integrated sampling. The PDMS fiber coating is used to carry out integrated sampling those compounds studied in Chapter 2 (Table 2.1) and PFBHA sorbed onto PDMS/DVB fibers for the on-fiber derivatization of formaldehyde (Chapter 4).

5.1.1. Use of grab samples to obtain a time-weighted concentration

For grab sampling, i.e., when the sampling time is less than ten minutes, detailed

information can be gathered regarding the analyte concentration in air as a function of time. Also, the time-weighted average (TWA) analyte concentrations can be obtained for the time period from a large number (n) of grab samples (Equation 5.1),

$$\overline{C}_{t_n} = \frac{C_1 t_1 + C_2 t_2 + C_3 t_3 + \ldots C_n t_n}{t_1 + t_2 + t_3 + \ldots t_n} \qquad \text{Equation 5.1}$$

where C_1 is the analyte concentration for time t_1, C_2 is the analyte concentration for time t_2, etc. If the sampling time, t, in Equation 5.1 are all equal, e.g. 10 minutes, then forty-eight samples will be acquired over a 480 minute sampling time, 96 samples for 5 minute sampling times, etc. Therefore, smaller sampling time intervals would yield larger data sets which could be used to both accurately describe the average analyte concentration and indicate trends in concentration for the total time. This method to obtain TWA concentrations, though, is extremely impractical and very costly.

An alternative approach to obtaining a TWA sample is with one air sample where $t_1=t_n$ (Equation 5.1). In this case, the sampler accumulates an amount of analyte per unit time in direct proportion to the concentration of analyte directly outside of the sampler, then averages the analyte concentration for the sampling time period. The following section presents TWA sampling with one sampler where the average airborne analyte concentration is desired for a total sampling time, t_n.

5.1.2. Time-weighted average sampling with one sampler

Time-weighted average sampling possibilities can be carried out with either active sampling or passive sampling (1). Figure 5.1 shows the SPME fiber coating position for TWA passive sampling, with the fiber in the retracted position relative to the needle opening. For passive sampling, three assumptions must be considered (2,3,4). From Figure 5.1, the

first assumption is that the analyte concentration, C_{BULK}, must equal the analyte concentration at the face of the sampling device, C_{FACE} (Figure 5.1). This assumption is easily satisfied with SPME due to the fact the cross sectional area of the face of the needle is extremely small. The second assumption is that the sampling device must respond proportionally to the changing analyte concentration at the face of the device, which is satisfied with SPME for a number of compounds, as discussed herein. The third assumption is that the sorbent or organic phase (Figure 5.2) should be a 'zero sink' for the target analytes, i.e., $C_{SORBENT}=0$. A zero sink ensures that once an analyte is sorbed that analyte does not alter the mass loading rate of additional analyte.

It must be emphasized that doing integrated or time-weighted average sampling automatically eliminates the possibility of describing the transient analyte concentrations in C_{BULK}. Therefore, the only reason to use a time-weighted average sampling device is when the average analyte concentration in C_{BULK} is required. Grab samples will allow a description of C_{BULK} as a function of time (Equation 5.1).

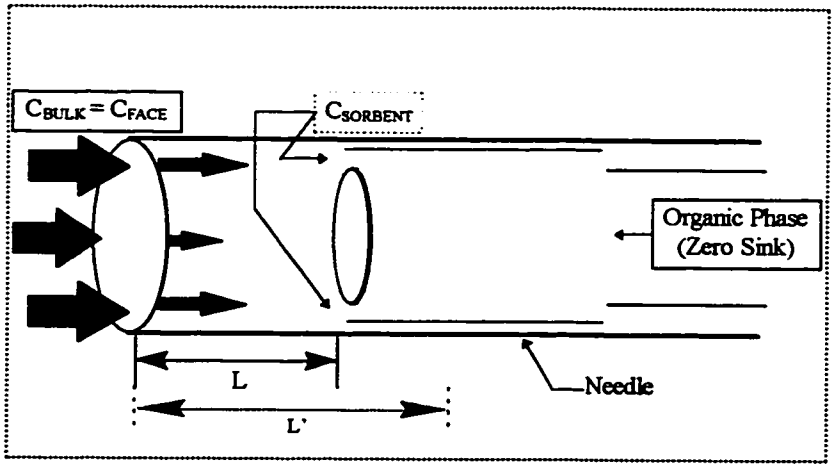

Figure 5.1: The *retracted* fiber position to achieve time-weighted average sampling with SPME.

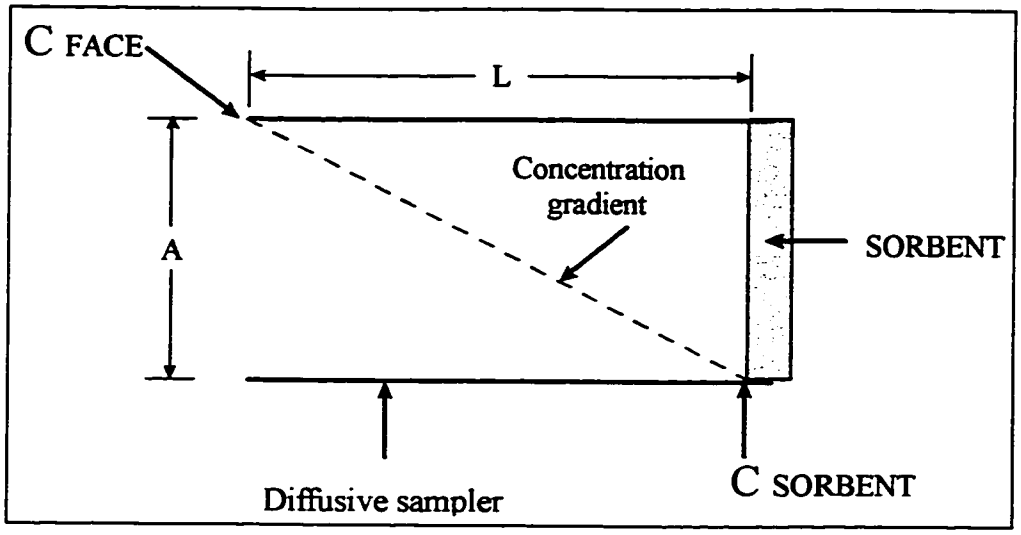

Figure 5.2: The concentration gradient of analyte from the face of the diffusive sampler to its sorbent. L is the path length and A is the surface area of the opening.

5.2 Theory

The mass loading rate of an airborne analyte onto a sorbent with *active* sampling depends on the sampling pump flow rate and the average analyte concentration (Equation 5.2),

$$\frac{M}{t} = R \times \overline{C} \qquad \text{Equation 5.2}$$

where M is the mass of analyte sorbed (ng), t is the sampling time (min), R is the pump sampling flow rate (cm^3/min), $\overline{C}$ is the average analyte concentration (ng/cm^3) for the sampling time. As shown below, a similar description is possible for *passive* sampling.

A sampler controlled by diffusion would show a dependence quite similar to those for the active sampler; however, no pump is used for passive sampling. From Fick's First Law of Diffusion (Equation 5.3),

$$J = -D\left(\frac{dc}{dz}\right) \qquad \text{Equation 5.3}$$

where D is the analyte diffusion coefficient (cm^2/min), and dc/dz is the analyte concentration gradient from the opening of the sampling device to the surface of the sorbent. Equation 5.3 can be modified to include the dimensions of the passive sampling device, as shown (Equation 5.4),

$$\frac{dJ}{dAdt} = -KD\frac{dc}{dz} \qquad \text{Equation 5.4}$$

where J is the weight (ng) of analyte passing through a cross section, A (cm^2) during a time, t (min). This amount is proportional to the concentration gradient in the sampler (dc/dz), the analyte diffusion coefficient D (cm^2/min), and a factor, K, which equals 1 when there is no barrier to the face. For a given passive sampling device, such as that shown in Figure 5.1, A and the path length, z, will be constant, therefore, dA=A and dz=L and with K=1 from Equation 5.4 yielding Equation 5.5,

$$\frac{dJ}{dt} = -\frac{DA}{L}dc \qquad \text{Equation 5.5}$$

When the product of D and A are divided by L, the result is a sampling rate in cm^3/min (R) (Equation 5.6),

$$D\left(\frac{A}{L}\right) = R \qquad \text{Equation 5.6}$$

Therefore, when Equations 5.5 and 5.6 are merged, Equation 5.7 results,

$$\frac{dJ}{dt} = -Rdc \qquad \text{Equation 5.7}$$

Furthermore, Equation 5.7 can be integrated with limits to concentration and time (Equation 5.7a), with the result shown in Equation 5.8,

$$J = -R\int_{0}^{t}\int_{C_F}^{C_S} dc\,dt = -Rt\int_{C_F}^{C_S} dc \qquad \text{Equation 5.7a}$$

where $C_{FACE}=C_F$ and $C_{SORBENT}=C_S$ and recognizing that J/t will be an average sampling rate directly proportional to the average bulk analyte concentration,

$$\frac{J}{t} = -R(C_s - C_F) = R(C_F - C_S) \qquad \text{Equation 5.8}$$

and when $C_S=0$, given J=M (mass of analyte), Equation 5.9 can be realized,

$$\frac{M}{t} = R \times \overline{C}_F \qquad \text{Equation 5.9}$$

where $\overline{C}_F$ is the average concentration of analyte at the face of the passive sampling device. In addition, Equation 5.9 can be rearranged to solve for the TWA concentration of airborne analyte (Equation 5.9a),

$$\frac{M}{R\,t} = \overline{C}_{(t)} \qquad \text{Equation 5.9a}$$

Equation 5.9a indicates that the rate of analyte mass loading in the passive sampling device (M/t) is dependent on the sampling rate of the system (R) and is directly proportional to the average analyte concentration. When the analyte concentration does not change with time, Equation 5.9a can be used to determine a first order rate constant, K' (Equation 5.10) (4,5,6),

$$K' = R = \frac{M}{t\,C_F} \qquad \text{Equation 5.10}$$

Equation 5.10 that the K' will be a constant for a given diffusive sampling device and with constant analyte concentration; however, once the K' is determined for an analyte with this device, the K' can then be used to quantify the average analyte concentration by measuring the mass of analyte loaded, *M*, for a given sampling time, *t*. In other words, the TWA concentration can be determined (4,7,8). Therefore, the SPME sampling device can be used as a TWA sampler. For example, if the K' is known for styrene with TWA sampling on the 100 μm PDMS, then quantitation of unknown styrene concentrations only requires a determination of the mass of styrene loaded on the fiber for a given sampling time, *t*. (Equation 5.11),

$$\frac{\frac{M_f}{t}}{K'} = \frac{ng}{cm^3} = \overline{C}_{(t)} \qquad \text{Equation 5.11}$$

where n_f is the mass of analyte measured on the fiber for a sampling time, *t* (min) and where K' is the sampling rate constant determined under specific conditions, $K' = \frac{ng_f}{ng/cm^3 \times \min}$.

Furthermore, the power of the SPME sampling device for TWA sampling is that L can be increased or decreased to accommodate high concentrations, or long sampling times, or decreased to accommodate low concentrations or short sampling times (Figure 5.1, Equation 5.6). Therefore, with a K' determined with a path length *L*, moving the coating to path length L' would proportionally change the analyte sampling rate. The effect of changing the path length from *L* to L' is shown in Equation 5.12

$$\overline{C}_{(t)} = \frac{\frac{M_f \times L'}{t}}{K' \times L} \qquad \text{Equation 5.12}$$

Equation 5.12 predicts that if the K' is determined at L and if the sampling occurred at L', then a factor of L'/L is required to correctly describe the analyte $\overline{C}_{(t)}$. A factor greater than 1 is required when $L' > L$, less than 1 when $L' < L$, and no factor when $L' = L$.

The key to using SPME for time-weighted average sampling is with the K' which is experimentally determined at a constant L, for a specific analyte(s) at known concentrations with specific fiber coatings. This new method will further simplify the use of SPME for TWA sampling.

Finally, consider the response time of the passive sampling device given in Equation 5.13 (9),

$$T_{\text{Response}} = \frac{1.5L^2}{D} \qquad \text{Equation 5.13}$$

where T_{Response} is the time for the sampling system to begin accurately responding to the analyte concentration. For example, for L=0.3 cm and D=0.09 cm²/s (benzene, 10), the response time is approximately 1.5 seconds and is approximately 19 seconds when L is increased to 1 cm, similar response times to those reported for other passive sampling devices (9). There is no concern for long response times since this time is typically considered the lag time between a varying analyte concentration and a proportional response (6).

5.3 Experimental

All retracted fiber path lengths (L) were measured by inserting a steel tube of equal fiber diameter into the needle, then measuring the depth of its insertion.

5.3.1 Integrated sampling with the PDMS coating

All chemicals, materials, and sampling methods were as described in Chapter 2.

5.3.2 Integrated sampling with the PDMS/DVB coating and on-fiber derivatization

All chemicals, materials and sampling methods were as described in Chapter 4.

5.4 Results and Discussion

Two different SPME fiber coatings were used as sorbents to test the feasibility of TWA sampling with SPME. The PDMS coating was used for benzene, toluene, ethylbenzene, *p*-xylene, *o*-xylene, 1,3,5-trimethylbenzene (mesitylene), α-pinene, d-limonene, n-pentane, n-hexane, and n-undecane. The PDMS/DVB fiber coating with on-fiber derivatization using PFBHA was used for formaldehyde. Both of these fiber coatings have been extensively discussed as grab sampling devices in Chapters 2 and 4 of this thesis.

The main strategies employed in this aspect of the research focused on using the mentioned fiber coatings as sampling media for TWA sampling with SPME. Each fiber coating was tested under different conditions, and as such they are presented separately.

5.4.1 Integrated Sampling with 100 μm PDMS Fibers

Table 5.1 summarizes the data obtained from the SPME TWA sampling of benzene, toluene, ethylbenzene, *p*-xylene, *o*-xylene, 1,3,5-trimethylbenzene (mesitylene), α-pinene, d-limonene, *n*-pentane, *n*-hexane, and *n*-undecane each at 34 μg/L (25 °C). These experiments were designed to determine the efficiency of the sorbent to act as a zero sink (6). The general concept is that a highly efficient sorbent will strongly retain the analyte even when the sorbent is exposed to a gas with zero concentration of that analyte (6). If the sorbent does not strongly retain the analyte, then the sorbent can still be used for TWA sampling except

only for short TWA sampling times, e.g., 15 to 30 minutes. Air samples acquired for these times are often used to determine whether analyte concentrations have exceeded a short-term exposure limit (1,11).

Column **A** from Table 5.1 indicates the amount of analyte detected on the fiber after a 15 minute exposure to the standard gas where the fiber was retracted during sampling, L=3 mm (Figure 5.1).

The data in Column **B** present the amount of analyte detected on the fiber after a 5 minute exposure to the standard gas, then 5 minutes to gas with zero concentration of the analytes, then a 5 minute exposure to the standard gas, etc., until a total of 15 minutes exposure time to the standard gas plus 15 minutes of unexposed time. The data between Columns **A** and **B** will be compared (below).

Column **C** presents the amount of analyte detected on the fiber after the fiber was exposed (out of the needle) for 10 minutes to the analytes (Figure 1.1), i.e., the amount of analyte which was detected on the fiber at *equilibrium* for each of the analytes. These data represent the maximum mass of analyte which can be loaded onto the 100 μm PDMS fiber at 25 °C for each analyte at 34 μg/L, and are used to determine the percent of equilibrium for retracted fiber sampling. It is emphasized that with TWA sampling, only a fraction of the gaseous analytes will be absorbed onto the fiber for a given time due to the cross sectional area and path length (Equation 5.9). Typically, no more than approximately 5 % of equilibrium for that analyte mass loaded during retracted fiber sampling can be tolerated before the amount of sorbed analyte begins to affect the mass rate uptake of the passive sampling device (6). This percentage will decrease will less efficient sorbents.

The data from Column **B** were divided by the data from Column **A**. The ratio of these data are the percent of analyte on the fiber detected with intermittent exposure compared to continuous exposure. Therefore, if **B/A** = 1, then there is no analyte desorption during

non-exposure to the analyte mixture; however, if **B/A** < 1, then analyte desorption occurs during the non-exposure period of the sampling. The data in Column **B/A** indicate that for the sampling time comparison, there an 81 % retention of pentane (81%) but 97 % for undecane. From Chapter 2 (Table 2.2) the K_{fg} for pentane was 95 and 25,000 for undecane. Therefore, the data show a trend that with increasing K_{fg}, there is a corresponding increase in the ratio of **B/A**. These data indicate that analytes with large affinities for the PDMS fiber coating will less readily desorb from the fiber during the sampling time. In other words, the efficiency of TWA sampling with PDMS increases with increasing analyte K_{fg}. Therefore, a method to discern which analytes are best long-term sampled by retracted sampling with 100 μm PDMS is possible by considering the analyte K_{fg}. The data show that 19 % of *n*-pentane desorbs from the fiber coating during the period of non-exposure while only 3 % of *n*-undecane desorb under these conditions. If a 10 % loss of analyte is tolerable (Column **B/A**), then from Table 5.1 the proposed cutoff for integrated sampling would start with toluene. Which suggests that short term TWA sampling (less than 30 minutes) is possible with the 100 μm PDMS fiber coating for compounds with K_{fg}>1,000.

The data in Table 5.1 were further analyzed by taking the ratio of Column **A** to Column **C, A/C**. The data in this column are the percent of analyte on the fiber between continuous retracted samplings for 15 minutes and the amount of analyte at equilibrium (10 minute) with the fiber completely exposed. The data indicate that *n*-pentane has reached 58 % of the mass at equilibrium while *n*-undecane has only reached 1% for the 15 minute sampling period. Therefore, if we set the **A/C** limit to 5 %, it would be possible to TWA sample-undecane for 75 minutes with L=0.3 cm (15 minutes x 5% / 1%) with this integrated sampling device without overly compromising the initial uptake rate.

The data in Column ***K'* (1)** represent the first order rate uptake for each of the tabulated analytes using μg/L and the data from Column ***K'* (2)** are the first order rate uptakes

for each analyte based on the analytes using ppm_v. (Equation 5.10). These data were calculated by dividing the data from Column **A** by the sampling time (15 minutes) and by the analyte concentration in both μg/L and ppm_v, yielding the apparent first order rate uptake given by $K' = \frac{M}{C \times t}$. The data from Column K'**(1)** indicate an interesting trend in that with increasing analyte K_{fg} there is a corresponding increase in the K' up to ethylbenzene where it begins to level off. The reason the K' is smaller for pentane compared to ethylbenzene can be explained with Equation 5.8. If $C_S \neq 0$, then there is a vapour tension of analyte from the surface of the sorbent which reduces the tendency of additional analyte to proportionally mass load onto the sorbent. This is most likely occurring when pentane absorbs into the PDMS fiber coating. Therefore, those compounds with K_{fg}<2,000 cannot be properly TWA sampled, i.e., the mass loading rate will not be representative of the analyte concentration.

Another observation made from the data in Table 5.1 was that the K'**(2)** values increase with increasing analyte LTPRI. Therefore, the values were plotted as a function of LTPRI (Figure 5.3). The findings were that K' linearly increased as a function of LTPRI value. In addition, the data in Figure 5.3 were plotted on the basis of analyte category, i.e., benzene, toluene, ethylbenzene, xylenes and mesitylene (1,3,5-trimethylbenzene), with the resulting plot presented in Figure 5.4. The rational for this was that it was expected that analytes within a homologous series would have similar solute activity coefficients (12). Recall also that the $\log K_{fg}$ is linearly related to LTPRI (Chapter 3). Therefore, K' should also be linearly related to $\log K_{fg}$, as was found (data not shown). In addition, recall from Equation 5.9 the mass sampling rate is directly proportional to R, the sampling constant for a given analyte and geometry of the passive sampler (Equation 5.6), which includes the diffusion coefficient.

Table 5.1: Summary of data obtained from the integrated sampling (retracted to 0.3 cm) of benzene, toluene, ethylbenzene, *p*-xylene, *o*-xylene, 1,3,5-trimethylbenzene (mesitylene), α-pinene, d-limonene, *n*-pentane, *n*-hexane, and *n*-undecane, each at 34 µg/L and 25 °C.

Column **A**: Amount of analyte detected on the fiber after a 15 minute (retracted fiber) exposure to the standard gas.

Column **B**: Amount of analyte detected on the fiber after a 5 minute exposure to the standard gas, then 5 minutes to gas with zero concentration of analyte, etc., until a total of 15 minutes exposure time plus 15 minutes unexposed time.

Column **C**: Amount of analyte detected on the fiber after the fiber was completely exposed for 10 minutes to the analytes.

Column **B / A**: Percent of analyte on the fiber detected when comparing the intermittent exposure to continuous exposure.

Column **A / C**: This is the percent of analyte detected on fiber between continuous retracted sampling for 15 minutes and the amount of analyte at equilibrium with the fiber completely exposed.

Column K' **(1)**: Calculated first order rate constant for the analyte uptake when the fiber was retracted, with data from Column A, using 34 µg/L and 15 minute sampling time.

Column K' **(2)**: Calculated first order rate constant for the analyte uptake when the fiber was retracted, with data from Column A, using ppmv and 15 minute sampling time.

Analyte	A (ng)	B (ng)	C (ng)	B / A	A / C	K' (1) (ng/min µg/L)	K' (2) (ng/min ppmv)	ppm_v
Pentane (n-)	1.1	0.9	1.8	81%	58%	0.0021	0.0062	12
Hexane (n-)	1.7	1.5	4.5	88%	39%	0.0034	0.0119	9.7
Benzene	2.3	2.1	7.5	89%	31%	0.0046	0.0146	11
Toluene	3.1	2.8	21.1	90%	15%	0.0061	0.0228	9.1
Ethylbenzene	3.8	3.5	52.7	93%	7%	0.0074	0.0321	7.8
Xylene (p-)	3.9	3.6	59.1	93%	7%	0.0076	0.0331	7.8
Xylene (o-)	4.1	3.8	72.5	94%	6%	0.0080	0.0349	7.8
Pinene (a-)	4.1	3.9	120	94%	3%	0.0081	0.0452	6.1
Mesitylene	4.5	4.3	157	95%	3%	0.0089	0.0436	6.9
Limonene	4.5	4.3	261	96%	2%	0.0087	0.0486	6.1
Undecane (n-)	5.1	5.0	658	97%	1%	0.0098	0.0640	5.3

Table 5.2: Summary of K_{fg} and LTPRI values for the compounds. The LTPRI values for pinene and mesitylene were calculated from $\log K_{fg}=0.0042LTPRI-0.188$ (Chapter 3).

i.d.	Analyte	LTPRI	$K_{fg\ (25°C)}$
1	*Pentane (n-)*	500	95
2	*Hexane (n-)*	600	150
3	*Benzene*	639	300
4	*Toluene*	747	880
5	*Ethylbenzene*	836	2100
6	*Xylene (p-)*	846	2400
7	*Xylene (o-)*	868	3100
8	*Pinene*	915	4500
9	*Mesitylene*	964	5800
10	*Limonene*	1000	10300
11	*n-Undecane*	1100	25000

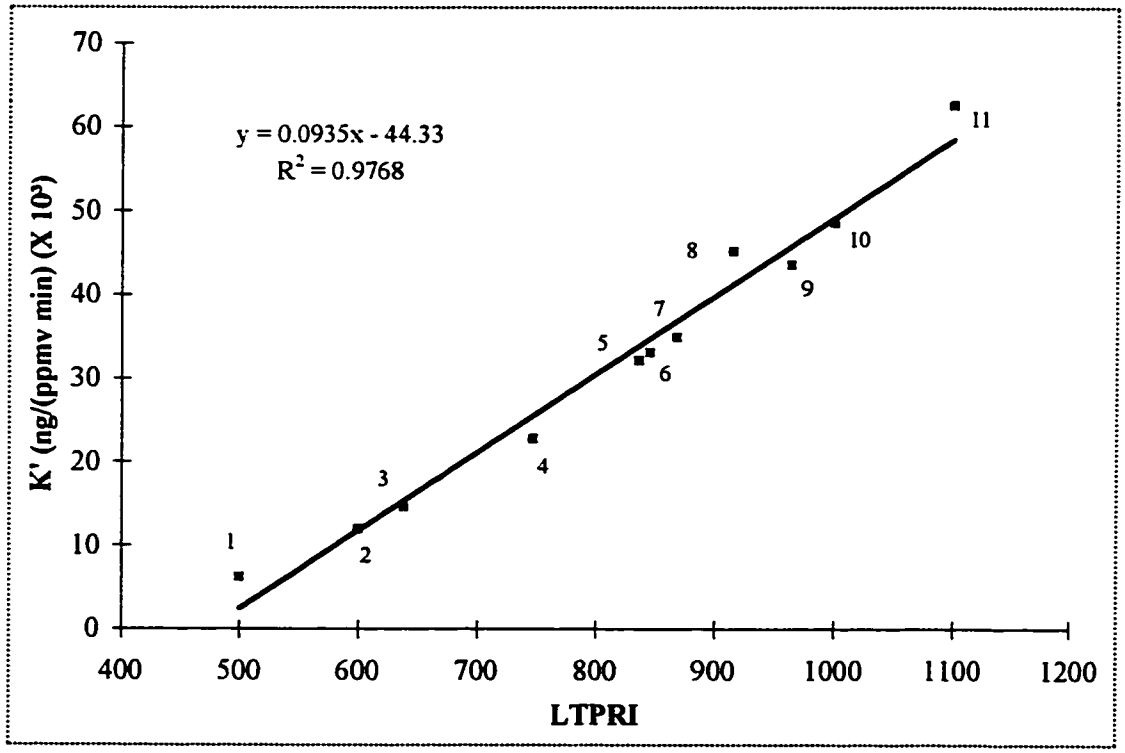

Figure 5.3: Plot of the K' from Table 5.1 for each of the compounds indicated in Table 5.2 as a function of the compound's LTPRI (Table 5.2).

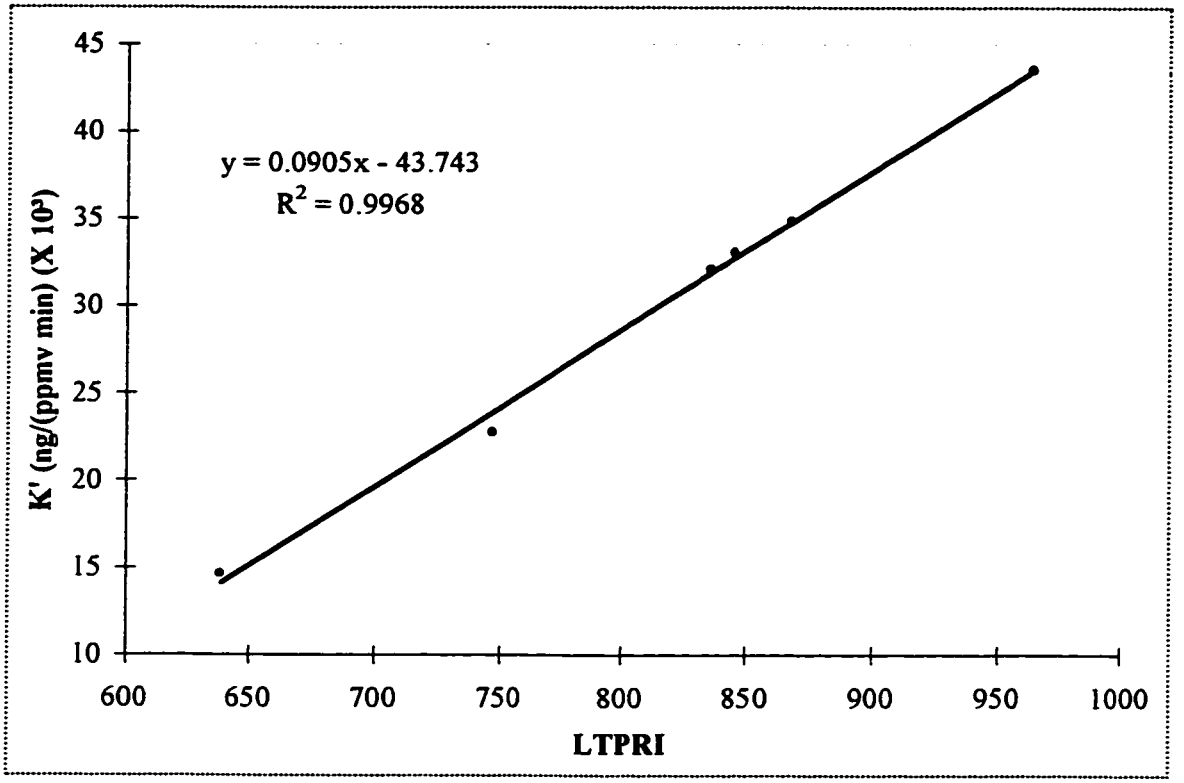

Figure 5.4: Plot of the relationship between *K'* and LTPRI for the aromatic compounds from Table 5.2. The data indicate there is an excellent linear relationship between the *K'* and LTPRI.

The practical application to these findings was that with the data shown in Figure 5.4, it seemed possible to use the LTPRI for a class of compounds, say the alkyl-substituted mono-aromatics, to obtain an estimated *K'* at 25 °C for analyte uptake rate on the 100 μm PDMS fiber coating. In this way, if short-term TWA sampling, e.g., 30 minutes, was required for a compound with K_{fg}>2000, which could be estimated as shown in Chapters 2 and 3, then the *K'* could be estimated without experimentation. This has been proven useful for the confirmation of a *K'* for styrene which is discussed in Chapter 6. A dynamic standard gas mixture of styrene was generated with the standard gas generator described in Chapter 2. The 100 μm PDMS fiber was used, in the integrated sampling position, to sample the gas for 15

minutes. The amount of styrene detected on the fiber was then divided by the sampling time and the concentration, in ppm_v. The K_{fg} for styrene was found to be 3090, essentially identical to that for *o*-xylene. Also, the LTPRI value for styrene was 870. Therefore, the estimated K' was 35×10^{-3} ng/(ppmv min), from the relationship shown in Figure 5.3, while the actual value is 34×10^{-3} ng/(ppmv min). Also, in using the relationship shown in Figure 5.1, the value was estimated to be 37×10^{-3} ng/(ppmv min), not unacceptable given this is an estimate. It seems, then, that a simple method is available to establish K' for the 100 μm PDMS fiber, a point discussed, and proven with a field study (Chapter 6).

5.4.2 Integrated sampling with PFBHA coated PDMS/DVB fibers: on-fiber derivatization as a method to yield a zero sink

Theory indicates that the rate of analyte uptake is ideal when C_S=0 for the TWA sampling device (Figure 5.2, Equation 5.9). Probably the best method to achieve C_S=0 is with analyte derivatization. In Chapter 4 of this thesis, PDMS/DVB fibers sorbed with PFBHA successfully sampled formaldehyde gas while the fiber was in the 'exposed' position. Also, as indicated in Chapter 4, the stability of the product, PFBHA-HCHO oxime, was extremely high, indicating the sampling system was of a very high efficiency. Therefore, using this sampling device for TWA sampling of HCHO would potentially yield the ideal zero sink, as will be shown herein.

The data summarizing the exposure routines for PDMS/DVB fibers adsorbed with PFBHA to sample HCHO are provided in Table 5.3. The exposure routines were designed to challenge the HCHO sampling system. The data indicate there is cumulative amount of PFBHA-HCHO oxime formed with intermittent fiber exposure to the HCHO standard gas, with no observable losses, thus substantiating the fact this sampling system yields an ideal zero

sink. For example (Table 5.4), essentially no losses were observed for a total sampling time of 60 minutes, where 30 minutes of the time the fiber sampled inside the sampling vessel and for the other 30 minutes the fiber sampled a gas stream with zero concentration of HCHO (Run No.4). In addition, this accumulated amount was directly proportional to the amounts obtained with different intermittent sampling procedures indicating that detectable consumption of the sorbed PFBHA had not occurred, even at the extremely high HCHO concentration used for the tests (>600 ppb_v).

Table 5.3: Exposure routines for integrated sampling (0.3 cm retracted fiber L). The PFBHA/PDMS/DVB fiber uptake of HCHO in the integrated sampling mode (move from left to right for the exposure pattern). All exposures were consecutive. The gas with zero concentration of HCHO was a diversion of the gas used to generate the standard gas mixture of HCHO. The diverted gas was passed over the fiber at the same velocity as that for the HCHO standard gas mixture.

Exposure Routines							
Run No.							Total Sampling Time (min.)
1	**E (10 min)**						10
2	**E (30 min)**						30
3	**E (10 min)**	*NE (10 min)*	**E (10 min)**	*NE (10 min)*	**E (10 min)**	*NE (10 min)*	40
4	**E (30 min)**	*NE (30 min)*					60
E = Exposure to HCHO (636 ppbv) (25 °C) *NE = No Exposure to HCHO - exposed to gas with zero concentration HCHO*							

The data in Table 5.4 summarize the mass of PFBHA-HCHO oxime produced from each of the runs shown in Table 5.3. Each run was carried out in duplicate over a period of

three days where the relative standard deviations were less than 3 %. The K' was determined for the TWA sampling device and found to be 0.000348 ng/(sec ppbv) for L=0.3 cm. With this K', the system was vigorously tested by exposing the fiber to 640 ppbv HCHO, with L=3.0 cm, for 1007 minutes (16 hours and 47 minutes, an overnight exposure). The amount of PFBHA-HCHO oxime formed after the exposure time was determined and found to be 23.8 ng. Then, this amount as a function of time was divided by the K' obtained at L=0.3 cm. The concentration was then multiplied by 10, the ratio between the path lengths (Equation 5.12). The result was that the actual concentration was within 7 % of the expected HCHO concentration. This was repeated two more times, and each time the findings were similar. These data indicate that long-term or integrated sampling HCHO is possible with SPME using PFBHA coated onto PDMS/DVB fibers. Since this is the same commercially available fiber used for grab sampling of HCHO discussed in Chapter 4, it is now possible to achieve both general aspects of air sampling with the same fiber for measurement of gaseous HCHO concentrations. This will allow for occupational monitoring as well as ambient monitoring of HCHO, and was tested and proven with a field study (Chapter 6).

Table 5.4: Summary of data obtained from the long-term sampling (TWA) (integrated sampling) of 636 ppbv HCHO with PFBHA/PDMS/DVB fibers. The Run No. are described in Table 5.1 - Exposure Routines.

Run No.	Sampling Time (min)	ng(fiber)	L (mm)	ng/min	K' ng/[HCHO]time/3.0 mm	
1	10	2.2	3.0	0.22	0.000346	
2	30	6.7	3.0	0.22	0.000351	
3	30 / 30	6.7	3.0	0.22	0.000349	
4	30 / 30	6.6	3.0	0.22	0.000346	
				average K'-	**0.000348**	
Overnight Sample	1007	23.8	30	0.024	ng/time/K' = ppbv 679	*%Er* *6.8%*

5.5 Summary

The use of K' for the quantitation of long term samples for hydrocarbons and formaldehyde with PDMS and PFBHA coated PDMS/DVB fibers proved successful.

Chapter 6 demonstrates the practical application of TWA sampling with both PDMS and PFBHA/PDMS/DVB fibers using the experimentally obtained and estimated K' values for quantitation.

5.6 References

1.. *The Industrial Environment - its Evaluation and Control*, U.S. Department of Health and Human Services, Public Health Service, Center for Disease Control, National Institute for Occupational Safety and Health, 1973

2. Lautenberger, W.J., Kring, E.V., Morello, J.A., Am. Ind. Hyg. Assoc. J., **41** (10) 1980 pp. 737-747

3. Brown, R.H.; Harvey, R.P.; Purnell, C.J.; Saunders, K.J. A Diffusive Sampler Evaluation Protocol, Am. Ind. Hyg. Assoc. J., **45**, 1984, 67-75

4. Namiesnik, J., Górecki, T. and Kozlowski, E., *Passive Dosimeters - An Approach to Atmospheric Pollutants Analysis*, The Science of the Total Environment, **38**, 1984 pp. 225-258

5. Brown, R.H., Harvey, R.P., Purnell, C.J., and Saunders, K.J., Am. Ind. Hyg. Assoc. J. **45** (2) 1984, pp. 67-75

6. Underhill, D.W., Am. Ind. Hyg. Assoc. J. **44** (3) 1983, pp. 237-239

7. Harper, M. and Purnell, C.J., Am. Ind. Hyg. Assoc. J. **48** (3) 1987, pp. 214-218

8. Kozdron-Zabiegata, B., Namiesnik, J., and Przyjazny, A., Indoor Environ. **4**, 1995 pp. 189-203

9. Einfeld, W., Am. Ind. Hyg. Assoc. J. **44** (1) 1983, pp. 29-35

10. Lugg, G.A., Anal. Chem.**40** (7) 1968 pp.1072-1077

11. *American Conference of Governmental Industrial Hygienists*, TLVs and BEIs, 1996

12. Zhang, Z., University of Waterloo, Ph.D. Thesis, 1995

CHAPTER 6

FIELD SAMPLING WITH SPME

6.1 Background

The ultimate challenge of the new sampling methods described in this thesis involved testing it under field conditions with side-by-side comparisons to at least two other standard (accepted) sampling methods. In this way, an unbiased agreement between the SPME methods and other methods can strengthen the validity of our understanding of the physical chemical processes of air sampling with SPME. It can also provide potential users with a point of reference against which the SPME sampling methods can be compared similar to other new air sampling method protocols (1,2,3,4).

One of the key aspects to obtaining an accurate representation of the analyte concentration from the field is to ensure the integrity of the sample once it is acquired. Sample stability becomes increasingly important as the time increases between sample collection and analysis (4). Transporting the samples from a field site to the laboratory for analysis often places the sampling media under a number of different environmental conditions. For example, ground transportation can often place the samples at extremely high temperatures, while transportation via aircraft can impose a dramatic decrease in barometric pressure since the samples are typically shipped in the plane's luggage compartment. For these reasons, it would also be quite advantageous to have the flexibility to analyze the samples directly in the field, immediately after they are acquired. This point is feasible due to the development of a field portable GC redesigned specifically for SPME introduction (5).

The field GC was used as a component of one of the following studies and my thanks go out to Dr. Górecki for his efforts (6).

This chapter presents the results obtained from using SPME with the 100 μm PDMS (Chapters 2, 3, and 5) fiber coating for air sampling styrene in an industry. It also presents data from using PFBHA/PDMS/DVB fibers (Chapters 4 and 5) for air sampling HCHO in a pathology room storage facility at the University of Guelph. Both sampling sessions used the commercially available SPME fibers for grab and TWA sampling (see Chapter 5 for TWA sampling).

For the styrene study involving PDMS, the samples were all analyzed in the laboratory, but for the HCHO study involving PFBHA/PDMS/DVB, samples were both analyzed in the field with the field GC and in the laboratory.

Finally, the results from both studies were compared to standard methods involving different sampling and analysis protocols, showing extremely promising results.

6.2 Field Sampling with SPME for Airborne Styrene Using 100 μm PDMS Fibers

6.2.1 Experimental

Four different methods were used to determine the airborne concentration of styrene from a styrene based resin used in an industry. Three charcoal tubes with active sampling, three charcoal passive badge monitors (3M), a portable photo-ionization detector (PID) which was based on active air sampling and eight SPME using 100 μm PDMS, three for grab sampling, three for integrated sampling, and two blanks, were used.

Active sampling through charcoal tubes was carried out following National Institute for Occupational Safety and Health (NIOSH) methods 1500 and 1501 for the determination of airborne hydrocarbons. A mass flow controlled air sampling pump equipped with a very fine metering valve was used to draw air through small charcoal tubes at 100 mL/min which was calibrated with a bubble flow meter at 25 °C. Chemical desorption from charcoal was facilitated with 1.0 mL CS_2 in Teflon capped 4 mL vials. The air samples were collected in triplicate. Sampling and analysis with the 3M passive badges was carried out as per the manufacturer's instructions.

The real-time gas detector used was a RAE portable PID set to 10.6 eV for non-halogenated compounds and it was calibrated the day before the study with a 100 ppm_v standard of isobutylene at 296 K and certified by the supplier of the equipment. The supplier indicated styrene response on the PID was 42% that for isobutylene. It was possible to use a PID in this study because previous analyses at other similar locations and activities showed

that of the airborne compounds, styrene was present at greater than 99 % of all the detectable airborne hydrocarbons.

For SPME with PDMS, eight 100 μm PDMS fibers were each conditioned at 250°C for one hour, then retracted and capped with a silicone septum. Three of the fibers were used for fast grab sampling concurrent to active sampling with charcoal tubes, three were used for testing the viability of integrated sampling, and the last two were used as a field blank and a trip blank. For fast grab sampling, the fibers were exposed to the test air for 5 minutes which was the same amount of time used for the active sampling on charcoal tubes. For integrated sampling, the fibers were left retracted in the assembly and exposed to the air for 30 minutes concurrent to the acquisition of 30 minute active sampling through charcoal tubes. Immediately after sampling with SPME with PDMS, all of the fibers were removed from the fiber holder and retracted approximately L=1.5 cm in the needle (Figures 5.1 and 6.1) which was followed by capping the end with a new and clean 6 mm silicone septum then placed on a bed of dry ice (7) along with the charcoal tubes. All SPME with PDMS and active charcoal tube samples were analyzed within 3 hours of acquisition. The sampling temperature averaged at 296 K and the relative humidity was 25 % during the sampling period. All analyses were carried with the same instrumental conditions as those described in Chapter 2.

A standard gas mixture of styrene in air was generated using the standard gas generator described in Chapter 2 to calibrate the PDMS fiber with styrene. The PDMS/styrene K_{fg} was determined at 25 °C and 1 atm, and the first order rate constant described in Chapter 5 was determined with the fiber retracted to 0.3 cm.

6.2.2 Results and Discussion

The laboratory work required before field sampling could proceed involved establishing both the K_{fg} for styrene on the 100 μm PDMS and its K' with the fiber retracted to 0.3 cm. This presented a good opportunity to use the K_{fg} temperature dependence (Chapter 2), the LTPRI relationship to K_{fg} (Chapter 3) and the estimation of K' (Chapter 5). First, the K_{fg} for styrene was determined (25 °C) using a standard gas mixture and found to be 3090 while the estimated K_{fg} using Equation 3.17 (Chapter 3) was calculated as 2920 with LTPRI=870, a relative error of -5.5%. Therefore, without experimentation, the K_{fg} could have been accurately estimated thus saving time without compromising the validity of the analytical result, given the required accuracy for new sampling methods is ±25 % (4). Then, using Equation 2.18, and the estimated K_{fg} and given the slope (a) from Equation 2.18 was 2105, the 'b' could be calculated thus providing a temperature correction factor should the sampling temperature be different than 25 °C. Also, with the K_{fg} available, it is possible to estimate the limit of detection using Equation 3.29. Therefore, using Equation 3.29 and with a detector detection limit of 1 ng with the FID and a K_{fg}=3090, the styrene in air detection limit was estimated at 0.47 μg/L (25 °C), better than 450 times lower than the allowable occupational exposure level of 215 μg/L (8). From these data, it appeared that grab sampling for styrene with 100 μm PDMS should not suffer from low analyte mass loading given the anticipated C_{air} for styrene was greater than 10 μg/L. The next step was to determine the K' for styrene with the 100 μm PDMS coating retracted to 0.3 cm. The experimentally determined K' was found to be 35 pg/(ppmv min) compared to the estimated K' of 37 pg/(ppmv min) (estimated using the relationship shown in Figure 5.3). This represents a relative error of +5.7%. Again, no experimentation would have been necessary to establish

this other sampling parameter; however, corroboration of these estimation techniques can only enhance method validity.

Table 6.2.1 summarizes the results from the field sampling session for styrene at the industry which had levels of styrene as a result of the application of a large quantity of vinyl-ester resin from which styrene evaporated. The results show very good agreement for the styrene concentrations using 100 μm PDMS for grab sampling and the charcoal tube samples and are summarized in Table 6.2.1. In addition, for the 30 minute integrated samples with PDMS, there was excellent agreement between the SPME result and the 30 minute charcoal tube results. Of interest are the results from the 3M passive badges. These badges, and other similar versions, are limited to a large extent by the fact they require large face velocities to maintain an appreciable exchange of analyte from the C_B and the C_F (Chapter 5) (9).

Table 6.2.1: Industrial concentrations of styrene, μg/L (23 °C), using different methods of field sampling, comparing PDMS to active sampling with charcoal, passive badge sampling and an active sampling portable photoionization detector, PID. The data in the first column represent the observed concentration of styrene with SPME 100 μm PDMS at 25 % R.H. for both grab sampling and integrated sampling.

Sample Type	***SPME 100 μm PDMS***	**Charcoal Tubes**	**Passive Badge (for the sample time)**	**PID**
5 min. sample	130	97	90	50 to 250
30 min. integrated	56	54	72	N/A

6.3. Field Sampling with SPME for Airborne Formaldehyde Using PFBHA loaded PDMS/DVB Fibers

6.3.1. Experimental

The field study for HCHO involved both 30 sec grab sampling with analysis by GC/PID and TWA sampling (7 hours). Two standard methods were used to compare the results obtained with SPME.

Work on the use of a field portable GC modified specifically for SPME sample introduction and narrow band detection has been published (5). A commercially available SRI gas chromatograph model 9300 B has been adapted to enable the use of SPME as the sample preparation and introduction technique for fast GC separations in the field. Modifications to the instrument included a new injector and to the photoionization detector (PID). The injector enables very fast fiber heating rates (~4000°C/s), which produce narrow injection bands suitable for fast GC and most appropriate for analyte desorption from SPME. The method to load the PDMS/DVB fiber with the derivatization reagent was presented in Chapter 4, and was used here; however, for the field work the fiber exposure time to the PFBHA solution was 3 minutes instead of 10 minutes. A calibration curve was generated of the PID response as a function of a 30 second exposure to various standard gas HCHO concentrations from the standard gas generator discussed in Chapter 4. Once in the field, the GC was placed within 5 m of the test sample locations so that all grab sampling and analyses occurred within two minutes. Each site was grab sampled four times, with the average value reported.

For TWA sampling, each of twelve PDMS/DVB fibers were loaded with PFBHA, in a HCHO free environment, as per the method described in Chapter 4, and there was no concern for PFBHA stability on the fibers since there is no loss of PFBHA while the fiber is retracted (even after 16 hours, Chapter 4). Each of the SPME needles was then placed in a clean Teflon capped 2 mL vial (Figure 7.1) with the fiber retracted to 3.0 cm and then transported to the test site, at ambient temperature (27 °C). Once in the field, four of the twelve fibers were left inside the vial during the sampling session (as blanks), and three fibers were used at each of the locations. One fiber from each of the three locations were retracted to 0.3 cm while the other two from each location were retracted to 3.0 cm. Therefore, each sampling site had a blank, one fiber which should have a high mass loading and two fibers which should have lower mass loading, for a total of twelve fibers. The sampling was considered active as soon as the fiber was withdrawn from the protective vial, at which point the timer was activated (a similar concept to other passive samplers, 10). The total sampling time was 420 minutes for each of fibers deployed for TWA sampling. Two other standard sampling methods were deployed as soon as the SPME fibers were exposed to the air. The first was a 3M passive badge specific for HCHO. This sampling device does not yield a derivative during the sampling; it passively absorbs the HCHO in a small amount of sodium bisulfite solution, then the absorbed HCHO is reacted with a chromogenic species followed by a spectrophotometric analysis (11). The second sampling method was that following NIOSH Method 2541, where air is drawn, with a mass flow controlled pump, over a bed of hydroxymethyl piperidine (HMP) with the product formed from the reaction between HMP and HCHO analyzed by GC/FID.

Upon termination of sampling with the SPME fibers, the total sampling time was recorded, and the fibers were returned to their original protective vials. The fibers were *not* cooled or stored under any special conditions for the 45 minute trip back to the laboratory for analysis, and a thermometer in the vehicle recorded a temperature of 30 °C. More than two hours passed once the samples were returned to the laboratory, primarily because the instrument had to be properly calibrated prior to sample analysis.

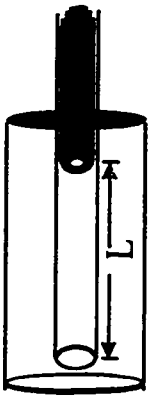

Figure 6.1: Strategy for transportation for SPME needles. The fiber is retracted to L=3.0 cm from the needle opening and with the needle placed in a small (1.8 mL) Teflon capped vial.

6.3.2. Results and Discussion

The data from the field sampling and analysis of HCHO with various methods, including SPME, are presented in Table 6.2. The data show that there is excellent agreement between the SPME sampling results for HCHO for both grab and integrated sampling. It can be seen from the SPME grab sampling data that high concentrations of HCHO were present during that particular sampling period. Recall that the SPME grab sampling took only 30 seconds, a true grab sampling device; however, there was no problem detecting the amount of

PFBHA-HCHO oxime formed, even with the low airborne HCHO concentration. It is also of interest that some of the sampling locations within the pathology sample storage room included positions immediately adjacent to jars containing 10-20 % formalin (HCHO stabilized with methanol). Even though the jars were tightly sealed, and with a layer of aluminum foil, they obviously leaked HCHO. The SPME grab sampling data presented in Table 6.2 also show good agreement with the integrated sampling methods, which is expected since the integrated sampling methods should provide an average concentration.

For the TWA HCHO sampling with SPME, the K' used was that for 0.3 cm retracted fiber length, 0.348 $\frac{pg}{\min(ppb_v)}$ (Table 5.4). Then, upon analysis the average rate of HCHO uptake (pg/min) was divided by 0.348 $\frac{pg}{\min(ppb_v)}$ yielding the 7 hour average HCHO concentration in ppb_v (Table 6.2). The data in Table 6.2 also show that two of the three 3M sampling devices have lower HCHO concentrations compared to the SPME integrated sampling devices, except for location number 2. For both locations 1 and 3, the 3M sampling device was positioned with the face towards the center of the storage room and 180° away from the major source of the contamination, i.e., large shelves of improperly sealed jars containing preserved tissues and organs. The 3M passive sampling device has one cross sectional face area of approximately 10 cm^2 with essentially a hemispherical exposure to the contaminated air. On the other hand, the cross sectional face area for the SPME needle opening is roughly 0.05 cm^2 but more importantly, its needle opening is open to the contaminated air in essentially a complete spherical range, thus allowing it to respond very well to all air changes. The 3M sample for location 2 was facing a ventilation air stream

during the sampling, thus rendering it less sensitive to casual air currents. By comparison, the SPME sampling device actually acts similarly to active sampling since the tube opening from the active sampling system also samples a spherical range.

These data indicate that this new SPME grab sampling method with field GC could be used to determine the HCHO concentration in areas of concern. In addition, the long-term sampling systems can then be deployed in strategic locations once the problematic areas are quickly identified. Often, the time to achieve control of a gaseous contaminant can be quite lengthy due to limitations in analysis time. For example, it would have taken at least 48 hours to acquire HCHO concentrations with either the active NIOSH sampling or 3M methods, but with SPME grab sampling and field GC, it took less than 2 hours to acquire more than 20 samples, not only in the main storage room, but also immediately outside of the area where other employees were located. Finally, the costs with the standard methods would have been more than 20 times that of SPME to achieve the same results.

Table 6.3.1: Summary of data obtained from a field study using PFBHA/PDMS/DVB fibers for airborne HCHO in a pathology storage facility. The sampling key is also presented.

Location	3-M (ppb_v)	SPME-1 (ppb_v)	2541 (ppb_v)	SPME-2 (ppb_v)
1	88	*109*	102	*106*
2	149	*152*	160	*140*
3	38	*57*	51	*93*

3M: 3501 Passive Badges for HCHO, 420 minutes, colorimetric
SPME-1: Time Weighted Average Sampling, 420 minutes
2541: NIOSH Method 2541, HMP/XAD-2, GC/FID
SPME-2: 30 seconds grab sampling + field portable (analysis)

1ppbv= 1.25 $\mu g/m^3$ = 1.25 ng/L @ 25 °C

6.4 Summary

The use of SPME retracted fiber sampling for TWA sampling HCHO by derivatization with PFBHA sorbed onto PDMS/DVB presents a considerable number of advantages over the traditional sampling methods.

6.5 References

1. Pristas, R. Am. Ind. Hyg. Assoc. J. **52** (7) 1991 pp. 297-304

2. Kring, E.V., Ansul, G.R., Basilio, A.N., McGibney, P.D., Stephens, J.S., and O'Dell, Am. Ind. Hyg. Assoc. J., **45** (5) 1984 pp. 318-324

3 Borders, R.A., Melcher, R.G., and Gluck, S.J., Am. Ind. Hyg. Assoc. J., **45** (5) 1984 pp.299-305

4. Kennedy, E.R., Fischbach, T.J., Song, R., Eller, P.M., and Shulman, S.S., Analyst, **121** 1996 pp. 1163-1169

5. Górecki, T. and Pawliszyn, J., Anal. Chem., **34** 1995 pp. 3265-3274

6. Martos, P., Górecki, T., and Pawliszyn, J., article in progress

7. Chai, M. and Pawliszyn, J. Environ. Sci. Tech., **29** 1995 pp. 693-701

8. *NIOSH Pocket Guide to Chemical Hazards*, U.S. Department of Health and Human Services, Public Health Service, Center for Disease Control, National Institute for Occupational Safety and Health, 1994

9. Lautenberger, W.J., Kring, E.V., Morello, J.A., Am. Ind. Hyg. Assoc. J., **41** (10) 1980 pp. 737-747

10. Hearl, F. and Manning, M.P., Am. Ind. Hyg. Assoc. J. **41** 1980 pp. 778-783

11. 3M Company, Occupational Health and Safety Products Laboratory, Organic Vapor Analytical Method No. 4D, 1985

CHAPTER 7

SUMMARY

7.1 Air Sampling with Solid Phase Microextraction

SPME has been shown with the work presented herein to be a viable air sampling analytical tool. It has equal or better reproducibility and accuracy than conventional air sampling methods, but is by far simpler to use and more versatile. The two SPME fiber coatings studied in this thesis were the 100 μm PDMS and the PDMS/DVB adsorbed with PFBHA.

Figure 7.1 presents the flow chart of suggested air sampling strategies for the newly developed sampling methods which were not possible with SPME prior to this work. Note that the figure indicates the choice of fiber coating depends on the analytes of interest.

7.1.1. The 100μm PDMS fiber coating

The sampling strategies with the PDMS fiber coating are presented on the left hand side of Figure 7.1. The 100 μm PDMS fiber coating can be used for air sampling general hydrocarbons, such as octane and benzene. For grab sampling, quantification with the 100 μm PDMS fiber coating can be achieved without am external calibration procedure, as shown with Equation 7.1 (in Figure 7.2). First, the K_{fg} can be determined experimentally from a small sampling vessel (Eqn. 7.2) or when either a dynamically generated standard gas was used or when $V_g > 100 \times K_{fg} \times V_f$ (Eqn. 7.3). Quantification of unknown airborne analyte concentrations can be achieved with Eqn. 7.1 provided the K_{fg} was determined at the same temperature at which sampling occurred. Alternatively, the K_{fg} (25 °C) can be estimated with

the analyte's linear temperature programmed retention index value using the established relationship for the homologous series of n-alkanes (Eqn. 7.4). In either case, if the sampling temperature is not the same as that at which K_{fg} was determined, then a temperature correction can be implemented given knowledge of the analyte's ΔH^v (Eqn. 7.5). If the analyte's ΔH^v is not known, then one can be estimated (Figure 3.3).

Finally, the same SPME air sampling device with PDMS can be used for time-weighted average sampling using the analyte's first order rate uptake, K', which is also related to the analyte's LTPRI (Chapter 5). In this way, the average sampling rate is divided by the analyte's K' yielding the TWA concentration of that analyte (for that sampling time).

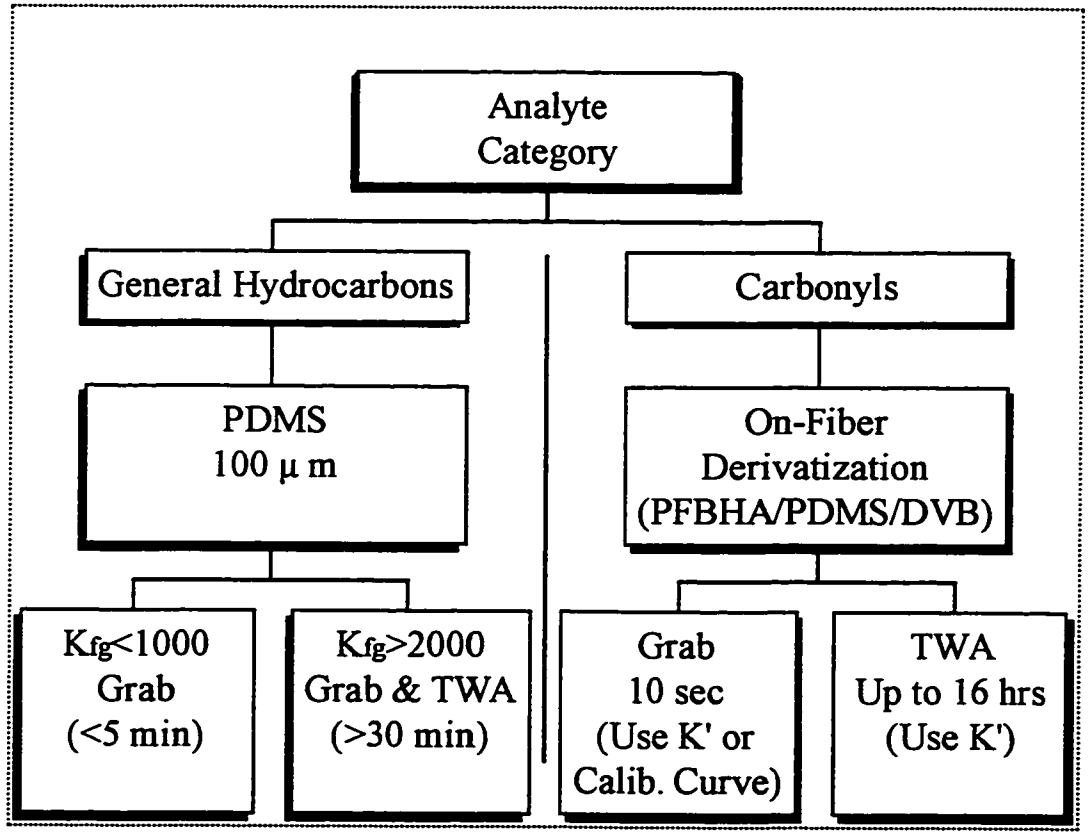

Figure 7.1: Selection of the suitable SPME fiber coating for the analyte category of interest.

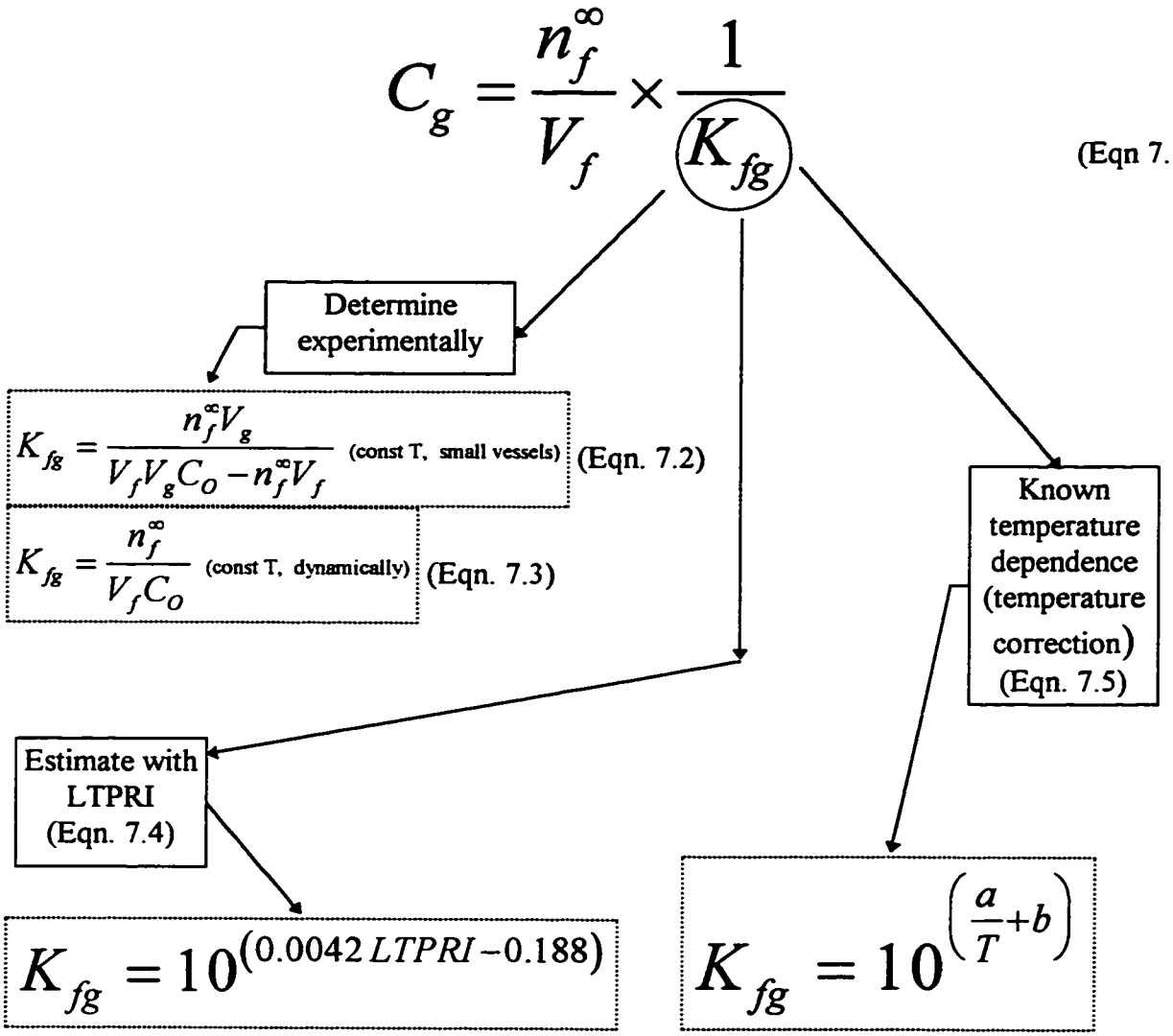

Figure 7.2: Summary of the grab sampling quantification method, using 100 μm PDMS without an external calibration procedure. If the K_{fg} is determined experimentally, then no temperature correction is required provided the calibration temperature for K_{fg} is the same as that for sampling. If the sampling temperature is not the same as that which K_{fg} was determined, then a temperature correction can be implemented given knowledge of the analyte's ΔH^v. If the K_{fg} is not known and one is required either quickly or cannot be determined, then one can be estimated with the LTPRI using the established relationship for the homologous series of n-alkanes.

The same SPME air sampling device with PDMS (in the retracted fiber position) can be used for integrated sampling using the analyte's first order rate constant for uptake (see Chapter 5).

7.1.2. The PDMS/DVB fiber coating sorbed with PFBHA

The right hand side of Figure 7.1 shows the sampling strategies for the on-fiber derivatization of gaseous formaldehyde. Also, Figure 7.3 shows how to use the PDMS/DVB fiber with on-fiber derivatization for quantification.

Both grab and TWA sampling formaldehyde with PDMS/DVB using on-fiber derivatization is possible (Figure 7.3). The method is highly reproducible and accurate, but most importantly, re-usable, and extremely cost effective (approximately 50 cents per sample) unlike conventional carbonyl sampling methods ($40/sample) for the non-reusable sampling device alone. Figure 7.3 shows that the derivatization reagent, PFBHA, is loaded onto the fiber (via an aqueous headspace extraction of a PFBHA solution), then the fiber is either exposed to the test gas as shown, or it is retracted into the needle for TWA sampling (Chapter 5, Figure 5.1).

For grab sampling, the fiber is exposed as shown in Figure 7.3. Following sampling, the mass of product formed is determined, the sampling rate calculated, then divided by 3.0 $\frac{pg}{ppb_v \sec}$. The result will be the concentration of HCHO. Typical grab sampling times can range from 10 seconds to 300 seconds, depending on the consumption rate of PFBHA. The amount of consumed PFBHA should not exceed 5 %.

For TWA sampling, the fiber is retracted during sampling HCHO as shown in Figure 5.1. Following TWA sampling, the amount of PFBHA-HCHO oxime product formed is analyzed. The sampling rate is determined, and the K'=0.35 $\frac{pg}{ppb_v \min}$ for L= 0.30 cm, is divided into the empirically obtained sampling rate yielding the average HCHO concentration for the sampling time (Chapters 4 and 5).

This method is highly desirable because PFBHA, unlike other extremely reactive carbonyl derivatization reagents, is not considered to be a toxin, mutagen, skin irritant, or mucous membrane irritant. The derivatization agent is purchased as a HCl salt which has a very high water solubility, has no offensive odours, and is very easy to clean away with water.

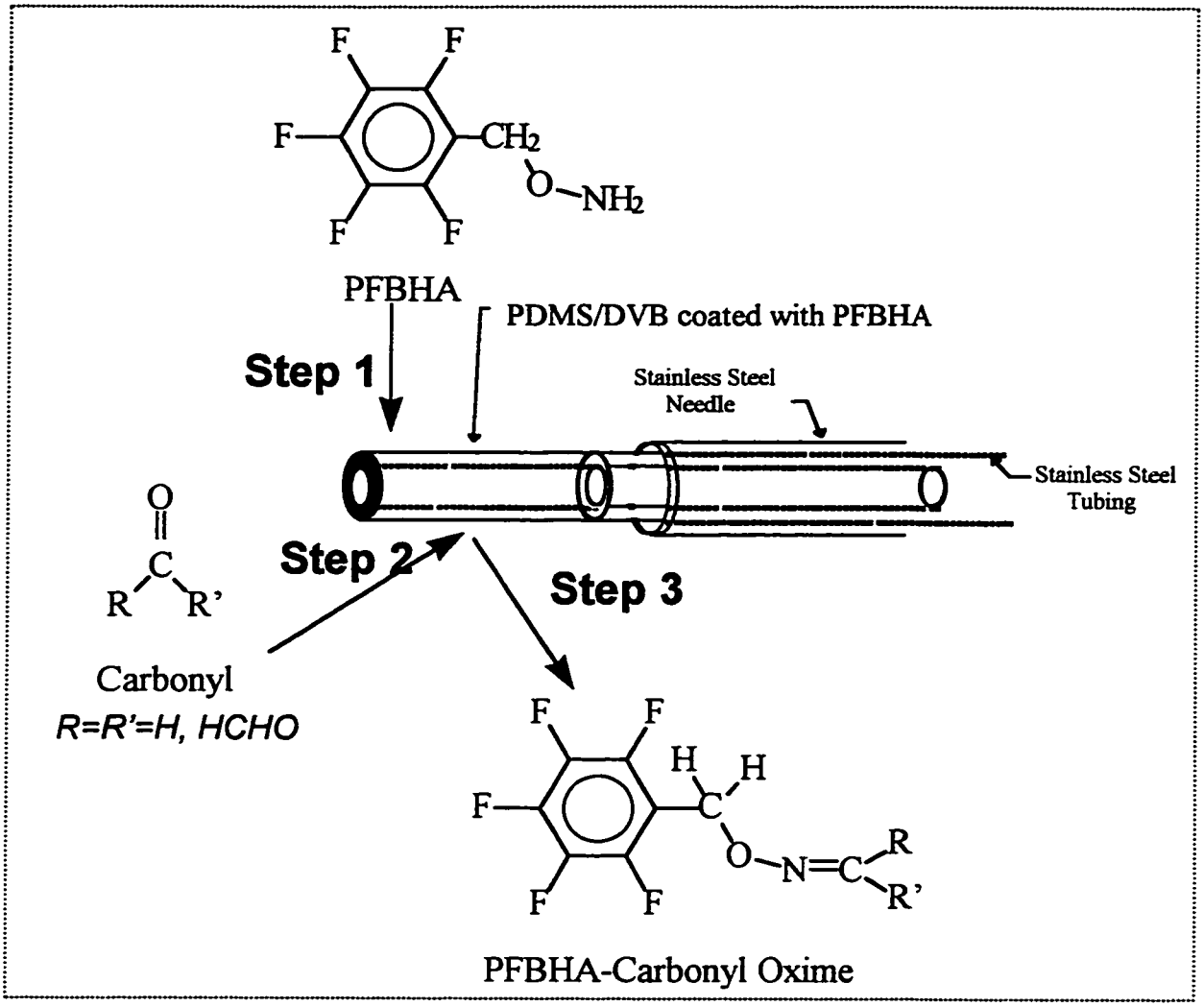

Figure 7.3: Procedure to quantify airborne formaldehyde with on-fiber derivatization using PFBHA adsorbed onto PDMS/DVB fibers, for both grab and TWA sampling. Step 1, load the fiber with PFBHA. Step 2, expose the fiber to air suspected of containing HCHO, either exposed (as shown) or retracted (Figure 5.1). Step 3, analyze the amount of product formed for the sampling time.

For grab sampling, expose the fiber as shown, obtain the sampling rate and divide this by 3.0 $\frac{pg}{ppb,\,sec}$. The result will be the concentration of HCHO. Grab sampling times can be as small as 10 seconds.

For TWA sampling, retract the fiber (Figure 5.1), sample the HCHO gas (minutes to hours), obtain the sampling rate and divide this by K'=0.35 $\frac{pg}{ppb,\,min}$. The result will be the average HCHO concentration for the sampling time (see Chapters 4 and 5 for grab and TWA sampling, respectively).

GLOSSARY

A ..... Area of needle opening
ACGIH ..... American Conference of Governmental Industrial Hygienists
Analytes ..... Test compounds under study or of interest
BP ..... Boiling point
C_f^{∞} ..... Equilibrium concentration of analyte on the fiber
C_g^{∞} ..... Equilibrium concentration of analyte in the gas
C_w^{∞} ..... Equilibrium concentration of analyte in water
C_O ..... Initial analyte concentration in the sample
CS_2 ..... Carbon disulphide used to chemically desorb analytes from charcoal
CXN/PDMS ..... Carboxen 1006 supported by PDMS
DNPH 2,4-Dinitrophenylhydrazine
ECD ..... Electron capture detector
Er ..... Percent relative error between actual and theoretical or expected
EPA ..... U.S. Environmental Protection Agency
F-test ..... Test for equal variances
FID ..... Flame ionization detector
GC ..... Gas chromatograph or gas chromatography
H_C ..... Henry's Law distribution coefficient
HCHO ..... Formaldehyde
HMP ..... Hydroxymethyl piperidine
HPLC ..... High pressure (performance) liquid chromatography
ΔH^v ..... Analyte heat of vaporization
K' ..... First order rate constant
K_{fg} ..... Partition coefficient - PDMS fiber to gas
K_{fw} ..... Partition coefficient - PDMS fiber to water
L ..... Path length for retracted fiber sampling
LC_{50} ..... Concentration of analyte which kills 50 % of test organisms
LD_{50} ..... Dose of analyte which kills 50 % of test organisms
LTPRI ..... Linear Temperature Programmed Retention Index
MDL or LOD ..... Method detection limit
MS ..... Mass spectrometer
n_f^{∞} ..... Equilibrium mass of analyte loaded on the PDMS fiber
NIOSH ..... National Institute for Occupational Safety and Health
n_{Total} ..... Total mass of analyte in a closed system
NIST ..... National Institute of Standards and Technology
NTP ..... Normal temperature (25 °C / 298 K) and pressure (760 mm Hg / 1 atm)
OSHA ..... Occupational Health and Safety Administration
PDMS ..... Poly (dimethylsiloxane)
PDMS/DVB ..... Poly (dimethylsiloxane) supporting divinylbenzene
PFBHA ..... *o*-(2,3,4,5,6-pentafluorobenzyl) hydroxylamine to derivatize carbonyls
PFBHA-HCHO oxime .. Product of the reaction between HCHO and PFBHA

PFBHA.HCl ..... HCl salt of PFBHA
PFBHA/PDMS/DVB ... PFBHA sorbed onto PDMS/DVB fiber coatings
PID ..... Photo ionization detector
ppm_v ..... Parts per million in air (μL/L)
ppb_v ..... Parts per billion in air (nL/L)
ppt_v ..... Parts per trillion in air (pL/L)
Re ..... Reynolds number
RH ..... Relative humidity
RSD ..... Relative standard deviation
SD ..... Standard deviation
SPI ..... Septum equipped temperature programmable injector, used for Varian
SPME ..... Solid phase microextraction
t-test ..... Test for equal means
TLV ..... Threshold limit value
TVOC or TPH ..... Total volatile organic carbons or total petroleum hydrocarbon (air)
TWA ..... Time-weighted average sampling or Integrated sampling
V_f ..... Fiber coating volume for PDMS
V_g ..... Sample volume
VP ..... Vapour pressure

IMAGE EVALUATION
TEST TARGET (QA-3)

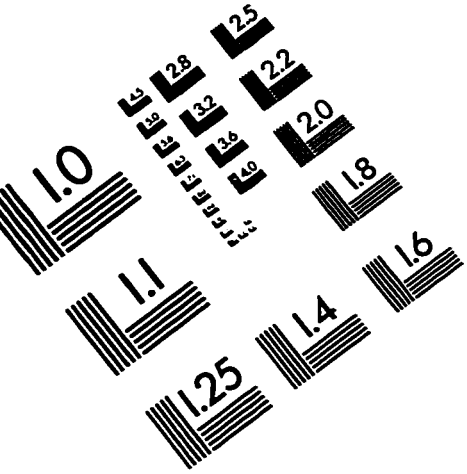

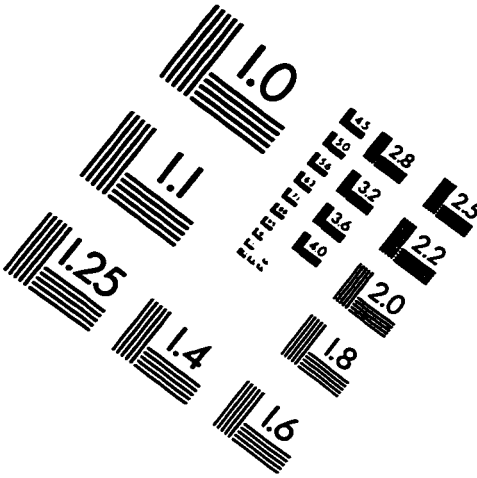

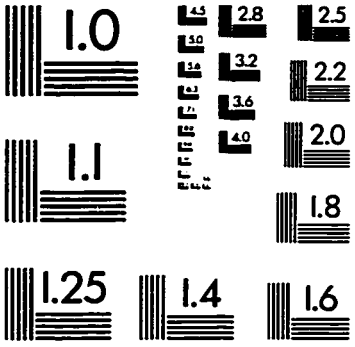

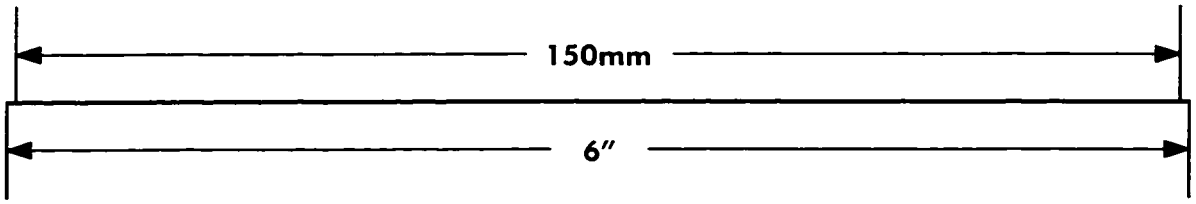

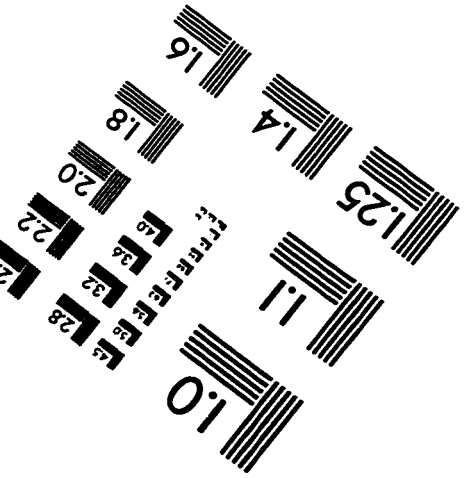

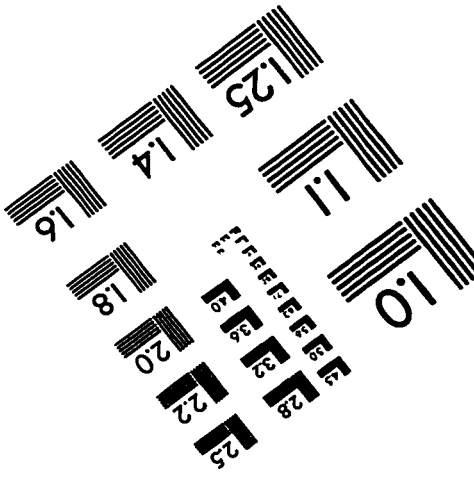

APPLIED IMAGE, Inc
1653 East Main Street
Rochester, NY 14609 USA
Phone: 716/482-0300
Fax: 716/288-5989